Mechanisms of Inflammation in Response to Wnt5A and IL-4 in Human Vascular Endothelial Cells

---

Dissertation

zur

Erlangung der naturwissenschaftlichen Doktorwürde (Dr. sc. nat.)

vorgelegt der

Mathematisch-naturwissenschaftlichen Fakultät

der

Universität Zürich

von

TOM SKARIA

von Indien

Promotionskomitee

Prof. Dr. Christoph Renner (Vorsitz)

Prof. Dr. Gabriele Schoedon-Geiser

Prof. Dr. Christian Münz

Zürich, 2015

1. PREFACE

The work of this PhD thesis was performed at the Inflammation Research Unit, Division of Internal Medicine, University Hospital of Zurich. This work is a part of the project number 31-124861 of Swiss National Science Foundation.

The aim of this thesis was to investigate novel mechanisms of inflammation in response to the emerging inflammatory mediators Wnt5A and IL-4 in human vascular endothelial cells.

The data of this study are presented in the form of following manuscripts submitted for publication.

1. **Wnt5A/Ryk Signaling Critically Affects Barrier Function in Human Vascular Endothelial Cells**
   Tom Skaria, Esther Bachli, Gabriele Schoedon

2. **IL-4 Causes Hyperpermeability of Vascular Endothelial Cells through Wnt5A Signaling**
   Tom Skaria, Julia Burgener, Esther Bachli, Gabriele Schoedon

TABLE OF CONTENTS

2. ABBREVIATIONS

AJ	Adherens junctions
CAM	Cell adhesion molecules
CAMKII	Calmodulin dependent protein kinase II
CFL	Cofilin
ECIS	Electric cell-substrate impedance sensing
Fzd	Frizzled
GO	Gene ontology
GPCRs	G-protein-coupled receptors
HCAEC	Human coronary artery endothelial cells
HUVEC	Human umbilical vein endothelial cells
IEJ	Inter-endothelial junctions
LIMK	LIM kinase
PCP	Planar cell polarity
ROCK	Rho-associated protein serine/threonine kinase
RTKs	Receptor tyrosine-protein kinases
sFRP	secreted Frizzled related protein
SIR	Systemic inflammatory response
TEER	Trans-endothelial electric resistance
T_H2 cell	Type 2 helper T cell
TLR	Toll-like receptor
WIF	Wnt inhibitory factor

3. ZUSAMMENFASSUNG

Bei schwerer Sepsis und septischem Schock kommt es zu einer systemischen Entzündungsreaktion (systemic inflammatory response SIR) durch die grosse Anzahl von Zytokinen, welche infolge der Kommunikation zwischen aktivierten Immunzellen und Gefässendothelzellen freigesetzt werden. Die mit der SIR assoziierte Endotheldysfunktion ist der Auslöser für eine schwere Leckage der Gefässe und die Bildung von systemischen Gewebsödemen. Sepsis und Septischer Schock sind noch immer die häufigste Todesursache auf der Intensivstation. Es besteht ein grosser Bedarf an wirksamen Therapien, denn die Blockade der „klassischen Entzündungsmediatoren“ wie TNF-α und IL-1β konnte das Ueberleben der Patienten nicht verbessern. Andere Therapieversuche waren ebenfalls erfolglos. Vor kurzem entdeckte man hohe Konzentrationen von Wnt5A im Serum und Knochenmark von Patienten mit SIR und septischem Schock. Wnt5A, ein neues Chemokin, wird von menschlichen Makrophagen durch Aktivierung des Toll-like Rezeptors freigesetzt und ist massgeblich beteiligt an der Aufrechterhaltung der Entzündungsantwort dieser Zellen. Wie Wnt5A auf humane Gefässendothelzellen wirkt ist jedoch noch nicht bekannt. Mikrovaskuläre Leckage als Folge gestörter endothelialer Barrierefunktion tritt häufig bei Typ2 T-Helferzell abhängigen allergischen Entzündungsreaktionen auf. IL-4, ein aus Typ2 T-Helferzellen stammendes Zytokin mit inflammatorischen Eigenschaften, beeinträchtigt die Funktion der endothelialen Barriere. Allerdings ist auch über den effektiven Mechanismus der IL-4 abhängigen Endotheldysfunktion wenig bekannt.

Ziele der vorliegenden Arbeit sind (1) Die Prozesse und Signalwege zu identifizieren welche durch Wnt5A in humanen Gefässendothelien aus Koronararterien (HCAEC) reguliert werden, (2) Die Effektoren und den Mechanismus zu identifizieren welcher die Barrierefunktion in IL-4 behandelten Gefässendothelzellen beeinträchtigt.

Mittels systembiologischer Vorgehensweise fanden wir, dass Wnt5A in HCAEC überwiegend Gene und Pathways beeinflusst, welche massgeblich beteiligt sind an der Bildung des Aktinzytoskeletts. Wnt5A beeinflusst die Rho-assoziierte Protein- Serin/Threonin- Kinase (ROCK), welche durch Phosphorylierung LIM-Kinase (LIMK)-2 aktiviert und diese wiederum den Aktin-Depolymerisierungsfaktor Cofilin (CFL)-1 deaktiviert. Durch Anfärbung von Aktinfasern in lebenden Zellen zeigte sich, dass Wnt5A-behandelte HCAEC wegen der gestörten Depolymerisierung vermehrt Aktin- Stressfasern bilden. Dies konnte durch WIF-1, den Ryk-Rezeptor spezifischen Wnt-Antagonisten, verhindert werden. Ausserdem wurden durch Wnt5A die zellulären Adhäsionsverbindungen über b-Catenin und VE- Cadherin gestört, was zu Lücken

zwischen den Zellen in HCAEC Monolayers führte. Kontinuierliche Messung des transendothelialen Widerstandes in lebenden Zellen wies auf erhöhte Permabilität der Wnt5A-behandelten HCAEC Monolayers hin. Knock-down des Ryk-Rezeptors konnte dies verhindern. Diese Daten deuten darauf hin, dass Wnt5A hauptsächlich Prozesse reguliert, die für die Gestaltung des Zytoskeletts in HCAEC verantwortlich sind. Wnt5A, welches während einer systemischen Entzündungsreaktion von aktivierten Immunzellen freigesetzt wird, könnte somit für die Störung der endothelialen Barrierefunktion verantwortlich sein.

Differentielle Genexpressionsanalyse von IL-4 behandelten HCAEC zeigte überraschenderweise, dass Wnt5A eines der am höchsten hochregulierten Gene ist. Die ontologische Gruppierung der Gene in entsprechenden Pathways zeigte, dass die signifikantesten Pathways diejenigen sind, welche Gene enthalten, die für die Zytoskelettstruktur verantwortlich sind. Gene, die diesen Pathways gehäuft zugeordnet wurden, waren wiederum *LIMK-2* und *CFL-1*. Nach Behandlung von HCAEC mit IL-4 waren LIMK-2 und CFL-1 phosphoryliert, ein Hinweis auf vermehrte Bildung von Aktin-Stressfasern. Durch Sichtbarmachung der Aktinfasern in lebenden Zellen konnte die erhöhte Stressfaserbildung in IL-4 behandelten HCAEC bestätigt werden. Die Stressfaser-bildung in IL-4 behandelten HCAEC war in Gegenwart von WIF-1 erheblich geringer. Nicht-invasive elektophysiologische Aufzeichnung des Widerstandes in HCAEC Monolayers zeigte, dass die Zellpermeabilität durch IL-4 erhöht wird. Durch spezifisches Silencing der Wnt5A-Epression konnte die Barrierefunktion in IL-4 behandelten HCAEC signifikant verbessert werden. IL-6, welches von IL-4 behandelten HCAEC in grossen Mengen gebildet wird, und von dem man bisher annahm, dass es die Gefässpermeabilität beeinflusst, hatte überraschenderweise keinen Effekt. Durch diese Untersuchung konnte Wnt5A als das Molekül identifiziert werden, welches massgeblich an der erhöhten Gefässpermeabilität beteiligt ist, die durch IL-4 verursacht wird.

Die vorliegende Arbeit weist folglich darauf hin, dass der Wnt5A/Ryk/ROCK Signalweg ein neuer Entzündungspathway ist, welcher unabhängig von proinflammatorischen Zytokinen wie TNF-α und IL-1β die Gefässpermeabilität beeinflusst. Gezielte Angriffspunkte im Wnt5A Signalweg könnten neue therapeutische Möglichkeiten für Patienten mit Sepsis und schweren systemischen Entzündungskrankheiten bieten.

4. SUMMARY

In severe sepsis and septic shock, immune cells and vascular endothelial cells communicate with each other by releasing and responding to an array of pro-inflammatory cytokines and chemokines, thereby provoking a systemic inflammatory response (SIR). SIR associated endothelial dysfunction is the trigger for severe vascular leakage and systemic tissue edema formation. Sepsis/septic shock is still a major cause of death in intensive care. Efficient therapeutic strategies are in demand since blockade of classical inflammatory mediators like TNF-α and IL-1β failed to improve patient survival. Other therapeutic trials were also not successful so far. Recently, high levels of Wnt5A have been detected in sera and bone marrow of patients with severe systemic inflammation and septic shock. Wnt5A is a novel chemokine secreted by Toll-like receptor-activated human macrophages, and is crucially involved in sustaining their inflammatory response. However, the targets and functional effects of Wnt5A on human vascular endothelial cells remain unclear. Microvascular leakage due to endothelial barrier dysfunction is a prominent feature of type 2 helper T cell (T_H2 cell) mediated allergic inflammation. IL-4, a T_H2 cell-derived cytokine with proposed inflammatory properties impairs the barrier function of vascular endothelial cells. However, the effector mechanism responsible for IL-4-induced endothelial barrier dysfunction remains poorly defined.

The present study aims to (1) identify the targets and processes regulated by Wnt5A signaling in human coronary artery endothelial cells (HCAEC), (2) identify the effector and the downstream mechanism impairing barrier function in IL-4-activated HCAEC.

By using a systems biology approach, we found that predominant targets of Wnt5A in HCAEC are clusters of genes significantly involved in actin cytoskeleton remodelling. Wnt5A targeted Rho-associated protein serine/threonine kinase (ROCK) to phosphorylate LIM kinase (LIMK)-2 and inactivate the actin depolymerization factor Cofilin (CFL)-1. Live actin staining in Wnt5A-treated HCAEC showed enhanced stress fiber formation in consequence of reduced actin depolymerization that was prevented by Ryk-specific antagonist Wnt inhibitory factor (WIF)-1. Wnt5A disrupted β-catenin and VE-cadherin adherens junctions forming inter-endothelial gaps in HCAEC monolayers. Live recording of trans-endothelial electric resistance revealed increased permeability of Wnt5A-treated HCAEC monolayers that was prevented by knockdown of Ryk. These data indicate that Wnt5A principally regulates the process of cytoskeleton remodelling in HCAEC. Thus Wnt5A released by activated immune cells during systemic inflammatory response might be responsible for endothelial barrier dysfunction.

Differential gene expression profiling in IL-4-treated HCAEC surprisingly identified Wnt5A among the top upregulated genes, and gene ontology pathway clustering revealed that among the top most significant pathways were those containing genes associated with cytoskeleton remodelling. Genes clustered in these pathways were again *LIMK-2* and *CFL-1*. Following IL-4 treatment of HCAEC, LIMK-2 and CFL-1 were phosphorylated, thereby indicating the possibility of actin stress fiber formation. Live imaging of actin proved the enhanced formation of stress fibers in IL-4-treated HCAEC. Stress fiber formation in IL-4-treated HCAEC was notably decreased in the presence of WIF-1. Non-invasive electrophysiologic recording of HCAEC monolayer resistance demonstrated that IL-4 increased the cellular permeability. Specific silencing of Wnt5A expression significantly improved the barrier function of the HCAEC monolayer upon IL-4 treatment. Surprisingly, IL-6 which is generated in large amounts by IL-4-treated endothelial cells and which is supposed to be responsible for IL-4-induced vascular permeability, had no such effect. This study identifies Wnt5A as an effector molecule critically involved in IL-4 mediated vascular hyperpermeability.

In conclusion, the present study reveals Wnt5A/Ryk/ROCK signaling as a novel inflammatory pathway that affects vascular permeability independent of the pro-inflammatory cytokines TNF-α and IL-1β. Targeting Wnt5A signaling could provide novel therapeutic options for patients with sepsis and severe systemic inflammatory diseases.

5. INTRODUCTION

5.1 Inflammation and sepsis

Inflammation is a pathophysiological process that develops in response to different stimuli such as infections or tissue injury. It involves the coordinated movement of blood leucocytes and plasma components to the site of infection or injury to minimize tissue damage, thereby providing an early protection to the host. Inflammatory responses caused by microbial infections are well characterized and involve the following mechanisms. Firstly, the innate immune receptors such as nucleotide-binding oligomerization-domain protein (NOD)-like receptors and Toll-like receptor (TLR) present on host mast cells and tissue resident macrophages recognize structures on microbial cells. These microbial structures belong to two major classes; the pathogen-associated molecular patterns (PAMPs) and virulence factors. PAMPs are present in all microorganisms while virulence factors are carried by only pathogens. The binding of these microbial structures by TLR and NOD-like receptors activate macrophages and mast cells, resulting in the production of various inflammatory mediators including tissue factor (TF), cytokines, chemokines, proteolytic enzymes, complement components, eicosanoids, platelet activating lipid factors, vasoactive peptides and vasoactive amines [1]. These mediators along with complement components (eg.C5a) function via autocrine and paracrine signaling to further activate tissue resident macrophages, monocytes and endothelial cells. For example, macrophages challenged with bacterial lipopolysaccharide (LPS) secrete pro-inflammatory cytokines including TNF-α and IL-1β. These pro-inflammatory cytokines paracrinically act on the local endothelial cells and activate them to upregulate the expression of inflammatory mediators like IL-6, IL-8 and MCP-1 [2] and cell adhesion molecules (CAM).

Sepsis/septic shock is defined as a severe systemic inflammatory response (SIR) to an infectious agent. Clinically, severe SIR also occurs without any obvious infection upon heavy trauma, in cancer, and in states of autoimmune inflammation. Prominent symptoms are rapid rise of body temperature accompanied by drop of systemic blood pressure, persistent hypotension despite fluid resuscitation [3], leucocytosis, thrombocytopenia, disseminated coagulation, hypoxemia, tachycardia and tachypnea, oliguria due to renal failure, metabolic acidosis, and finally organ failure and death. Still, septic shock is the major cause of death in intensive care units with mortality rates ranging from 40 to 70% [3]. A major symptom related with SIR is severe vascular leakage causing systemic tissue edema formation. Dysfunction of the vascular endothelium is suggested to be the major reason for vascular leakage during severe systemic inflammation and sepsis. Therapeutic trials targeting the prototypic

inflammatory mediators TNF-α and IL-1β have not been successful in treating sepsis and septic shock [4]. The effectors and associated molecular mechanisms responsible for endothelial dysfunction and consequent tissue edema formation in sepsis still remain not fully understood.

5.2 Endothelial cells

The vessel wall of arteries and veins is composed of three layers. The innermost layer is called intima which is constantly exposed to the blood flow as well as to cellular and soluble blood components. The vascular endothelial cells are located in this intima where they attach together at intercellular junctions and form a continuous monolayer to line up the blood vessels [5]. Vascular smooth muscle cells form the middle layer called media [6]. The media is separated from the endothelial and the outer adventitia layers by elastic lamina [7]. The adventitia is composed of fibroblasts, small capillaries, lymphatic vessels, nerves, endothelial progenitor cells and immune cells such as macrophages and dendritic cells [7]. The walls of tiny capillaries are composed of endothelial cells surrounded by basal lamina and few pericytes (Figure 1).

The vascular endothelial cells play an important role in maintaining vascular homeostasis. They preserve blood fluidity [8,9], control blood pressure, prevent the adherence of leucocytes [8] and platelets [9] and regulate vascular permeability [8]. Endothelial cells control coagulation through the surface expression of tissue factor pathway inhibitors such as heparin sulphate proteoglycans and thrombomodulin. Moreover, resting endothelial cells retain the von Willebrand factor in their storage granules called Weibel-Palade bodies (WPBs), thus preventing interaction between endothelial membrane and platelets [8].

Endothelial cells control blood pressure by secreting a number of vasodilator and vasoconstrictor mediators that increase and decrease the tone of the neighboring smooth muscle cell layers. Among such endothelium-derived mediators, nitric oxide acts as a vasodilator whereas endothelin type-1 acts as a vasoconstrictor for smooth muscle cells [9].

Under resting conditions, endothelial cells mask leucocyte interaction proteins such as chemokines and CAM like P-selectin by storing them in WPBs. Moreover, the expression of other CAM like VCAM-1, E- selectin and ICAM-1 are suppressed. This prevents the adherence of leucocytes to resting endothelial cells [8].

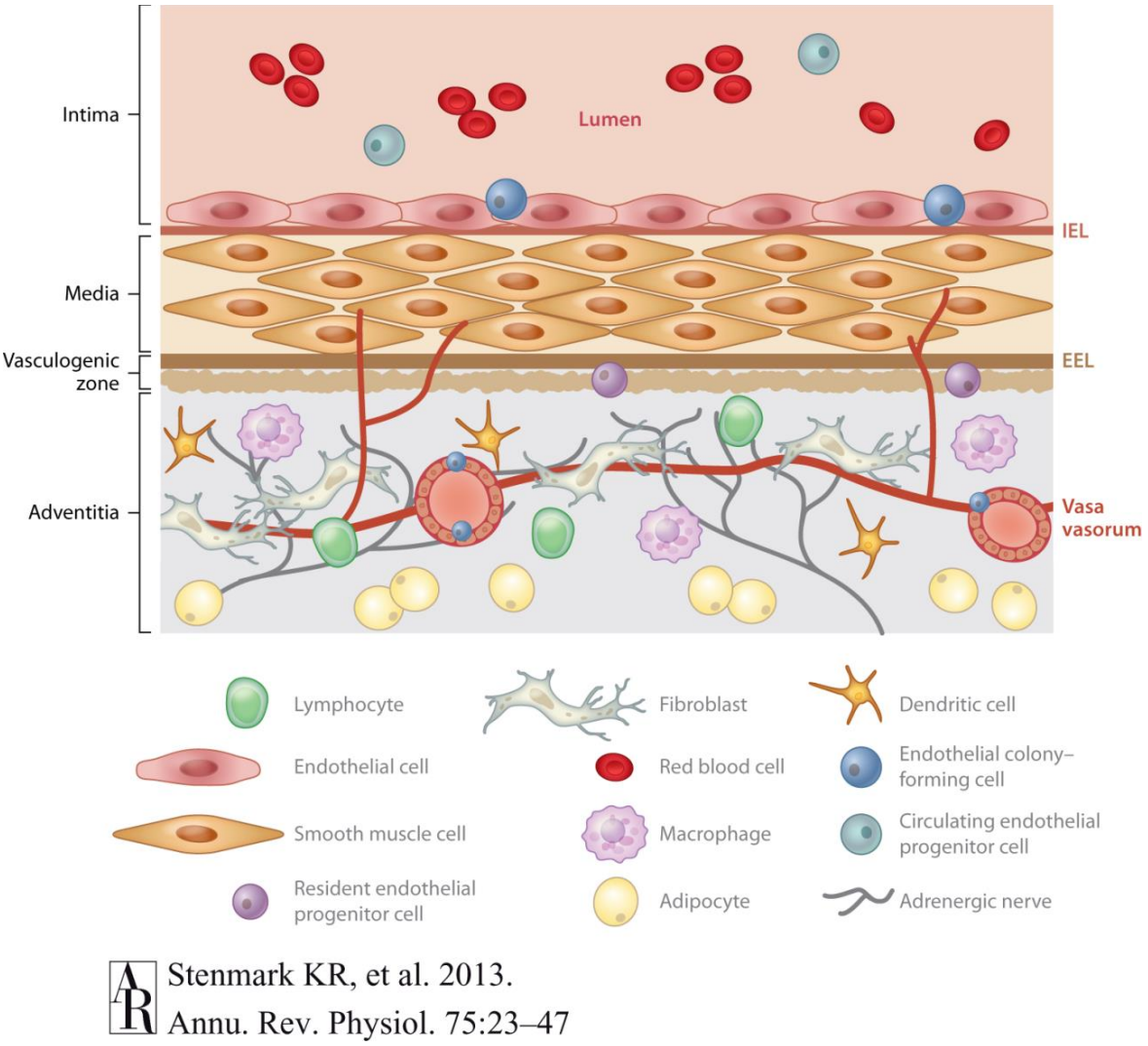

Figure 1. Composition of the vascular wall. IEL, internal elastic lamina; EEL, external elastic lamina. Figure adapted and modified from reference [7].

Under physiological conditions, endothelial cells tightly control vascular permeability with the aid of ion channels and intercellular junction proteins. The free efflux of liquid, plasma proteins and blood cells to the underlying interstitial space and tissues are restricted. Thus, endothelial cells act as a semipermeable barrier that maintains the selective passage of blood components at a low rate.

Endothelial cells from different parts of the vascular system exhibit different phenotypic characteristics. It means that even endothelial cells from different anatomic sites within the same individual express different receptors and surface antigens and produce different responses to identical stimuli [9].

5.2.1 Structural components of endothelial barrier

The barrier function of endothelial cells depends on the integrity of the structure that comprises of endothelial cell cytoskeleton, intercellular junction complexes, and cell attachments to basement membrane and extracellular matrix [10].

Endothelial cytoskeleton

Endothelial scaffold structures are microtubules, intermediate filaments and actin filaments. Among these, actin filaments represent the most important cytoskeletal structure to regulate endothelial permeability. Actin filaments are polymers of filamentous actin (F-actin) arranged in a linear fashion. Their stability is highly dependent upon the concentration of intracellular globular actin (G-actin). G-actin monomers polymerize to form F-actin filaments when the intracellular concentration of G-actin reaches above the critical concentration of 0.1 μM. Under physiological conditions, actin filaments are irregularly scattered all over the cell and even located at the cellular periphery as cortical actin. Signaling proteins such as Rho family GTPases (RhoA, Rac1 and Cdc42) modify the arrangement of the actin cytoskeletal network and generate specialized structures such as actin stress fibers or cortical actin [10]. Stress fibers are contractile actomyosin polymers with inverted polarity which are also linked to α-actinin [11]. Actin cytoskeleton rearrangement and stress fiber formation increase endothelial permeability through mechanisms that are still not fully elucidated [10] .

Microtubules are tubular polymers composed of dimers of alpha- and beta-tubulin subunits. The microtubule consists of 13 polymeric filaments which are arranged in parallel to form a ring. As microtubules are crosslinked to actin filaments in endothelial cells, they alter endothelial permeability via mechanisms involving actin filaments. Stabilization of microtubules by polymerization inhibits actin stress fiber formation and hyperpermeability in endothelial cells. On the other hand, depolymerization of microtubules increases actin stress fiber formation, possibly through activation of guanine nucleotide exchange factors and Rho family GTPases like RhoA [10]. Intermediate filaments are composed of protein polymers, especially those of vimentin.

Endothelial intercellular junction complexes

The endothelial intercellular junction complexes or inter-endothelial junctions (IEJ, also referred as inter-endothelial adhesions) in microvascular endothelial cells are of mainly two types, the adherens junctions (AJ) and tight junctions (TJ). AJ represent the most common endothelial cell-cell junctions found in microvascular endothelial cells including peripheral microvascular endothelial cells. AJ are impermeable to larger proteins such as albumin and thus act as

barriers to prevent the passage of macromolecules into tissues and organs. AJ are mainly composed of the transmembrane receptor protein VE-cadherin. The extracellular domain of VE-cadherin of one endothelial cell binds to the extracellular domain of another VE-cadherin expressed on the membrane of an adjacent cell. This forms a seal that prevents the passage of molecules through the inter-endothelial space. The intracellular domain of VE-cadherin is connected to the actin cytoskeleton with the help of catenin family of proteins such as α-, β-, γ- and p120-catenins. A proper assembly and maintenance of VE-cadherin-catenin-actin cytoskeleton complex is highly essential for preserving the structural integrity and function of endothelial barriers. In comparison with AJ, there is little expression of tight junction proteins in peripheral microvascular endothelial cells. TJ composed of proteins such as claudins, occludins and junctional adhesion molecule-A are commonly found in the microvascular endothelial cells of specialized tissues such as blood retinal or blood brain barriers [10].

Endothelial focal adhesions

Focal adhesions attach endothelial cells to their basement membrane. Focal adhesions are small regions in the basolateral membrane, composed of transmembrane receptors called integrins. Integrins are normally present as heterodimers of α- and β- subunits. The intracellular domain of integrins is associated with the actin cytoskeleton with the help of linker proteins such as α-actinin, talin, vinculin or paxillin. They are also able to associate with the actin cytoskeleton directly and function independent of linker proteins. The extracellular domain of integrins binds to matrix proteins such as fibronectin, fibrinogen and vitronectin lodged in the laminin and collagen fibers of endothelial basement membrane. Focal adhesions keep the endothelial cells attached to the substratum and preserve endothelial barrier integrity [10]. Focal adhesion disassembly is regulated by RhoA through the activation of its downstream target Rho-associated protein serine/threonine kinase (ROCK). Activation of ROCK leads to the activation of LIM kinase (LIMK) by phosphorylation, which in turn phosphorylates cofilin (CFL). Phosphorylation inactivates CFL and favours the stabilization of filamentous actin contained within the actomyosin bundles [11].

5.3 Endothelial response in severe systemic inflammation and sepsis

The functions of endothelial cells are heavily altered in diseases like severe systemic inflammation and sepsis [9]. These alterations include a change from the anticoagulant phenotype to a procoagulant state, increased production of vasoactive substances, expression of CAM, and the synthesis of inflammatory mediators including chemoattractants. The

endothelium at this stage is said to be activated. The pro-inflammatory cytokines TNF-α and IL-1 secreted by activated leucocytes act as the prototypic mediators of endothelial activation. The binding of these pro-inflammatory cytokines to their corresponding receptors on endothelial cells initiate signaling mechanisms that activate mitogen-kinase kinase kinases (MAPKKKs). Activated MAPKKKs trigger the pathways activating the transcription factors nuclear factor-kappa-light-chain-enhancer of activated B cells κB (NF-κB) and activator protein-1 (AP-1). The activated transcription factors turn on the gene expression of CAM and pro-inflammatory proteins (Figure 2). The CAM expressed on activated endothelial cells, E-selectin, ICAM-1 and VCAM-1 promote the recruitment and adhesion of leucocytes to endothelial cells. The pro-inflammatory mediators include cytokines such as IL-6, chemokines such as IL-8 and MCP-1, enzymes such as cyclooxygenase-2 (COX-2) and effector proteins that are responsible for the rearrangements of actin filaments [8]. Cytokines such as IL-6 and chemokines act on leucocytes and facilitate their recruitment to inflamed tissue. COX-2 aids the biosynthesis of prostaglandin-I_2 to raise the blood pressure. Actin filament rearrangements disrupt IEJ [8] and might induce endothelial barrier dysfunction. But the exact mechanisms mediating these rearrangements remain still unidentified.

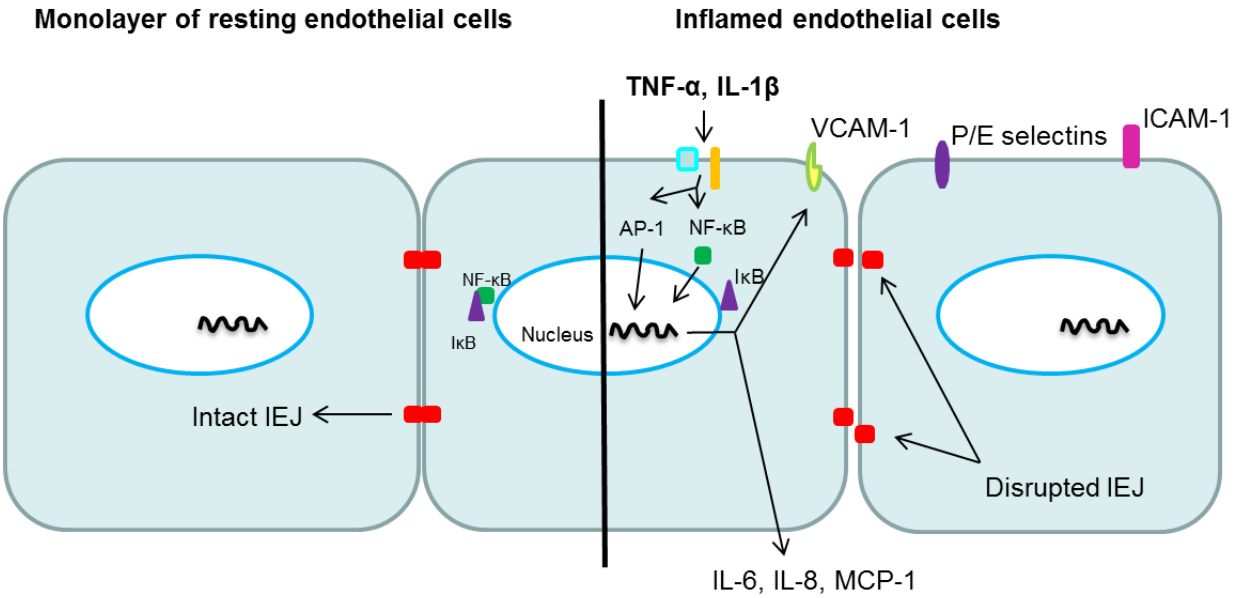

Figure 2. Phenotypic changes in resting and activated vascular endothelial cells. Left side: vascular endothelial cells forming a tight cell-cell contact under resting conditions. Right side: activated endothelial cells showing upregulated expression of CAM and chemokines followed by disruption of inter-endothelial contacts. IEJ, inter-endothelial junction.

5.3.1 IL-4 signaling

Activation of the vascular endothelium is also associated with cytokines such as IL-4, secreted by type 2 helper T cell (T_H2 cell) population. IL-4 is a multifunctional cytokine that has crucial roles in the regulation of homeostasis and pathogenesis of diseases. Although activated T_H2 cells represent the major source of IL-4, it is also produced by basophils, eosinophils and mast cells [12]. IL-4 can bind to two different cell surface receptor complexes known as type I IL-4R and type II IL-4R. Type I IL-4R is composed of IL-4Rα and γc chains and mainly found in hematopoietic cells. Type II IL-4R is expressed by both hematopoietic and non-hematopoietic cells and formed of IL-4Rα and IL-13Rα1 chains. The subunits of both IL-4 receptor complexes are constitutively associated with members of Janus protein kinases (Jaks) family such as Jak1 (IL-4Rα), Jak2 (IL-13Rα1) and Jak3 (γc chain). Activation of Jaks followed by ligand-receptor interaction causes tyrosyl phosphorylation and dimerization of signal transducer and activator of transcription 6 (STAT6). STAT6 is then transported to the nucleus to activate the expression of IL-4 responsive genes [13].

IL-4 triggers functionally different intracellular signaling mechanisms by binding to alternative receptors [12]. It induces the differentiation of antigen encountered naïve T cells to form mature effector T_H2 cells capable of producing IL-4 and a number of other cytokines such as IL-5 and IL-13. It regulates immunoglobulin (Ig) class switching so that human B cells express IgE and IgG4 [14]. IL-4 induces the “alternative activation” of macrophages to form a group of highly specialized cells called M2 macrophages, the latter playing important roles in inflammation, parasite clearance and tissue repair [12]. Through its effects on multiple cell types, IL-4 plays critical roles in allergic inflammation including allergen-induced asthma, anaphylaxis and rhinitis [15], immune response to extracellular parasites, autoimmunity [14], and tumor inflammation and metastasis [12].

In vascular endothelial cells, IL-4 upregulates the expression of IL-6 and MCP-1 [16,17]. It induces endothelial cells to express VCAM-1 [17,18] that facilitates the adhesion of peripheral blood monocytes [19] and T cells to endothelial cells [20]. Further, IL-4 enhances endothelial permeability. Edema formation resulting from vascular leakage is an important symptom in allergy [21] and autoimmune inflammation. However, the effectors responsible for IL-4-induced endothelial barrier dysfunction remain so far unidentified.

5.3.2 Endothelial barrier dysfunction and vascular leakage

Endothelial barrier dysfunction causes increased efflux of plasma through the vessel wall into the neighboring tissues, leading to the formation of protein-rich tissue edema. Small molecules

and activated leucocytes can pass the endothelial monolayer either through transcellular or paracellular routes. Transcellular passage of proteins is supported by caveolae vesicles. Paracellular passage of leukocytes involves the IEJ. The permeability of the IEJ is dependent on the assembly of the adhesion proteins that constitute IEJ.

Inflammatory mediators increase endothelial permeability through the activation of RhoA/ROCK and its downstream target LIMK. When activated by ROCK-mediated phosphorylation, LIMK phosphorylates the actin deploymerization factor CFL-1. Phosphorylation inactivates CFL-1 and prevents its ability to depolymerize actin filaments leading to the formation of contractile actin stress fibers. The contractile force stretches VE-cadherin inward, requiring a VE-cadherin extracellular domain of one cell to detach from the VE-cadherin extracellular domain of a neighboring cell, forming inter-endothelial gaps [22]. The exact mechanisms are, however, still not well defined.

5.4 Wnts and their signaling mechanisms

Wnts constitute a large family of secreted lipid modified signaling proteins [23-25] that are potent regulators of multiple biological processes such as cell proliferation, cell fate decision and differentiation during embryogenesis and adult homeostasis, and immune responses [26,27]. In mammals, there are 19 genes coding for Wnt proteins [28]. Frizzled (Fzd) proteins are generally suggested to function as receptors for Wnts [26,29]. Wnts function through either the β-catenin dependent canonical pathway or the β-catenin independent non-canonical pathway, the latter being also referred as Wnt/planar cell polarity (PCP) pathway [29].

Canonical Wnt signaling

Canonical Wnt signaling is transduced mainly through Fzd receptors. Fzd receptors belong to the family of G-protein-coupled receptors (GPCRs) [29] and consist of a seven-pass transmembrane region and an extracellular cysteine-rich domain (CRD) homologous to the natural Wnt antagonist, secreted Frizzled related protein (sFRP)-1 [30]. A featured event in canonical Wnt signaling is an increase in cytoplasmic levels of β-catenin, followed by its translocation into the nucleus to regulate gene expression [25]. When Wnt ligands are absent, adenomatous polyposis coli (APC), glycogen synthase kinase 3 (GSK3), the scaffolding protein axin 1, casein kinase I (CKI) and others form a destruction complex. This destruction complex phosphorylates free β-catenin which is not bound to cadherin. The phosphorylated β-catenin gets ubiquitinated and is subsequently targeted for degradation by 26S proteasome, thereby maintaining β-catenin at low levels in resting cells [29,31]. Simultaneously, transcriptional

repressors like transducin-like enhancer proteins (TLEs) bind to DNA binding proteins of the T cell factor (TCF) and lymphoid enhancer-binding factor 1 (LEF1) in the nucleus, leading to the repression of Wnt target genes. Following interaction of a Wnt ligand with Fzd receptor-LRP6 co-receptor complexes, the conformation of LRP6 co-receptor is changed leading to phosphorylation of the co-receptor. This in turn activates G proteins as well as dishevelled proteins, thereby enabling the recruitment of axin 1 to the co-receptor to induce disruption of the destruction complex. As a result, β-catenin increases in the cytoplasm which then translocates to nucleus and interacts with TCF or LEF1. This interaction dissociates TLE repressors from TCF and LEF1 and thus activates the transcription of number genes including MYC and axin 2. Axin 2 aids the assembly of more destruction complexes and thus functions as a feedback inhibitor to the signaling [31]. The sequence of events involved in canonical Wnt signaling is shown in Figure 3. Two examples of canonical Wnt ligands which signal through β-catenin are Wnt3A and Wnt8A [31]. In contrast, Wnt5A has been suggested to repress or inhibit β-catenin dependent canonical Wnt signaling.

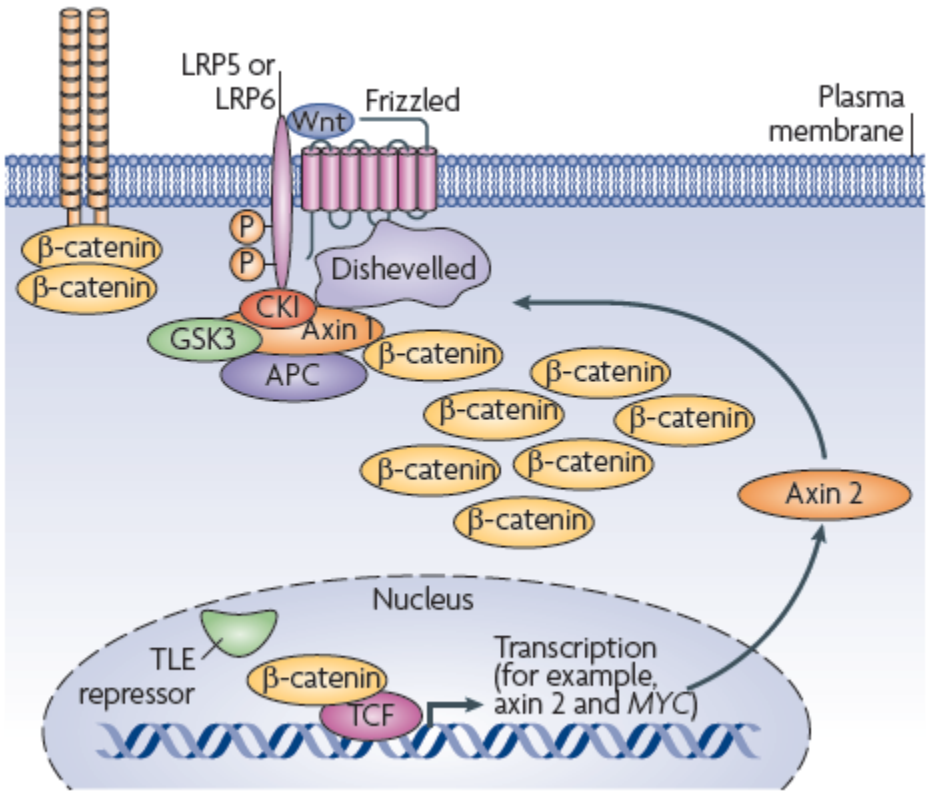

Figure 3. Canonical Wnt signaling. Interaction of Wnt with receptor releases β-catenin from the degradation complex. Gene transcription is activated following translocation of free β-catenin from cytoplasm to nucleus. Figure adapted and modified from reference [31].

Non-canonical Wnt signaling

Canonical Wnt signaling has been extensively studied while Wnt/PCP signaling still remains poorly understood with different β-catenin independent pathways existing in parallel [28,31]. The non-canonical Wnt signaling pathways involve either Fzd receptors or non-Fzd receptors such as receptor tyrosine kinase-like orphan receptor-2 (Ror2) and Ryk [29]. One branch is the Wnt/Ca^{2+} pathway and involves an increase in intracellular Ca^{2+} levels through the activation of phospholipase C (PLC). The Ca^{2+} flux in turn activates calmodulin-dependent protein kinase II (CAMKII), protein kinase C (PKC), and the nuclear factor of activated T cells (NFAT) transcription factor [29,31]. This pathway has been reported to be involved in dorsoventral patterning and separation of tissues in embryos and inhibition of Wnt3/β-catenin signaling. Recently, CAMKII activation was identified as an essential part of inflammatory Wnt5A/Fzd5 signaling in human macrophages [26]. Another branch of Wnt/PCP pathway involves the activation of Rho which through the regulation of ROCK mediate actin remodelling [29] and alter cytoskeleton arrangement [31]. Wnt4, Wnt5A and Wnt11 are generally classified as non-canonical Wnts [31]. Suggested pathways involved in non-canonical Wnt signaling are summarized in Figure 4.

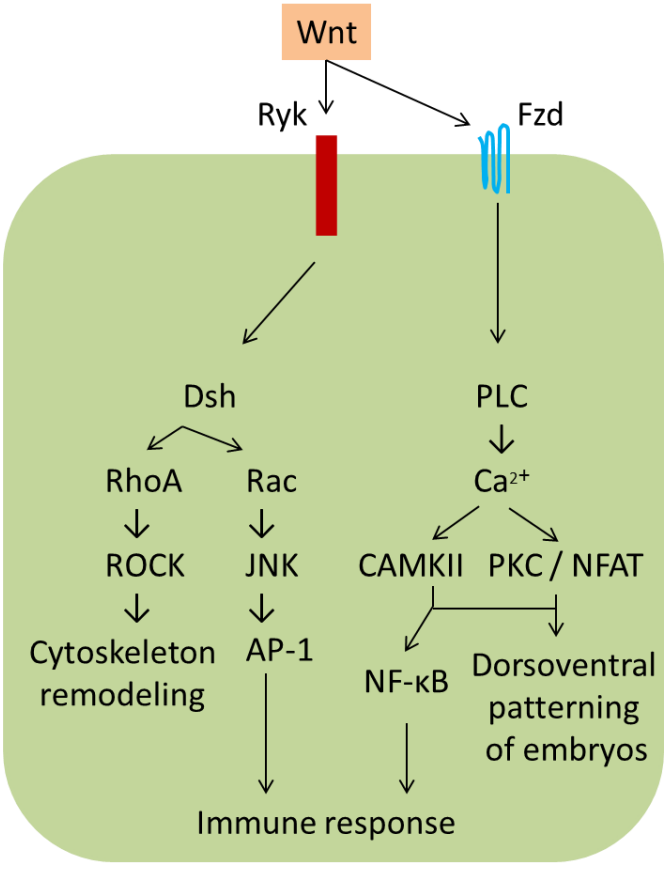

Figure 4. Non-canonical Wnt signaling. Interaction of Wnt with specific receptor leads to activation one of the three downstream pathways involving Rho GTPases, JNK and PLC. The type of cellular processes regulated depends on the downstream pathway involved. Dsh, dishevelled.

Receptor tyrosine-protein kinases

Wnts can function through transmembrane tyrosine kinase family members called Ror2 and Ryk. Ror2 belongs to the family of the Ror family of receptor tyrosine-protein kinases (RTKs) [32]. Ror2 is distinguished as receptor or co-receptor for Wnt5A and can regulate different Wnt5A signaling pathways by acting alone or in combination with Fzd receptors. Ror2 contains an extracellular CRD domain similar to the extracellular Wnt binding domain of Fzd receptors and sFRP [30], and activates intracellular signaling pathways in response to Wnt5A [28,33]. Wnt5A/Ror2 non-canonical signaling has been described to inhibit canonical Wnt signaling and to play important roles in polarized cell migration [29,32], tumor growth, invasion and metastasis [32].

Ryk is a member of the family of atypical RTKs. It is composed of an extracellular Wnt binding domain, a transmembrane domain and an intracellular kinase domain (Figure 5). Its extracellular domain is glycosylated and is homologous to the endogenous Wnt antagonist Wnt inhibitory factor (WIF)-1. The intracellular kinase domain of Ryk, unlike other members of RTK, is atypical because it lacks tyrosine kinase activity [34] due to the presence of mutations in its evolutionarily conserved tyrosine kinase regions [35]. Therefore, the precise mechanisms by which signals are transmitted from the cell surface to the intracellular compartment upon interaction of Ryk with Wnt ligands remain still unknown. It has been suggested that Ryk signaling activates MAPK pathway [36]. Ryk is overexpressed in epithelial ovarian cancer [37,38].

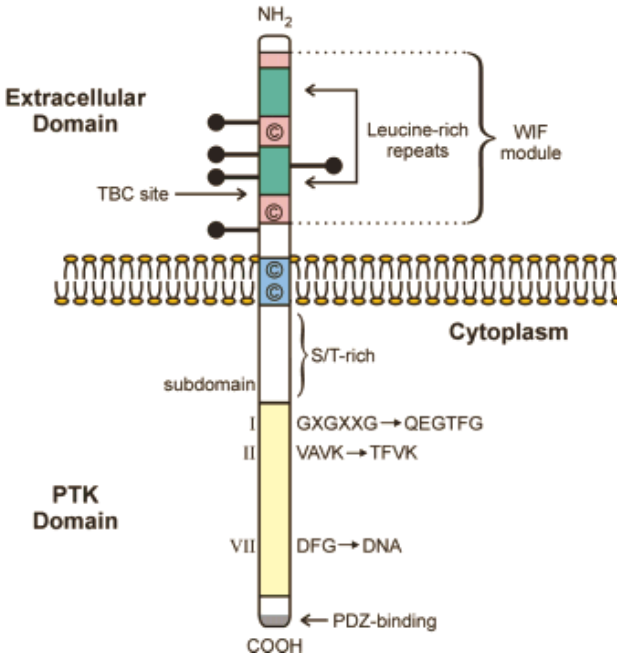

Figure 5. Structure of Ryk receptor. The extracellular domain is composed of a Wnt inhibitory factor (WIF) module containing two cysteine residues (pink) that surround a tetrabasic cleavage site (TBC site), two leucine-rich repeats (green), and many putative N-linked sites for adding carbohydrates (black sticks). The transmembrane region is composed of tandem cysteine residues. The intracellular domain is composed of a juxtamembrane serine- and threonine (S/T)-rich sequence (white), a catalytically inactive PTK-like domain and a PDZ-binding motif at the C-terminal end. Figure adapted and modified from [34].

A previous study demonstrated that Wnt5A/Ryk signaling inhibits the growth of adult rat corticospinal axons [39]. Moreover, Derailed, a member of Ryk family of receptors in *Drosophila* has been described to act as a receptor for Wnt5A in axon guidance [40]. Wnt5A signaling through Ryk causes repulsive axon guidance in mammals [41]. Recently, it has been shown that Wnt5A/Ryk suppresses the growth of mouse callosal axons [42]. Evidences are still scant to define the downstream mechanism of Wnt5A/Ryk signaling and how Wnt5A/Ryk signaling differs between non-differentiated and fully differentiated cells in terms of its targets and biological function. In the present thesis, we could define a Wnt5A/Ryk signaling pathway in human vascular endothelial cells, affecting vascular permeability (see chapter 6.1).

5.5 Role of Wnt5A in inflammation

Human Wnt5A is a 49kDa protein encoded by one of the Wnt family of genes located on chromosome 3 (in the region between 3p14-p21) [43]. Wnt5A regulates a number of cellular processes such as adhesion, differentiation, migration, polarity and proliferation and plays pivotal roles in post-natal cell functions, immune responses and developmental process of different organs. This suggests that Wnt5A regulates multiple signaling pathways depending on the availability of specific receptors [43,44] and other mediators of the signaling pathway [44], cellular conditions [43], and the presence of natural inhibitors like sFRP. Evidence indicating a crucial role for Wnt signaling in immune response was initially obtained from studies using a 'septic fly' model. It was demonstrated that WntD, a member of Wnt family of proteins in *Drosophila,* was induced through Toll/NF-κB signaling and regulated innate immune responses to infection. This study proved that mortality rates were higher in flies lacking WntD expression in comparison to flies expressing endogenous WntD. It suggested that under septic conditions, flies deficient of WntD would suffer overstimulated immune responses [45]. A consecutive study demonstrated a functional role for Wnt5A signaling in response to bacterial infections. In that study, human mononuclear cells stimulated with mycobacterial species upregulated Wnt5A and Fzd5 through the activation of Toll/NF-kB signaling. In response to microbial antigenic stimulation, Wnt5A/Fzd5 signaling upregulated the expression of IL-2 and IFN-γ by antigen presenting cells and T cells, respectively [27]. Increased expression of Wnt5A and Fzd5 has been detected in synovial tissues in rheumatoid arthritis [46], and blockade of Wnt5A/Fzd5 signaling prevented the activation of rheumatoid synovial tissues [47]. Moreover, expression of Wnt5A has been detected in the macrophage-rich regions of murine and human atherosclerotic plaques [48] .

Recently, inflammatory Wnt5A signaling in human macrophages was found to be critically involved in severe systemic inflammatory response. Wnt5A protein was highly induced and released upon TLR targeting of macrophages, and was found in substantial quantity in sera of patients with severe sepsis. The study further demonstrated that Wnt5A was capable of sustaining the inflammatory response of macrophages through an autocrine Wnt5A/Fzd5/CAMKII signaling pathway [26]. This study indicates a pivotal role for Wnt5A in inflammation and suggests therapeutic approaches targeting Wnt5A beneficial in treating diseases associated with severe systemic inflammation [49]. Wnt5A is released in substantial amounts from activated macrophages and the vascular endothelium plays an important role in systemic inflammation and septic shock. However, the knowledge of paracrine Wnt5A signaling in vascular endothelial cells is still scant. We addressed this issue in the course of this thesis.

Inflammatory Wnt5A signaling in endothelial cells

A previous study showed that human umbilical vein endothelial cells (HUVEC) treated with a cocktail of TNF-α, IL-1 and IL-8 upregulated the expression of Wnt5A mRNA [50]. As endothelial cells from different vascular environments exhibit functional heterogeneity, Wnt5A signaling in adult vascular endothelial cells may differ from the foetal tissue-derived HUVEC. Another study showed that human aortic endothelial cells (HAEC) treated with Wnt5A expressed pro-inflammatory cytokines such as IL-1, IL-6, and IL-8 [51]. However, the specific targets of Wnt5A in adult human vascular endothelial cells and the precise downstream mechanism by which Wnt5A induces endothelial inflammation have remained unclear.

5.6 Outline of the project

The aim of this thesis was to study the response of human vascular endothelial cells to Wnt5A and IL-4 to define novel mechanisms and signaling pathways of these emerging inflammatory mediators. Following specific aims were addressed:

1. Define all genes and biological processes regulated by Wnt5A signaling in primary human vascular endothelial cells using a standardized genome-wide expression profiling approach.

2. Identify the receptor(s) and the downstream signaling pathways specific for Wnt5A in human vascular endothelial cells.

3. Describe the biological functions of Wnt5A signaling in human vascular endothelial cells.

4. Identify the genes and pathways affecting barrier function in IL-4-activated human vascular endothelial cells using a whole genome transcriptome approach and specific endothelial barrier function assays.

5.7 References

1. Medzhitov R (2008) Origin and physiological roles of inflammation. Nature 454: 428-435.
2. Aird WC (2003) The role of the endothelium in severe sepsis and multiple organ dysfunction syndrome. Blood 101: 3765-3777.
3. Russell JA (2006) Management of Sepsis. New England Journal of Medicine 355: 1699-1713.
4. Hotchkiss RS, Karl IE (2003) The Pathophysiology and Treatment of Sepsis. New England Journal of Medicine 348: 138-150.
5. Sandoo A, van Zanten JJCSV, Metsios GS, Carroll D, Kitas GD (2010) The Endothelium and Its Role in Regulating Vascular Tone. The Open Cardiovascular Medicine Journal 4: 302-312.
6. Pacilli A, Pasquinelli G (2009) Vascular wall resident progenitor cells: a review. Exp Cell Res 315: 901-914.
7. Stenmark KR, Yeager ME, El Kasmi KC, Nozik-Grayck E, Gerasimovskaya EV, et al. (2013) The adventitia: essential regulator of vascular wall structure and function. Annu Rev Physiol 75: 23-47.
8. Pober JS, Sessa WC (2007) Evolving functions of endothelial cells in inflammation. Nat Rev Immunol 7: 803-815.
9. Galley HF, Webster NR (2004) Physiology of the endothelium. British Journal of Anaesthesia 93: 105-113.
10. Yuan SY RR (2010) Regulation of Endothelial Barrier Function. . San Rafael (CA): Morgan & Claypool Life Sciences.
11. Lamalice L, Le Boeuf F, Huot J (2007) Endothelial cell migration during angiogenesis. Circ Res 100: 782-794.
12. Luzina IG, Keegan AD, Heller NM, Rook GA, Shea-Donohue T, et al. (2012) Regulation of inflammation by interleukin-4: a review of "alternatives". J Leukoc Biol 92: 753-764.
13. Chatila TA (2004) Interleukin-4 receptor signaling pathways in asthma pathogenesis. Trends Mol Med 10: 493-499.
14. Nelms K, Keegan AD, Zamorano J, Ryan JJ, Paul WE (1999) The IL-4 receptor: signaling mechanisms and biologic functions. Annu Rev Immunol 17: 701-738.
15. Li-Weber M, Krammer PH (2003) Regulation of IL4 gene expression by T cells and therapeutic perspectives. Nat Rev Immunol 3: 534-543.
16. Colotta F, Sironi M, Borre A, Luini W, Maddalena F, et al. (1992) Interleukin 4 amplifies monocyte chemotactic protein and interleukin 6 production by endothelial cells. Cytokine 4: 24-28.

17. Lee YW, Eum SY, Chen KC, Hennig B, Toborek M (2004) Gene expression profile in interleukin-4-stimulated human vascular endothelial cells. Mol Med 10: 19-27.
18. Beekhuizen H, Verdegaal EM, Blokland I, van Furth R (1992) Contribution of ICAM-1 and VCAM-1 to the morphological changes in monocytes bound to human venous endothelial cells stimulated with recombinant interleukin-4 (rIL-4) or rIL-1 alpha. Immunology 77: 469-472.
19. Luscinskas FW, Kansas GS, Ding H, Pizcueta P, Schleiffenbaum BE, et al. (1994) Monocyte rolling, arrest and spreading on IL-4-activated vascular endothelium under flow is mediated via sequential action of L-selectin, beta 1-integrins, and beta 2-integrins. J Cell Biol 125: 1417-1427.
20. Thornhill MH, Kyan-Aung U, Haskard DO (1990) IL-4 increases human endothelial cell adhesiveness for T cells but not for neutrophils. J Immunol 144: 3060-3065.
21. Kotowicz K, Callard RE, Klein NJ, Jacobs MG (2004) Interleukin-4 increases the permeability of human endothelial cells in culture. Clin Exp Allergy 34: 445-449.
22. Vandenbroucke E, Mehta D, Minshall R, Malik AB (2008) Regulation of endothelial junctional permeability. Ann N Y Acad Sci 1123: 134-145.
23. Willert K, Brown JD, Danenberg E, Duncan AW, Weissman IL, et al. (2003) Wnt proteins are lipid-modified and can act as stem cell growth factors. Nature 423: 448-452.
24. Nelson WJ, Nusse R (2004) Convergence of Wnt, beta-catenin, and cadherin pathways. Science 303: 1483-1487.
25. Pereira CP, Bachli EB, Schoedon G (2009) The wnt pathway: a macrophage effector molecule that triggers inflammation. Curr Atheroscler Rep 11: 236-242.
26. Pereira C, Schaer DJ, Bachli EB, Kurrer MO, Schoedon G (2008) Wnt5A/CaMKII signaling contributes to the inflammatory response of macrophages and is a target for the antiinflammatory action of activated protein C and interleukin-10. Arterioscler Thromb Vasc Biol 28: 504-510.
27. Blumenthal A, Ehlers S, Lauber J, Buer J, Lange C, et al. (2006) The Wingless homolog WNT5A and its receptor Frizzled-5 regulate inflammatory responses of human mononuclear cells induced by microbial stimulation. Blood 108: 965-973.
28. van Amerongen R, Mikels A, Nusse R (2008) Alternative wnt signaling is initiated by distinct receptors. Sci Signal 1: re9.
29. Angers S, Moon RT (2009) Proximal events in Wnt signal transduction. Nat Rev Mol Cell Biol 10: 468-477.

30. Green J, Nusse R, van Amerongen R (2014) The role of Ryk and Ror receptor tyrosine kinases in Wnt signal transduction. Cold Spring Harb Perspect Biol 6.

31. McNeill H, Woodgett JR (2010) When pathways collide: collaboration and connivance among signaling proteins in development. Nat Rev Mol Cell Biol 11: 404-413.

32. Nishita M, Enomoto M, Yamagata K, Minami Y (2010) Cell/tissue-tropic functions of Wnt5a signaling in normal and cancer cells. Trends Cell Biol 20: 346-354.

33. Mikels AJ, Nusse R (2006) Purified Wnt5a protein activates or inhibits beta-catenin-TCF signaling depending on receptor context. PLoS Biol 4: e115.

34. Halford MM, Stacker SA (2001) Revelations of the RYK receptor. Bioessays 23: 34-45.

35. Lu W, Yamamoto V, Ortega B, Baltimore D (2004) Mammalian Ryk is a Wnt coreceptor required for stimulation of neurite outgrowth. Cell 119: 97-108.

36. Katso RM, Russell RB, Ganesan TS (1999) Functional analysis of H-Ryk, an atypical member of the receptor tyrosine kinase family. Mol Cell Biol 19: 6427-6440.

37. Wang XC, Katso R, Butler R, Hanby AM, Poulsom R, et al. (1996) H-RYK, an unusual receptor kinase: isolation and analysis of expression in ovarian cancer. Mol Med 2: 189-203.

38. Katso RM, Manek S, Biddolph S, Whittaker R, Charnock MF, et al. (1999) Overexpression of H-Ryk in mouse fibroblasts confers transforming ability in vitro and in vivo: correlation with up-regulation in epithelial ovarian cancer. Cancer Res 59: 2265-2270.

39. Miyashita T, Koda M, Kitajo K, Yamazaki M, Takahashi K, et al. (2009) Wnt-Ryk signaling mediates axon growth inhibition and limits functional recovery after spinal cord injury. J Neurotrauma 26: 955-964.

40. Yoshikawa S, McKinnon RD, Kokel M, Thomas JB (2003) Wnt-mediated axon guidance via the Drosophila Derailed receptor. Nature 422: 583-588.

41. Li L, Hutchins BI, Kalil K (2010) Wnt5a induces simultaneous cortical axon outgrowth and repulsive turning through distinct signaling mechanisms. Sci Signal 3: pt2.

42. Clark CE, Richards LJ, Stacker SA, Cooper HM (2014) Wnt5a induces Ryk-dependent and -independent effects on callosal axon and dendrite growth. Growth Factors 32: 11-17.

43. Kikuchi A, Yamamoto H, Sato A, Matsumoto S (2012) Wnt5a: its signaling, functions and implication in diseases. Acta Physiol (Oxf) 204: 17-33.

44. Pukrop T, Binder C (2008) The complex pathways of Wnt 5a in cancer progression. J Mol Med (Berl) 86: 259-266.

45. Gordon MD, Dionne MS, Schneider DS, Nusse R (2005) WntD is a feedback inhibitor of Dorsal/NF-kappaB in Drosophila development and immunity. Nature 437: 746-749.

46. Sen M, Lauterbach K, El-Gabalawy H, Firestein GS, Corr M, et al. (2000) Expression and function of wingless and frizzled homologs in rheumatoid arthritis. Proceedings of the National Academy of Sciences of the United States of America 97: 2791-2796.

47. Sen M, Chamorro M, Reifert J, Corr M, Carson DA (2001) Blockade of Wnt-5A/frizzled 5 signaling inhibits rheumatoid synoviocyte activation. Arthritis Rheum 44: 772-781.

48. Christman MA, 2nd, Goetz DJ, Dickerson E, McCall KD, Lewis CJ, et al. (2008) Wnt5a is expressed in murine and human atherosclerotic lesions. Am J Physiol Heart Circ Physiol 294: H2864-2870.

49. George SJ (2008) Wnt pathway: a new role in regulation of inflammation. Arterioscler Thromb Vasc Biol 28: 400-402.

50. Cheng CW, Yeh JC, Fan TP, Smith SK, Charnock-Jones DS (2008) Wnt5a-mediated non-canonical Wnt signaling regulates human endothelial cell proliferation and migration. Biochem Biophys Res Commun 365: 285-290.

51. Kim J, Kim J, Kim DW, Ha Y, Ihm MH, et al. (2010) Wnt5a induces endothelial inflammation via beta-catenin-independent signaling. J Immunol 185: 1274-1282.

6. MANUSCRIPTS

6.1 Wnt5A/Ryk Signaling Critically Affects Barrier Function in Human Vascular Endothelial Cells

Tom Skaria, Esther Bachli, Gabriele Schoedon

Submitted

6.2 IL-4 Causes Hyperpermeability of Vascular Endothelial Cells through Wnt5A Signaling

Tom Skaria, Julia Burgener, Esther Bachli, Gabriele Schoedon

Submitted

6.1 Wnt5A/Ryk Signaling Critically Affects Barrier Function in Human Vascular Endothelial Cells

Tom Skaria, Esther Bachli, Gabriele Schoedon

Wnt5A/Ryk Signaling Critically Affects Barrier Function in Human Vascular Endothelial Cells

Tom Skaria[1]; Esther Bachli[2]; Gabriele Schoedon[1]

[1]Inflammation Research Unit, Division of Internal Medicine, University Hospital Zürich, Switzerland; [2]Department of Medicine, Uster Hospital, Uster, Switzerland.

Running title: Wnt5A and endothelial barrier function

Name and Address for Correspondence:
Gabriele Schoedon, PhD
Inflammation Research Unit
Division of Internal Medicine
University Hospital of Zurich
Rämistrasse 100
CH-8091 Zurich
Switzerland
Email: klinsog@usz.uzh.ch
Tel: +41-44-255-2256

Key Words: Sepsis, Wnt5A, endothelium, vascular permeability, systemic inflammation

Subject Codes: [138] Cell signaling/signal transduction; [141] Functional genomics; [97] Other Vascular biology; [17] Peripheral vascular disease

Word count: 5879

Total number of figures: 6
Total number of tables: 3

TOC category- Basic
TOC subcategory- Vascular Biology

Abstract

Objective— Satisfactory therapeutic strategies for septic shock are still missing. Previously we found elevated levels of Wnt5A in patients with severe sepsis and septic shock. Wnt5A is released by activated macrophages but knowledge of its effects in the vascular system remains scant. Here we investigate the response of human coronary artery endothelial cells (HCAEC) to Wnt5A.

Approach and Results—We used a genome-wide differential expression approach to define novel targets regulated by Wnt5A. Gene ontology analysis of expression profiles revealed clusters of genes involved in actin cytoskeleton remodeling as the predominant targets of Wnt5A. Wnt5A targeted Rho-associated protein serine/threonine kinase (ROCK), leading to phosphorylation of LIM kinase-2 (LIMK2) and inactivation of the actin depolymerization factor cofilin-1 (CFL1). Functional experiments recording cytoskeletal rearrangements in living cells showed that Wnt5A enhanced stress fiber formation as a consequence of reduced actin depolymerization. The antagonist Wnt inhibitory factor 1 (WIF1) that specifically interferes with the WIF domain of Ryk receptors prevented actin polymerization. Wnt5A disrupted β-catenin and VE-cadherin adherens junctions forming inter-endothelial gaps. Functional experiments targeting the endothelial monolayer integrity and live recording of trans-endothelial resistance revealed enhanced permeability of Wnt5A-treated HCAEC. Ryk silencing completely prevented Wnt5A-induced endothelial hyperpermeability. Wnt5A decreased wound healing capacity of HCAEC monolayers; this was restored by the ROCK inhibitor Y-27632.

Conclusions—Here we show that Wnt5A acts on the vascular endothelium causing enhanced permeability through Ryk interaction and downstream ROCK/LIMK2/CFL1 signaling. Wnt5A/Ryk signaling might provide novel therapeutic strategies to prevent capillary leakage in systemic inflammation and septic shock.

Non-standard Abbreviations and Acronyms

CFL1	cofilin-1
ECIS	Electric Cell-substrate Impedance Sensing
Fzd	Frizzled
HCAEC	human coronary artery endothelial cells
IL	interleukin
LIMK2	LIM kinase-2
qRT-PCR	quantitative Real Time-PCR
ROCK	Rho-associated protein serine/threonine kinase
sFRP	secreted Frizzled-related peptide
WIF1	Wnt inhibitory factor 1

Sepsis is a systemic inflammatory response of the organism to an infection. The most serious manifestations of the disease are severe sepsis and septic shock with organ dysfunction and profound hypotension. The pathophysiology is highly complex and includes deregulation of the immune response, severe coagulopathy and endothelial dysfunction[1]. A small number of randomized clinical trials showed improved survival in septic patients; however three of these have been disproven in larger studies. The latest example has been trials with activated protein C, which lead to withdrawal of the drug from the market[2]. Despite optimized therapies with replacement of organ function using artificial systems, mortality remains high with a rate of 40-–70%[1]. The clinical manifestations of sepsis have a strong vascular component, predominantly seen as enhanced vascular leakage due to endothelial barrier dysfunction[3, 4].

During systemic inflammation, activated immune cells communicate with the vascular endothelium by release of and response to an array of inflammatory mediators[5]. Inflammatory mediators such as tumor necrosis factor and interleukin (IL)-1 were identified as responsible for disturbed endothelial function with increased leukocyte adhesion and transmigration, loss of control of systemic vascular tone, increased pro-coagulant activity and pronounced vascular leakage. Therapeutic trials targeting these inflammatory mediators have not been efficacious in treating human sepsis[6-8].

Recently, Wnt5A was identified as a novel chemokine highly induced and released following Toll-like receptor dependent inflammatory activation of human macrophages and was found in substantial quantities in sera of patients with severe sepsis[9, 10]. Wnt5A is one of the members of the Wnt family of secreted lipid modified signaling proteins. Wnt5A is capable of sustaining the inflammatory phenotype of macrophages through an autocrine mechanism involving Frizzled (Fzd)-5/CaMKII signaling. This pathway is a target for anti-inflammatory interventions in human macrophages[9, 11].

In systemic inflammation and sepsis, inflammatory mediators secreted by activated immune cells act paracrinically on endothelial cells[1, 12, 13]. Therefore, Wnt5A secreted by activated macrophages might act in a similar manner and contribute to endothelial dysfunction. A recent report indicates inflammatory activation of vascular endothelial cells may occur following Wnt5A exposure[14] but the exact mechanism by which Wnt5A contributes to the inflammatory response of vascular endothelial cells still remain unclear. In the present study, we applied a genome-wide transcriptome analysis to define the targets and pathways of paracrine Wnt5A signaling in our established system of primary vascular endothelial cells, human coronary artery endothelial cells (HCAEC)[5]. IL-1β, a leading inflammatory cytokine in the vascular system[5, 15], was used in parallel as a comparison to Wnt5A and a control for integrity and proper biological function of our HCAEC system. Our study revealed that Wnt5A principally regulated genes involved in cytoskeleton rearrangement. This contrasted with IL-

1β, which predominantly affected pathways and genes associated with an immune response. We found that Wnt5A critically affects endothelial barrier function and cell migration. We identified the receptor Ryk and downstream Rho-associated protein serine/threonine kinase (ROCK)/LIM kinase 2 (LIMK2)/cofilin-1 (CFL1) signaling as the pathway responsible for Wnt5A-induced cytoskeletal changes in HCAEC. Targeting the Wnt5A/Ryk interaction by either knockdown of Ryk expression or using the Ryk specific soluble antagonist Wnt inhibitory factor 1 (WIF1) abolished cytoskeletal changes and endothelial hyperpermeability. Wnt5A/Ryk signaling might provide novel strategies for therapeutic intervention in systemic inflammation and sepsis.

Materials and Methods

Materials and methods are available in the online-only Data Supplement.

Results

Differential gene expression profiling reveals that Wnt5A predominantly affects genes involved in cytoskeleton rearrangements

To define the genes regulated by Wnt5A treatment in HCAEC, we performed competitive two-color differential gene expression profiling. The transcriptome profiles of HCAEC treated with Wnt5A for 8 h were compared with that of untreated cells (cultured in parallel) using human whole genome oligomicroarrays. Transcriptome profiling of IL-1β treated HCAEC was performed using the same approach. The well-defined cytokine IL-1β was used to compare its inflammatory properties with the suspected but not elucidated effects of Wnt5A in the HCAEC system. GeneSpring analysis of the Wnt5A transcriptome in HCAEC revealed 9854 genes, of which 3317 genes were upregulated and 6537 genes were downregulated. GeneSpring analyses comparing Wnt5A and IL-1β transcriptomes showed that 3188 genes were commonly regulated by both treatments (Figure 1A). The presence of common targets for Wnt5A and IL-1β points to an inflammatory action of Wnt5A in HCAEC.

The list of two hundred genes highly regulated by Wnt5A and IL-1β is provided in Tables 1 and 2 of the Online Supplement. Complete data sets for Wnt5A and IL-1β are available in the NCBI GEO data repository with accession number GSE62281.

To identify the biological processes regulated by Wnt5A or IL-1β in HCAEC, Metacore gene ontology (GO) analyses were conducted. Using this tool, genes regulated at least 2-fold in

their expression were clustered on the basis of their function to generate statistically significant cellular pathways.

Gene ontology cluster analysis of genes regulated by Wnt5A treatment of HCAEC were mainly associated with cytoskeleton remodeling pathways. The “Cytoskeleton remodeling_TGF, WNT and cytoskeletal remodeling” appeared as the most significant pathway for Wnt5A (Figure 1B), but appeared as only 25th out of 50 pathways significant for IL-1β (not shown). Genes regulated by both Wnt5A and IL-1β (Table 1), such as MAPK13 and LIMK2, were mainly concerned with actin polymerization and cytoskeleton remodeling. Among the genes specifically regulated by Wnt5A (Table 2), ARPC1B and CFL1 are involved in actin polymerization, CRK is involved in cell motility and several other genes are involved in angiogenesis. The “Cell adhesion_Chemokines and adhesion” pathway was the second most statistically significant pathway for Wnt5A (Figure 1B), but it appeared as only 45th out of 50 pathways significant for IL-1β (not shown). In this pathway, Wnt5A-regulated genes were mainly associated with the cytoskeleton targets described above. Additionally, FLNA, a gene involved in branching of actin filaments, was downregulated by Wnt5A (Table 2).

In contrast to Wnt5A, gene ontology cluster analysis of genes regulated by IL-1β were mainly associated with immune response pathways. The “Immune response_HMGB1/RAGE signaling pathway” and “Immune response_HSP60 and HSP70/TLR signaling pathway” were the first and second most significant pathways for IL-1β in HCAEC (Figure 1C) which involved the upregulation of NFκB (Table 3). IL-1β significantly upregulated the expression of inflammatory mediators (IL-6, IL-8, CCL2; Online Supplement Table 2) and cell adhesion molecules (ICAM; Table 3) whereas the expression of these genes was not regulated by Wnt5A. This correlates with our qRT-PCR and flow cytometry analyses and thereby confirms that Wnt5A does not regulate the expression of cell adhesion molecules or proinflammatory cytokines in HCAEC (Online Supplement Figures 1, 2).

Wnt5A receptors in HCAEC

We previously described Wnt5A/Fzd5 signaling as an essential pathway maintaining the production of inflammatory mediators IL-1β, IL-6 and IL-8 in human macrophages[9]. Since HCAEC did not respond to Wnt5A stimulation with the production of these “Classical” inflammatory molecules or adhesion molecules, and Ryk and Ror2 are other receptors known to be involved in Wnt signaling pathways[16], we checked which of these three receptors (Fzd5, Ryk or Ror2) is responsible for Wnt5A signaling in HCAEC. Using qRT-PCR, we measured Fzd5, Ryk and Ror2 mRNAs expressed constitutively and upon Wnt5A or IL-1β treatment. Wnt5A treatment did not affect the mRNA levels of Fzd5 (Figure 2A) or Ryk (Figure 2B). In HCAEC treated with IL-1β, Ryk mRNA was increased approximately 2-

fold while no change was observed in the Fzd5 mRNA level (Figure 2A). We then measured Fzd5 and Ryk mRNA transcripts constitutively expressed in HCAEC. As shown in Figure 2C, Ryk mRNA expression is greater than six times the expression level of Fzd5 mRNA, the latter being very low. Ror2 mRNA expression was undetectable (data not shown). Immunofluorescence staining was performed to corroborate this finding and to verify if IL-1β upregulates Ryk receptor protein in HCAEC. HCAEC constitutively express substantial amounts of Ryk protein and, consistent with regulation at the mRNA level, HCAEC treated with IL-1β expressed significantly more Ryk protein compared with the non-treated cells (Figure 2D, upper panel). Constitutive Fzd5 protein expression was scant and remained unchanged with IL-1β treatment (Figure 2D, lower panel).

Wnt5A phosphorylates LIMK2 and CFL1 proteins through ROCK activation

Wnt5A mainly regulated the functional cluster of genes involved in endothelial actin cytoskeleton remodeling including the ROCK downstream targets *LIMK2* and *CFL1*. LIMK2 is a serine/threonine/tyrosine kinase which, when phosphorylated by ROCK activation, phosphorylates the actin depolymerization factor CFL1[17-19]. As Wnt/Planar Cell Polarity signaling involves the activation of ROCK[20] and Wnt5A regulated *LIMK2* and *CFL1*, we next checked if LIMK2 and CFL1 proteins are phosphorylated upon treatment with Wnt5A. HCAEC were treated with Wnt5A and the phosphorylated forms of both endogenous LIMK2 and CFL1 were detected by immunofluorescence staining using specific antibodies to phosphorylated LIMK2 and CFL1. Amounts of fluorescent phosphorylated LIMK2 and CFL1 in cells were further quantified using Fiji software. Compared with non-treated cells, a substantial increase in phosphorylated LIMK2 and CFL1 was observed in HCAEC treated with Wnt5A for 1 h and 4 h, respectively (Figure 3A–C).

As LIMK2 and CFL1 are phosphorylated by the activation of ROCK[17, 19], we next checked if inhibiting ROCK prevents their phosphorylation upon treatment with Wnt5A. Wnt5A-induced phosphorylation of both LIMK2 and CFL1 was notably suppressed when HCAEC were treated with a combination of Wnt5A and the ROCK-inhibitor Y-27632 (iROCK, Figure 3A–C).

Functional experiments in living cells reveal actin stress fiber formation upon Wnt5A treatment

Since ROCK-mediated LIMK2 and CFL1 phosphorylation causes increased actin fiber bundling and stress fiber formation[18, 19, 21], and Wnt5A induced phosphorylation of LIMK2 and CFL1, we next checked if Wnt5A causes actin stress fiber formation. Changes in actin arrangement and F-actin stress fiber formation were recorded in actin-RFP transduced cells. In non-treated HCAEC, an accumulation of non-fibrous g-actin in the perinuclear region was

obvious with few thin actin filaments present. In contrast to this, live actin-RFP showed significantly increased stress fiber formation in Wnt5A treated HCAEC. Similar changes were observed in cells treated with IL-1β (Figure 4A).

We then checked if Wnt5A-induced stress fiber formation can be prevented by the Wnt antagonists secreted Frizzled-related peptide (sFRP) 1 and WIF1. sFRP1, a member of sFRP family, contains a cysteine-rich domain homologous to the Wnt binding extracellular domain of Fzd and Ror receptors. WIF-Wnt binding domains are homologous to the Wnt binding extracellular domain of Ryk[16]. Treatment of HCAEC with Wnt5A in the presence of sFRP1 did not prevent Wnt5A-induced F-actin stress fiber formation, whereas stress fiber formation was notably decreased when HCAEC were treated with a combination of Wnt5A and WIF1 (Figure 4A). This suggests the involvement of Ryk as an upstream receptor for ROCK in Wnt5A triggered cytoskeletal rearrangements in HCAEC. Stress fiber formation induced by IL-1β remained unaffected by the presence of sFRP1 and WIF1 (Figure 4A).

Wnt5A disrupts adherens junction proteins

As increased stress fiber formation disrupts the assembly of β-catenin and VE-cadherin adhesion proteins in adherens junctions or inter-endothelial junctions[22], we next checked if Wnt5A disrupts these adhesion proteins in HCAEC. HCAEC monolayers were treated with Wnt5A for 8 h and the organization of β-catenin and VE-cadherin were examined by immunofluorescence staining. IL-1β treatment served as a positive control in these experiments. In non-treated cells, β-catenin and VE-cadherin were regularly distributed along the cellular periphery and formed tight contacts at cell borders (Figure 4B). Upon treatment with Wnt5A, β-catenin and VE-cadherin were lost specifically at cell borders resulting in small holes and separations (gaps) between cells. Similar effects were observed in HCAEC treated with IL-1β (arrowheads, Figure 4B).

Functional experiments targeting the monolayer integrity by live recording of trans-endothelial resistance reveal enhanced permeability through Wnt5A/Ryk signaling

Since Wnt5A disrupted inter-endothelial adherens junctions and induced the formation of intercellular gaps, we proposed that Wnt5A could impair the barrier functions and increase the permeability of an endothelial monolayer. To prove this, HCAEC monolayers cultured in 8W10E+ electrode arrays were treated with Wnt5A and changes in trans-endothelial electrical resistance of the endothelial monolayer were recorded in real time by Electric Cell-substrate Impedance Sensing (ECIS). Upon treatment with Wnt5A, there was a significant decrease in the resistance of HCAEC monolayers to alternating current. The Wnt5A-induced changes in electrical resistivity became significantly evident after 3 h after the addition of

Wnt5A and lasted for more than 10 h. Likewise, treatment with IL-1β significantly decreased the resistance of HCAEC monolayers (Figure 5A). Our data indicate that inflammatory activation of HCAEC with Wnt5A or IL-1β affects endothelial barrier function and increases monolayer permeability.

Since HCAEC express constitutively high levels of Ryk, and the Ryk specific Wnt antagonist WIF1 diminished Wnt5A-induced endothelial stress fiber formation, we checked if silencing Ryk expression would prevent Wnt5A induced hyperpermeability of HCAEC monolayers. To silence Ryk expression, HCAEC were transfected with Ryk-specific siRNA. Additionally, HCAEC were transfected with highly validated negative control siRNA to detect off target effects caused by siRNA or transfection reagents. To prove the efficiency of Ryk knockdown, Ryk mRNA expression was compared by qRT-PCR in cells transfected with Ryk-siRNA and in cells transfected with negative control siRNA. Ryk mRNA expression was approximately 70% lower in cells transfected with Ryk-siRNA than in cells transfected with negative control siRNA (Online Supplement Figure 3A). Immunofluorescence staining further confirmed that Ryk-siRNA transfected HCAEC expressed significantly lower amounts of Ryk receptor compared with cells transfected with negative control siRNA (Online Supplement Figures 3B, 3C). These results prove that efficient and specific silencing of Ryk was achieved in HCAEC. Next, Ryk-silenced HCAEC were seeded onto 8W10E+ electrode arrays, treated with Wnt5A or IL-1β and changes in trans-endothelial electrical resistance were measured in real time by ECIS. Treatment with Wnt5A did not alter the resistance of Ryk-silenced HCAEC. In contrast, IL-1β significantly decreased the resistance of Ryk-silenced HCAEC (Figure 5B). This result confirms that Wnt5A specifically signals through Ryk in HCAEC.

Wnt5A-impaired motility of endothelial cells is restored by ROCK inhibition

Since Wnt5A induced stress fiber formation and impaired the barrier function of endothelial monolayers, we hypothesized that Wnt5A could also affect the motility of endothelial cells. An ECIS assisted wounding assay was used to investigate whether Wnt5A influences the motility of HCAEC. HCAEC monolayers on single electrode (8W1E) arrays were treated with Wnt5A and subjected to electric current that killed cells in a defined area of the electrode and created a wound of standard size. The migration of viable cells to the wounded area was recorded in real time by ECIS. Treatment with Wnt5A significantly reduced the number of cells migrating to the wounded area (indicated by a significant decrease in impedance) resulting in delayed wound closure. A similar effect was observed in HCAEC treated with IL-1β whereby cell migration and subsequent wound closure were significantly affected (Figure 6A)

We have shown that Wnt5A-induced phosphorylation of LIMK2 and CFL1 could be suppressed by inhibiting ROCK. ROCK is involved in a variety of cellular processes including cell motility, actin cytoskeleton rearrangements and cell adhesion[19]. Therefore, we investigated whether inhibiting ROCK prevents Wnt5A-induced impairment of HCAEC motility in an ECIS assisted wounding assay. HCAEC treated with a combination of Wnt5A and the ROCK inhibitor Y-27632 showed significant increase in cell motility and faster wound closure compared with HCAEC treated with Wnt5A in the absence of ROCK inhibitor. Similar effects were observed in HCAEC treated with a combination of IL-1β and Y-27632 (Figure 6B). This data further indicate that ROCK is involved in Wnt5A/Ryk signaling in HCAEC.

Discussion

Using a genome-wide expression survey, we characterized the targets and determined the biological function of paracrine inflammatory Wnt5A signaling in a tightly controlled system of adult human vascular endothelial cells. Our study reveals that Wnt5A primarily regulates genes involved in actin cytoskeleton rearrangements in endothelial cells. We have identified a novel Wnt5A/Ryk signaling mechanism that targets the ROCK/LIMK2/CFL1 axis to induce cytoskeleton remodeling and barrier dysfunction in vascular endothelial cells. Gene expression profiling of IL-1β performed in parallel showed that IL-1β mainly regulates genes and pathways associated with immune responses, thereby confirming previous findings[5]. The response to IL-1β proves the integrity of biological functions in our HCAEC system.
Our previous study revealed that Wnt5A signals through Fzd5 to cause inflammatory activation of human macrophages[9]. In this study, we found that HCAEC constitutively express high levels of Ryk, and only trace amounts of Fzd5 (Figures 2C, 2D), thereby suggesting that Wnt5A could exert its function without upregulating the level of endogenous Ryk receptors. We further found that Wnt5A-induced stress fiber formation can be prevented by WIF1, thereby pointing to the involvement of Ryk as the receptor for Wnt5A-mediated cytoskeleton remodeling in HCAEC (Figure 4A). Additionally, the transcriptome analysis of the current study shows that Wnt5A downregulates the expression of LRP5 (Table 1). Since LRP5 acts as a co-receptor for Fzd5 in β-catenin dependent signaling[20, 23], the Wnt/β -catenin pathway involving Fzd receptors could be repressed by Wnt5A in HCAEC. This is supported by our finding that β-catenin remains sequestered on the plasma membrane of HCAEC after Wnt5A treatment and is not transported to the nucleus (Figure 4B) to signal via the β-catenin pathway. The subsequent functional experiments demonstrate that Wnt5A induced HCAEC barrier impairment can be prevented by silencing Ryk expression, thereby providing direct

evidence that Wnt5A signals through Ryk (Figure 5). Ryk is a member of the family of atypical receptor tyrosine-protein kinases. It comprises an extracellular Wnt binding domain, a PDZ binding motif and an intracellular atypical kinase domain lacking tyrosine kinase activity. Wnt5A/Ryk signaling has been functionally demonstrated in adult rat corticospinal axons[24]. Moreover, Derailed, a member of the Ryk family of receptors in Drosophila, has been described as acting as a receptor for Wnt5A in axon guidance[25]. Furthermore, abundant expression of the *Ryk* gene was reported in mouse pulmonary capillary endothelial cells.[26] Data obtained in the present study indicate that Wnt5A signaling via ROCK activation induces actin cytoskeletal rearrangements and disrupts VE-cadherin-mediated intercellular adhesion. The involvement of Ryk but not other known Wnt receptors such as Fzd or Ror is further evident from the observation that Wnt5A induced actin stress fiber formation was prevented by the Ryk specific antagonist WIF1, while sFRP1 was uneffective (Figure 4A). Previous studies have already established that inactivation of ROCK and RhoA prevents endothelial hyperpermeability[27, 28].

Our study reveals that Wnt5A decreases the motility of HCAEC and combining Wnt5A with the ROCK inhibitor Y-27632 restores the migratory capacity of HCAEC (Figure 6). This is in full accordance with the proposed model of Wnt5A/Ryk signaling. The reduction in endothelial cell motility caused by Wnt5A is due to actin cytoskeleton rearrangements and increased stress fiber formation (Figure 4A) induced by ROCK mediated phosphorylation of LIMK2 and CFL proteins (iROCK, Figure 3A–C).

Our study further demonstrates that IL-1β signaling significantly upregulates Wnt5A expression in HCAEC (Online Supplement Figure 4). Addressing the question of which transcription factors are involved in mediating IL-1β -induced expression of Wnt5A in endothelial cells, we found that IL-1β upregulated NF-κB (Table 3). As IL-1β induces Wnt5A in HCAEC, it can be inferred that IL-1β secreted by activated macrophages in systemic inflammation and sepsis paracrinically triggers endogenous Wnt5A signaling in vascular endothelial cells. Our present study further proves that Wnt5A, unlike IL-1β, does not induce a cytokine storm (*IL-6, IL-8, CCL2;* Online Supplement Figure 1) or cell adhesion molecules (*ICAM-1, VCAM-1;* Online Supplement Figure 2) in endothelial cells as has been reported previously[14]. Data from our genome-wide transcriptome analysis and functional studies indicate that Wnt5A/Ryk signaling in HCAEC is independent of the induction of any other inflammatory mediators. The biological integrity of the cells in our system is proven by the typical inflammatory response to IL-1β (Online Supplement Figures 1, 2).

Wnt5A expression is elevated in sepsis[9] and our present study finds Wnt5A as a critical mediator of endothelial hyperpermeablity. This warrants further studies to determine the correlation of Wnt5A levels with vascular leakage in appropriate septic animal models.

However, current sepsis animal models fail to mimic the human disease for a number of reasons, and most of the highly successful trials in animal models did not improve patient survival when translated to clinical settings[12, 29].

In conclusion, the present study shows for the first time that Wnt5A/Ryk signaling impairs the barrier functions and affects the wound healing of a damaged monolayer of human vascular endothelial cells. This suggests that Wnt5A, secreted by activated macrophages during a systemic inflammatory response, could cause capillary leakage and subsequent edema in severe sepsis. Restoring vascular integrity along with reducing edema is an established factor that improves the prognosis of septic shock. Considering the essential role for Rho/ROCK in Wnt5A signaling in adult human vascular endothelial cells, therapeutic approaches targeting the Wnt5A/Ryk/ROCK signaling pathway would probably improve the prognosis of sepsis.

Acknowledgments: We thank Cheryl Pech, PhD, for critical reading of the manuscript.

Source of Funding: This study was supported by the Swiss National Science Foundation No. 31-124861 to Gabriele Schoedon.

Disclosures: None

References

1. Russell JA. Management of sepsis. N Engl J Med. 2006:355:1699-1713.
2. Thachil J, Toh CH, Levi M, Watson HG. The withdrawal of Activated Protein C from the use in patients with severe sepsis and DIC [Amendment to the BCSH guideline on disseminated intravascular coagulation]. Br J Haematol. 2012:157:493-494.
3. Lee WL, Slutsky AS. Sepsis and Endothelial Permeability. N Engl J Med. 2010:363:689-691.
4. Mehta D, Ravindran K, Kuebler WM. Perspective: Novel regulators of endothelial barrier function. Am J Physiol Lung Cell Mol Physiol. 2014:307:L924-L935.
5. Franscini N, Bachli EB, Blau N, Leikauf M-S, Schaffner A, Schoedon G. Gene expression profiling of inflamed human endothelial cells and influence of activated protein C. Circulation. 2004:110:2903-2909.
6. Reinhart K, Karzai W. Anti-tumor necrosis factor therapy in sepsis: update on clinical trials and lessons learned. Crit Care Med. 2001:29:S121-125.

7. Fisher CJ, Jr., Dhainaut JF, Opal SM et al. Recombinant human interleukin 1 receptor antagonist in the treatment of patients with sepsis syndrome. Results from a randomized, double-blind, placebo-controlled trial. Phase III rhIL-1ra Sepsis Syndrome Study Group. J Am Med Assoc. 1994:271:1836-1843.
8. Opal SM, Fisher CJ, Jr., Dhainaut JF et al. Confirmatory interleukin-1 receptor antagonist trial in severe sepsis: a phase III, randomized, double-blind, placebo-controlled, multicenter trial. The Interleukin-1 Receptor Antagonist Sepsis Investigator Group. Crit Care Med. 1997:25:1115-1124.
9. Pereira C, Schaer DJ, Bachli EB, Kurrer MO, Schoedon G. Wnt5A/CaMKII signaling contributes to the inflammatory response of macrophages and is a target for the antiinflammatory action of activated protein C and interleukin-10. Arterioscler Thromb Vasc Biol. 2008:28:504-510.
10. Schulte DM, Kragelund D, Muller N, Hagen I, Elke G, Titz A, Schadler D, Schumacher J, Weiler N, Bewig B, Schreiber S, Laudes M. The wingless-related integration site-5a/secreted frizzled-related protein-5 system is dysregulated in human sepsis. Clin Exp Immunol. 2015:180:90-97.
11. George SJ. Wnt pathway: a new role in regulation of inflammation. Arterioscler Thromb Vasc Biol. 2008:28:400-402.
12. Riedemann NC, Guo R-F, Ward PA. Novel strategies for the treatment of sepsis. Nat Med. 2003:9:517-524.
13. Xu H, Ye X, Steinberg H, Liu SF. Selective blockade of endothelial NF-κB pathway differentially affects systemic inflammation and multiple organ dysfunction and injury in septic mice. J Pathol. 2010:220:490-498.
14. Kim J, Kim J, Kim DW, Ha Y, Ihm MH, Kim H, Song K, Lee I. Wnt5a induces endothelial inflammation via β-catenin–independent signaling. J Immunol. 2010:185:1274-1282.
15. Linscheid P, Schaffner A, Blau N, Schoedon G. Regulation of 6-pyruvoyltetrahydropterin synthase activity and messenger RNA abundance in human vascular endothelial cells. Circulation. 1998:98:1703-1706.
16. Green J, Nusse R, van Amerongen R. The role of Ryk and Ror receptor tyrosine kinases in Wnt signal transduction. Cold Spring Harb Perspect Biol. 2014:6:a009175.
17. Rath N, Olson MF. Rho-associated kinases in tumorigenesis: re-considering ROCK inhibition for cancer therapy. EMBO Rep. 2012:13:900-908.
18. Maekawa M, Ishizaki T, Boku S, Watanabe N, Fujita A, Iwamatsu A, Obinata T, Ohashi K, Mizuno K, Narumiya S. Signaling from Rho to the actin cytoskeleton through protein kinases ROCK and LIM-kinase. Science. 1999:285:895-898.

19. Liao JK, Seto M, Noma K. Rho kinase (ROCK) inhibitors. J Cardiovasc Pharmacol. 2007:50:17-24.
20. Angers S, Moon RT. Proximal events in Wnt signal transduction. Nat Rev Mol Cell Biol. 2009:10:468-477.
21. Fazal F, Bijli KM, Minhajuddin M, Rein T, Finkelstein JN, Rahman A. Essential role of cofilin-1 in regulating thrombin-induced RelA/p65 nuclear translocation and intercellular adhesion molecule 1 (ICAM-1) expression in endothelial cells. J Biol Chem. 2009:284:21047-21056.
22. Vandenbroucke E, Mehta D, Minshall R, Malik AB. Regulation of endothelial junctional permeability. Ann N Y Acad Sci. 2008:1123:134-145.
23. Zeng X, Tamai K, Doble B, Li S, Huang H, Habas R, Okamura H, Woodgett J, He X. A dual-kinase mechanism for Wnt co-receptor phosphorylation and activation. Nature. 2005:438:873-877.
24. Miyashita T, Koda M, Kitajo K, Yamazaki M, Takahashi K, Kikuchi A, Yamashita T. Wnt-Ryk signaling mediates axon growth inhibition and limits functional recovery after spinal cord injury. J Neurotrauma. 2009:26:955-964.
25. Yoshikawa S, McKinnon RD, Kokel M, Thomas JB. Wnt-mediated axon guidance via the Drosophila Derailed receptor. Nature. 2003:422:583-588.
26. Favre CJ, Mancuso M, Maas K, McLean JW, Baluk P, McDonald DM. Expression of genes involved in vascular development and angiogenesis in endothelial cells of adult lung. Am J Physiol Heart Circ Physiol. 2003:285:H1917-H1938.
27. Carbajal JM, Gratrix ML, Yu CH, Schaeffer RC, Jr. ROCK mediates thrombin's endothelial barrier dysfunction. Am J Physiol Cell Physiol. 2000:279:C195-204.
28. Carbajal JM, Schaeffer RC, Jr. RhoA inactivation enhances endothelial barrier function. Am J Physiol. 1999:277:C955-964.
29. Fink MP. Animal models of sepsis and its complications. Kidney Int. 2008:74:991-993.

Significance

Vascular leakage in severe systemic inflammation and septic shock is one of the major reasons that mulitiorgan failure occurs. With still no good treatment option available it can lead to death in these patients. There is limited knowledge concerning the pathophysiology leading to this leakage and so there are no targeted treatment options. Wnt5A/Ryk signaling in human vascular endothelial cells affects the endothelial cytoskeleton, disrupts inter-endothelial junction assembly, affects endothelial migration, and enhances monolayer permeability causing barrier dysfunction. The Wnt5A/Ryk pathway described here might provide potential novel targets for therapeutic interventions in severe systemic inflammatory diseases and septic shock.

Tables

Table 1. Genes regulated by both Wnt5A and IL-1β in "Cytoskeleton remodeling_TGF, WNT and cytoskeletal remodeling" and "Cell adhesion_Chemokines and adhesion" pathways.

Gene symbol	Accession number	Sequence description	Regulation	
			Wnt5A	IL-1β
LIMK2*†	NM_001031801	Homo sapiens LIM domain kinase 2	Down	Up
LRP5*	NM_001291902	Homo sapiens low density lipoprotein receptor-related protein 5	Down	Down
MAPK12*	NM_002969	Homo sapiens mitogen-activated protein kinase 12	Down	Down
MAPK13*	NM_002754	Homo sapiens mitogen-activated protein kinase 13	Down	Down
MMP1†	NM_002421	Homo sapiens matrix metallopeptidase 1	Up	Up
PLAU*†	NM_001145031	Homo sapiens plasminogen activator, urokinase	Down	Up
TAB1*	NM_006116	Homo sapiens TGF-beta activated kinase 1	Down	Down

* Genes regulated in "Cytoskeleton remodeling_TGF, WNT and cytoskeletal remodeling" pathway.
† Genes regulated in "Cell adhesion_Chemokines and adhesion" pathway.

Table 2. Genes regulated only by Wnt5A in ‘‘Cytoskeleton remodeling_TGF, WNT and cytoskeletal remodeling” and “Cell adhesion_Chemokines and adhesion” pathways.

Gene symbol	Accession number	Sequence description	Regulation
AKT2*†	NM_001626	Homo sapiens v-akt murine thymoma viral oncogene homolog 2	Down
ARPC1B*†	NM_005720	Homo sapiens actin related protein 2/3 complex, subunit 1B	Down
CDKN1A*	NM_078467	Homo sapiens cyclin-dependent kinase inhibitor 1A	Down
CFL1*†	NM_005507	Homo sapiens cofilin-1	Down
CRK*†	NM_016823	Homo sapiens v-crk sarcoma virus CT10 oncogene homolog (avian)	Down
FLNA†	NM_001110556	Homo sapiens filamin A	Down
MAPK3*†	NM_002746	Homo sapiens mitogen-activated protein kinase 3	Down
MAPK11*	NM_002751	Homo sapiens mitogen-activated protein kinase 11	Down
MAPK14*	NM_139013	Homo sapiens mitogen-activated protein kinase 14	Down
TSC2*	NM_000548	Homo sapiens tuberous sclerosis 2	Down

* Genes regulated in “Cytoskeleton remodeling_TGF, WNT and cytoskeletal remodeling” pathway
† Genes regulated in “Cell adhesion_Chemokines and adhesion” pathway

Table 3. Genes regulated by IL-1β in "Immune response_HMGB1/RAGE signaling pathway" and "Immune response_HSP60 and HSP70/TLR signaling pathway".

Gene symbol	Accession number	Sequence description	Regulation
ATF2[†]	NM_001880	Homo sapiens activating transcription factor 2	Up
CCL4[*]	NM_002984	Homo sapiens chemokine (C-C motif) ligand 4	Up
ICAM1[*†]	NM_000201	Homo sapiens intercellular adhesion molecule 1	Up
IL-1α[*]	NM_000575	Homo sapiens interleukin 1, alpha	Up
MAP2K6[*†]	NM_002758	Homo sapiens mitogen-activated protein kinase kinase 6	Down
NFκB1[*†]	NM_003998	Homo sapiens nuclear factor of kappa light polypeptide gene enhancer in B-cells 1	Up
NFκB2[*†]	NM_001077493	Homo sapiens nuclear factor of kappa light polypeptide gene enhancer in B-cells 2	Up
NFκBIA[*†]	NM_020529	Homo sapiens nuclear factor of kappa light polypeptide gene enhancer in B-cells inhibitor, alpha	Up
NFκBIE[*†]	NM_004556	Homo sapiens nuclear factor of kappa light polypeptide gene enhancer in B-cells inhibitor, epsilon	Up
SERPINE1[*]	NM_000602	Homo sapiens serpin peptidase inhibitor, clade E (nexin, plasminogen activator inhibitor type 1), member 1	Up
TLR2[*†]	NM_003264	Homo sapiens toll-like receptor 2	Up

* Genes regulated in "Immune response_HMGB1/RAGE signaling pathway"
† Genes regulated in "Immune response_HSP60 and HSP70/TLR signaling pathway"

Figure 1

A

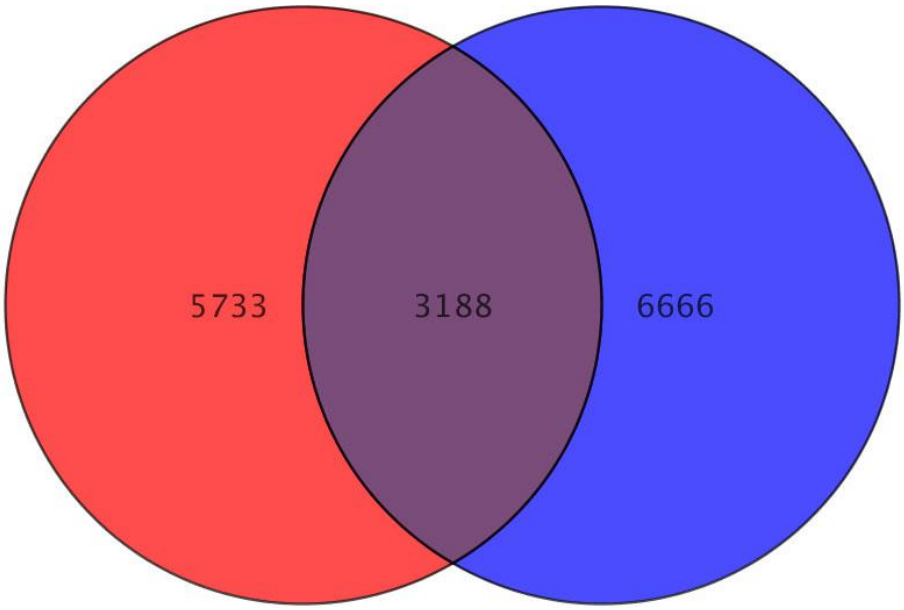
5733
3188
6666

B

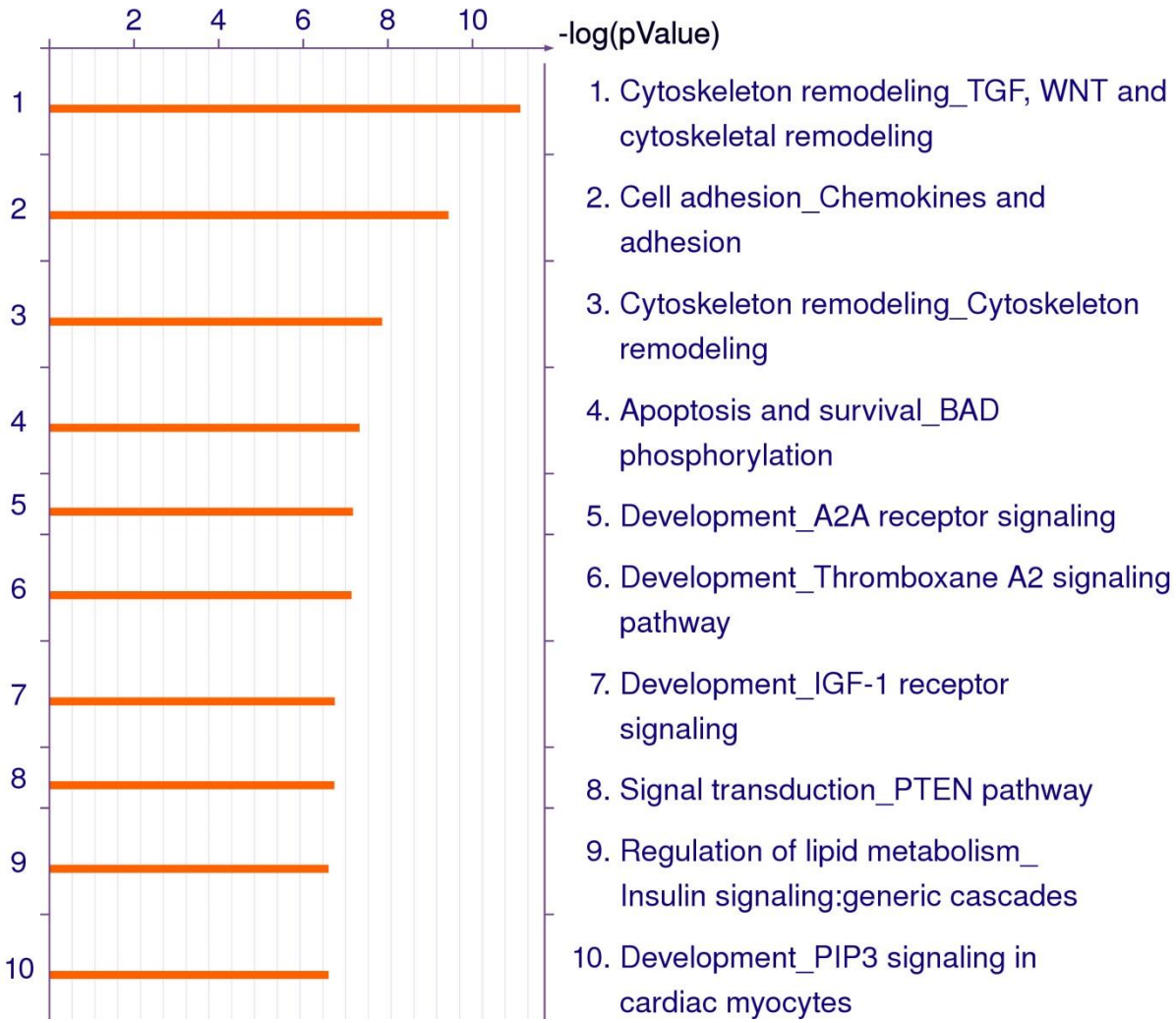
2
4
6
8
10
-log(pValue)
1
2
3
4
5
6
7
8
9
10
1. Cytoskeleton remodeling_TGF, WNT and cytoskeletal remodeling
2. Cell adhesion_Chemokines and adhesion
3. Cytoskeleton remodeling_Cytoskeleton remodeling
4. Apoptosis and survival_BAD phosphorylation
5. Development_A2A receptor signaling
6. Development_Thromboxane A2 signaling pathway
7. Development_IGF-1 receptor signaling
8. Signal transduction_PTEN pathway
9. Regulation of lipid metabolism_ Insulin signaling:generic cascades
10. Development_PIP3 signaling in cardiac myocytes

C

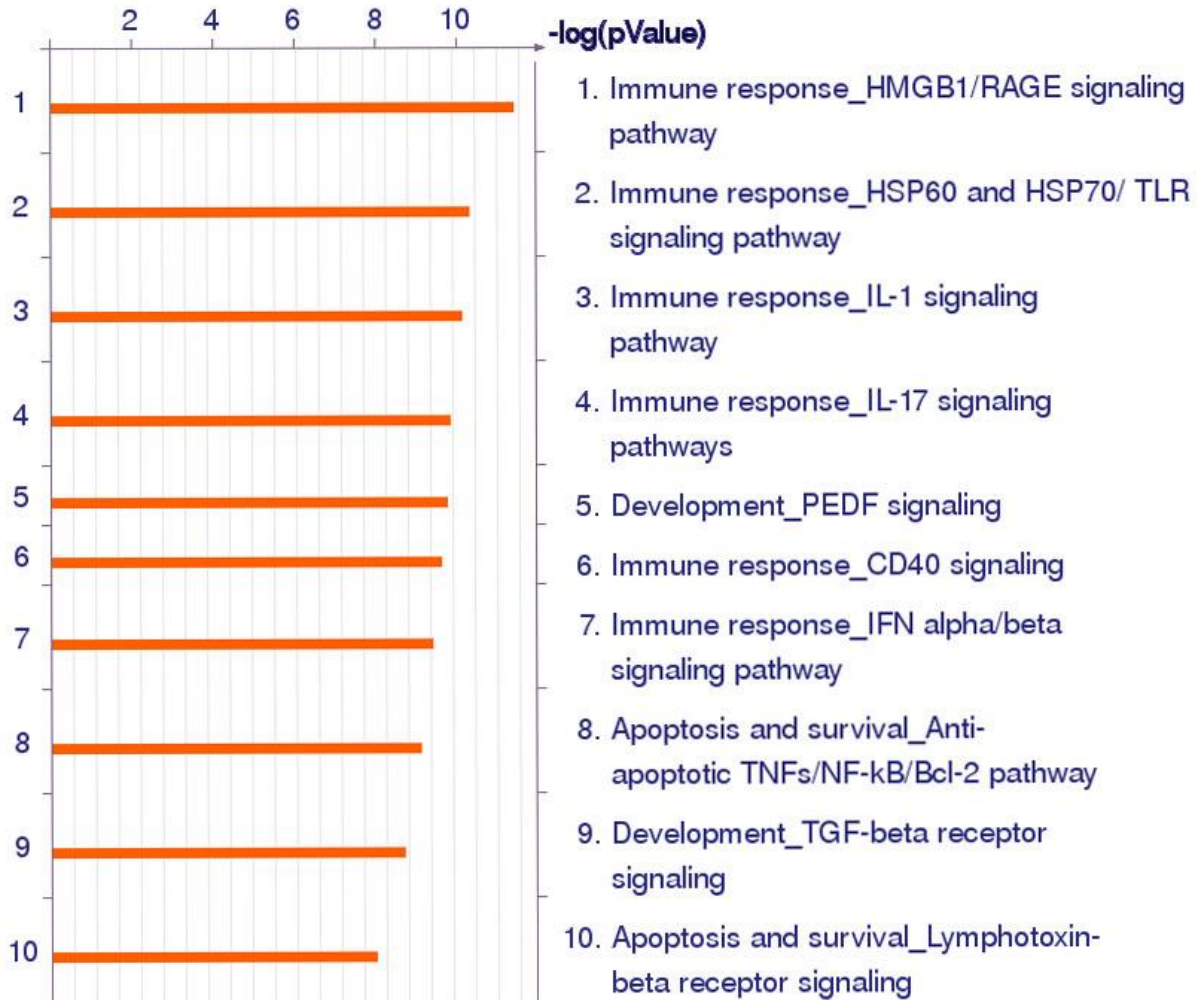

Figure 1. Whole genome expression survey of the inflammatory response of HCAEC to IL-1β and Wnt5A. (A) Venn diagram summarizing different and common genes regulated by IL-1β and Wnt5A in HCAEC. Feature extracted data was analyzed using GeneSpring under "Biological significance" work flow. Red circle, IL-1β specific genes; blue circle, Wnt5A specific genes; intersection, genes regulated by both Wnt5A and IL-1β. (**B, C**) GO pathway maps of regulated genes clustered according to biological processes. Pathways represented as histograms are ranked by the –log value *(P* value). Length of histogram corresponds to the number of genes associated with that specific pathway. Maps of the ten most significant processes regulated by (**B**) Wnt5A, corresponding to genes within blue circle of Venn diagram and (**C**) IL-1β, corresponding to genes within the red circle of Venn diagram.

Figure 2

A

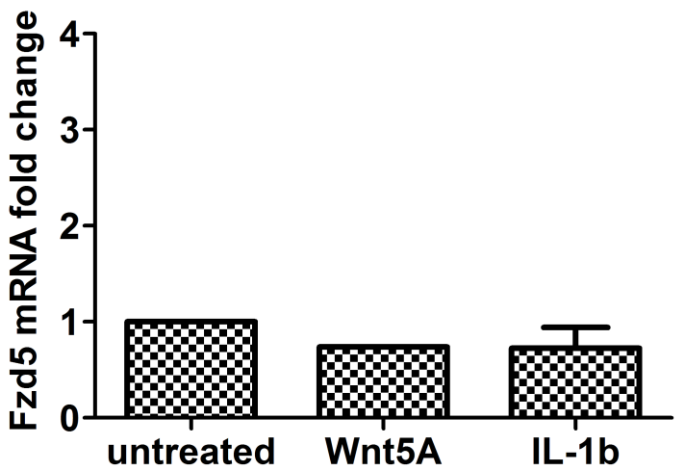
Fzd5 mRNA fold change
4
3
2
1
0
untreated
Wnt5A
IL-1b

B

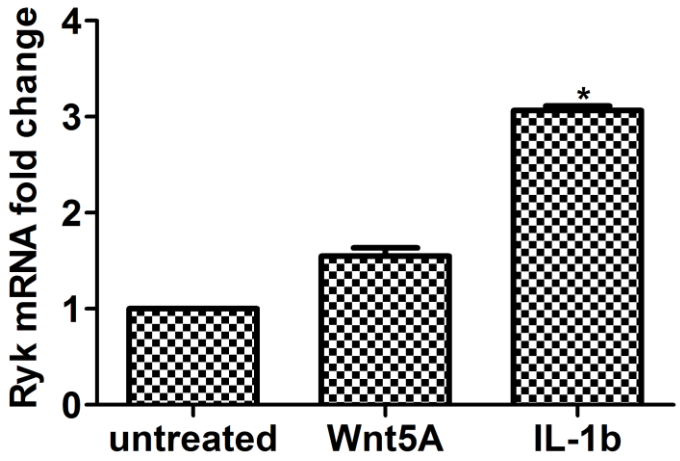
Ryk mRNA fold change
4
3
2
1
0
*
untreated
Wnt5A
IL-1b

C

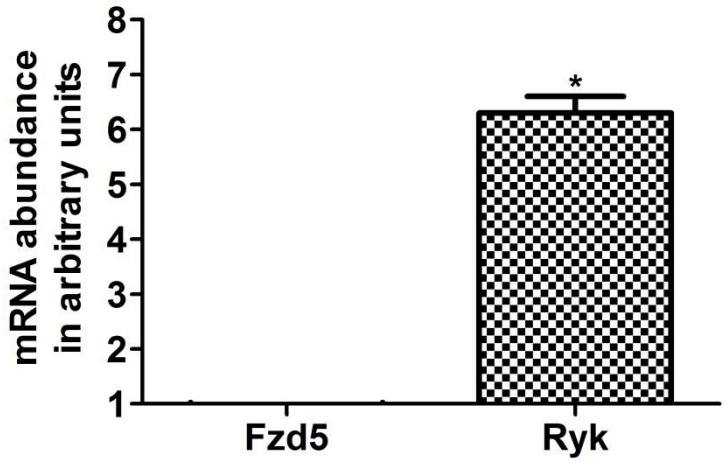
mRNA abundance in arbitrary units
8
7
6
5
4
3
2
1
*
Fzd5
Ryk

D

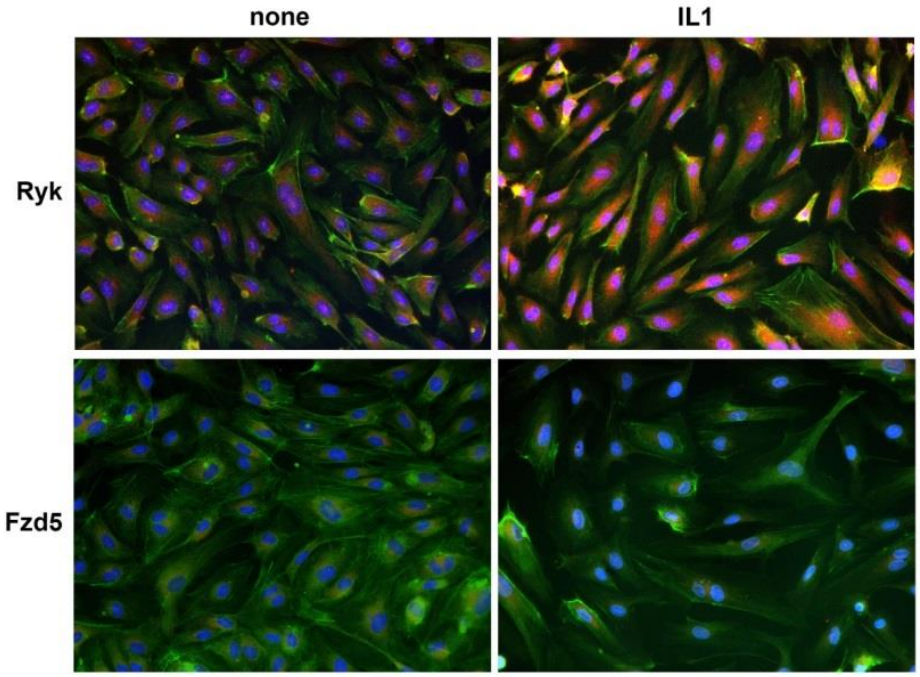

Figure 2. Expression of Fzd5 and Ryk receptors in HCAEC. Expression of mRNA levels of (**A**) Fzd5 and (**B**) Ryk in HCAEC treated with Wnt5A and IL-1β (IL-1b) for 8 h as outlined in Methods. Data were obtained from three independent qRT-PCR experiments with duplicate samples and expressed as the mean ± S.E.M. **P*<0.05 by Student's *t*-test. (**C**) Quantitative ratio of constitutive levels of Fzd5 and Ryk mRNAs in HCAEC. **P*<0.05 by Student's *t*-test. (**D**) Protein expression of Fzd5 and Ryk receptors in HCAEC either untreated (left panel) or treated with IL-1β (IL1) 24 h. Images show immunofluorescence staining using specific antibodies for Fzd5 and Ryk (red), F-actin (phalloidin, green) and nuclei (DAPI, blue). Zeiss Axioskope, magnification 200 fold.

Figure 3

A

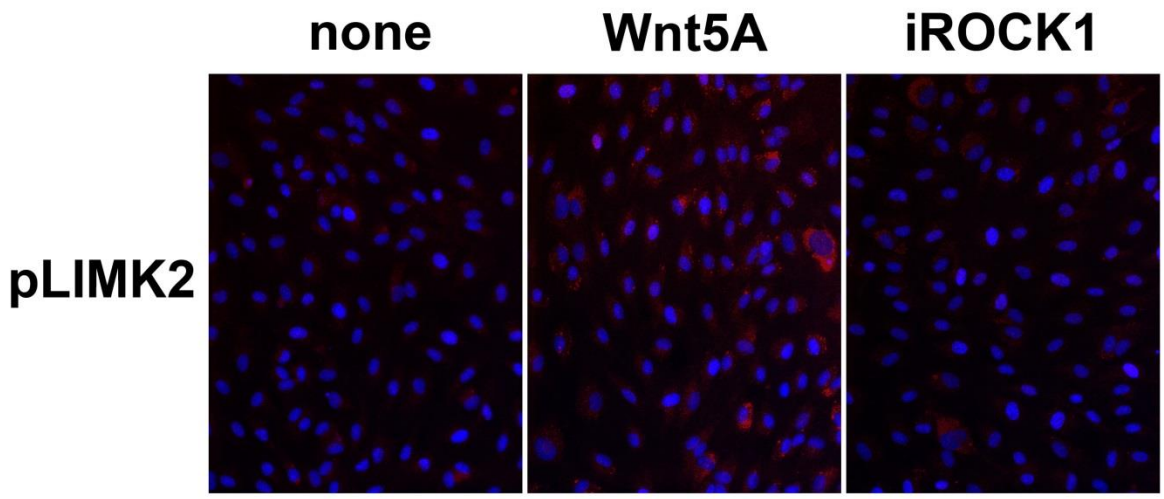
none
Wnt5A
iROCK1
pLIMK2

B

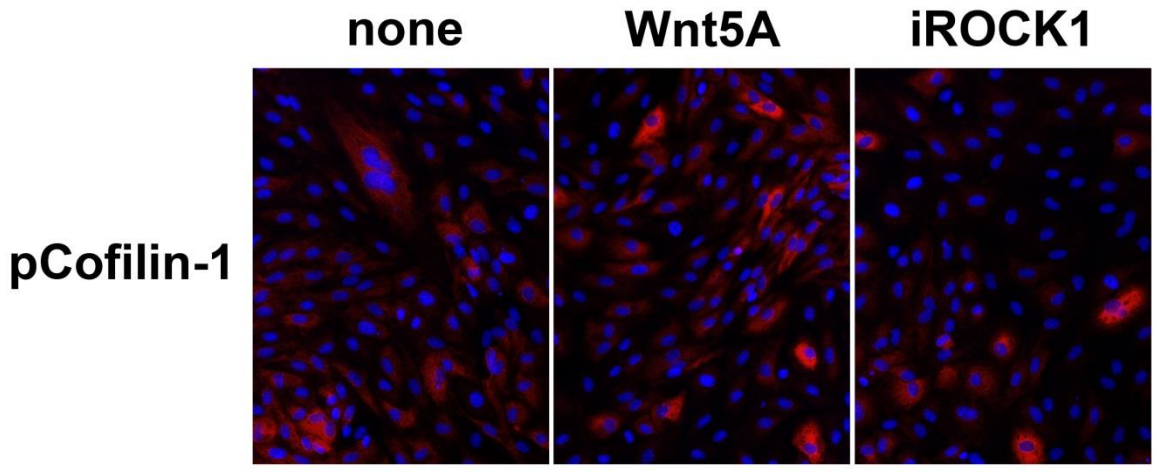
none
Wnt5A
iROCK1
pCofilin-1

C

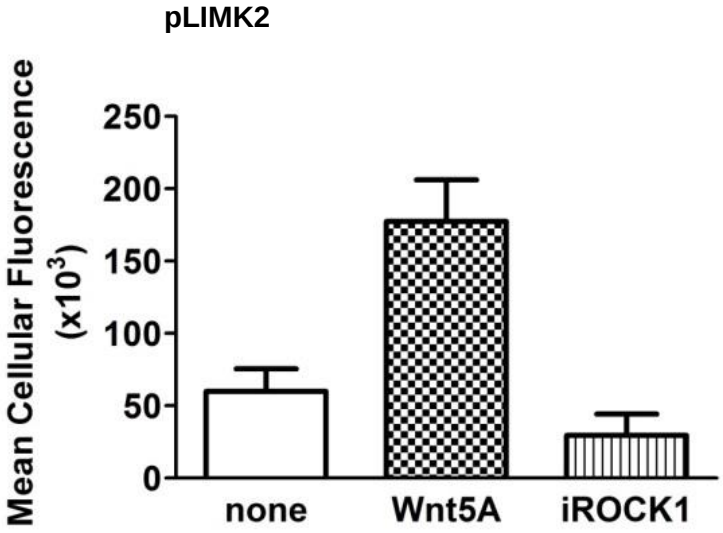
pLIMK2
Mean Cellular Fluorescence (x10³)
250
200
150
100
50
0
none
Wnt5A
iROCK1

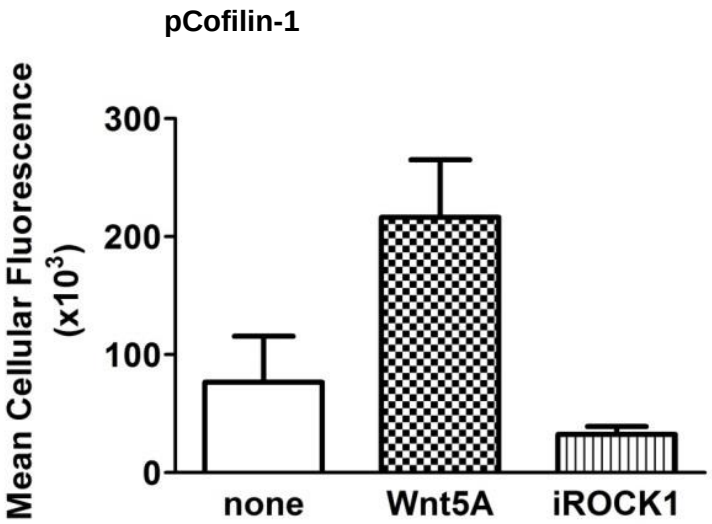

Figure 3. Effects of ROCK inhibition on Wnt5A-induced phosphorylation of LIMK2 and cofilin-1. Immunofluorescence staining of (**A**) phosphorylated LIMK2 and (**B**) phosphorylated cofilin-1 (both in red) and nuclei (blue) in HCAEC treated with either Wnt5A alone or in combination with the ROCK inhibitor Y-27632 (iROCK1) for 1 h and 4 h respectively. Zeiss Axioskope, magnification 200 fold. (**C**) Mean cellular fluorescent intensities of phosphorylated LIMK2 and cofilin-1 quantified by ImageJ based Fiji software. pLIMK2, phosphorylated LIMK2; pCofilin-1, phosphorylated cofilin-1.

Figure 4

A

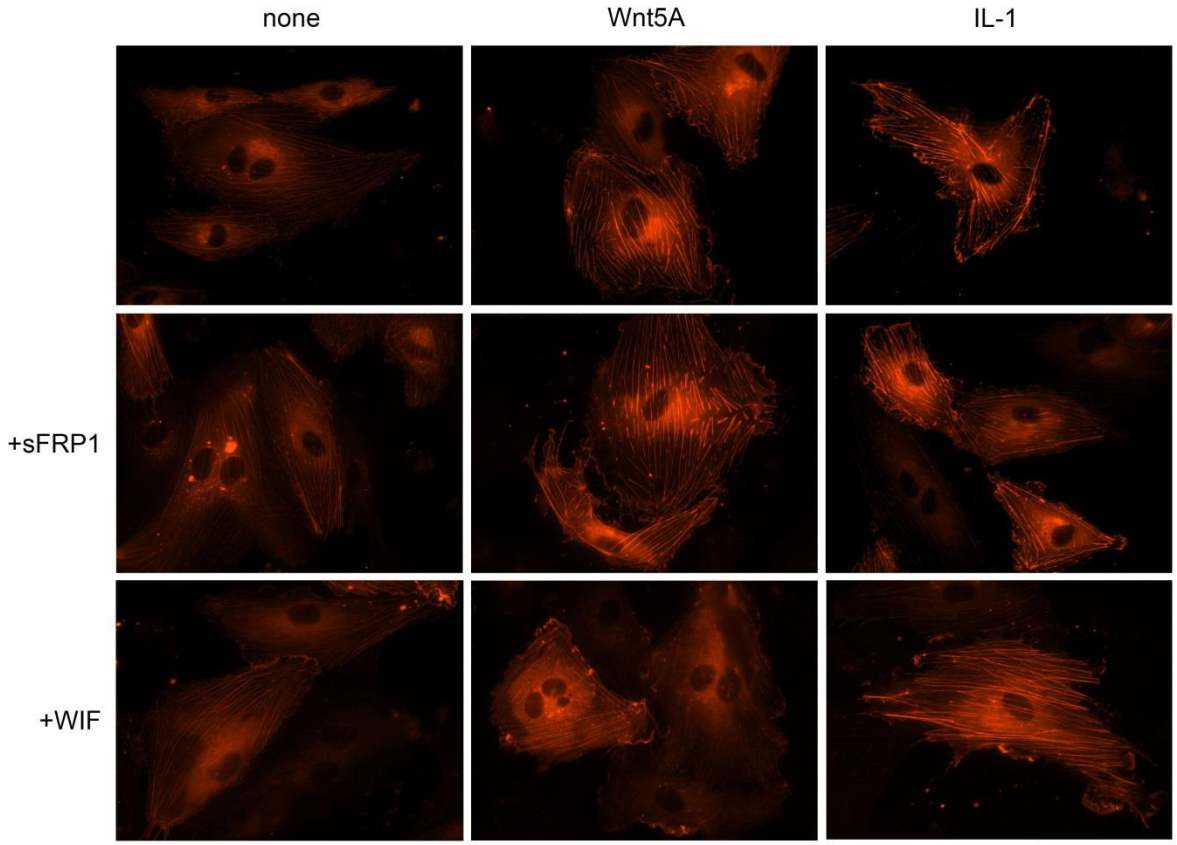

B

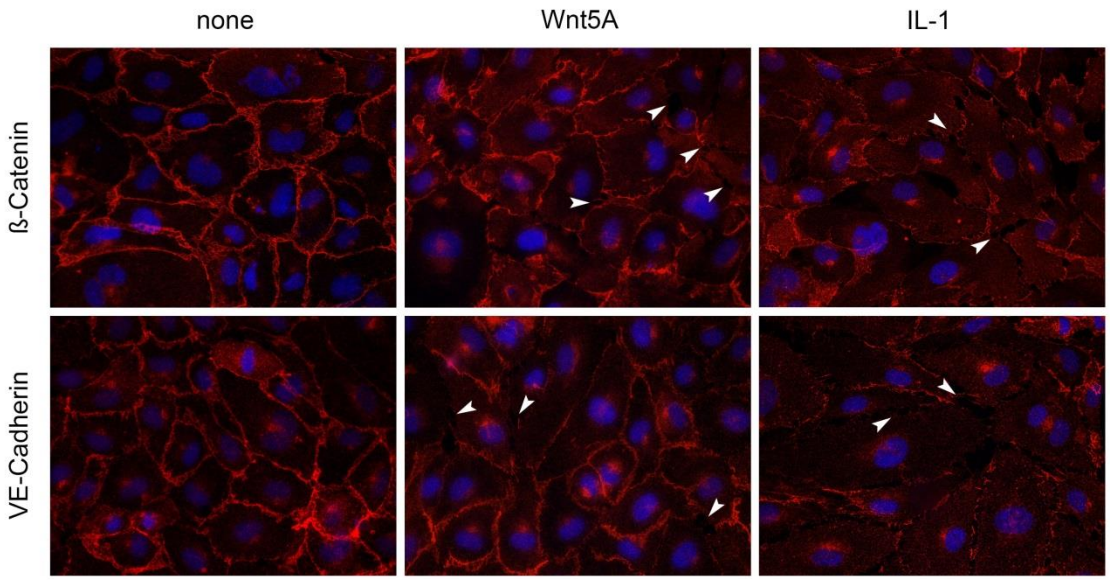

Figure 4. Actin stress fiber formation and adherens junction disruption in HCAEC in response to Wnt5A and IL-1β. (**A**) Actin stress fibers stained by live actin-RFP in HCAEC either untreated (left panel) or treated with Wnt5A (middle panel) or IL-1β (IL-1, right panel), in the absence or presence of sFRP1 or WIF. Stained cells were captured at 8 h after treatment using a Zeiss Axio Observer.Z1, magnification 400 fold. (**B**) Immunofluorescence staining for β-catenin and VE-cadherin (red) in HCAEC treated with either Wnt5A or IL-1β (IL-1) for 8 h. Nuclei are stained blue. Arrowheads point to inter-endothelial gaps. Zeiss Axioskope, magnification 400 fold.

Figure 5

A

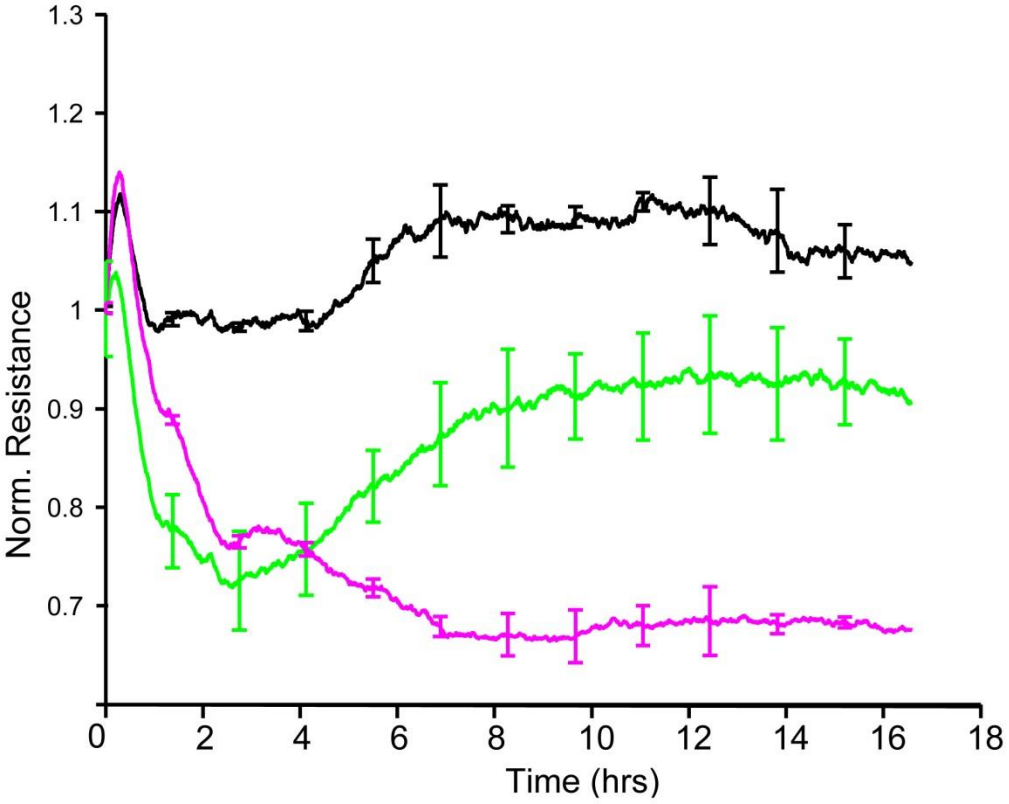
Norm. Resistance
1.3
1.2
1.1
1
0.9
0.8
0.7
0
2
4
6
8
10
12
14
16
18
Time (hrs)

B

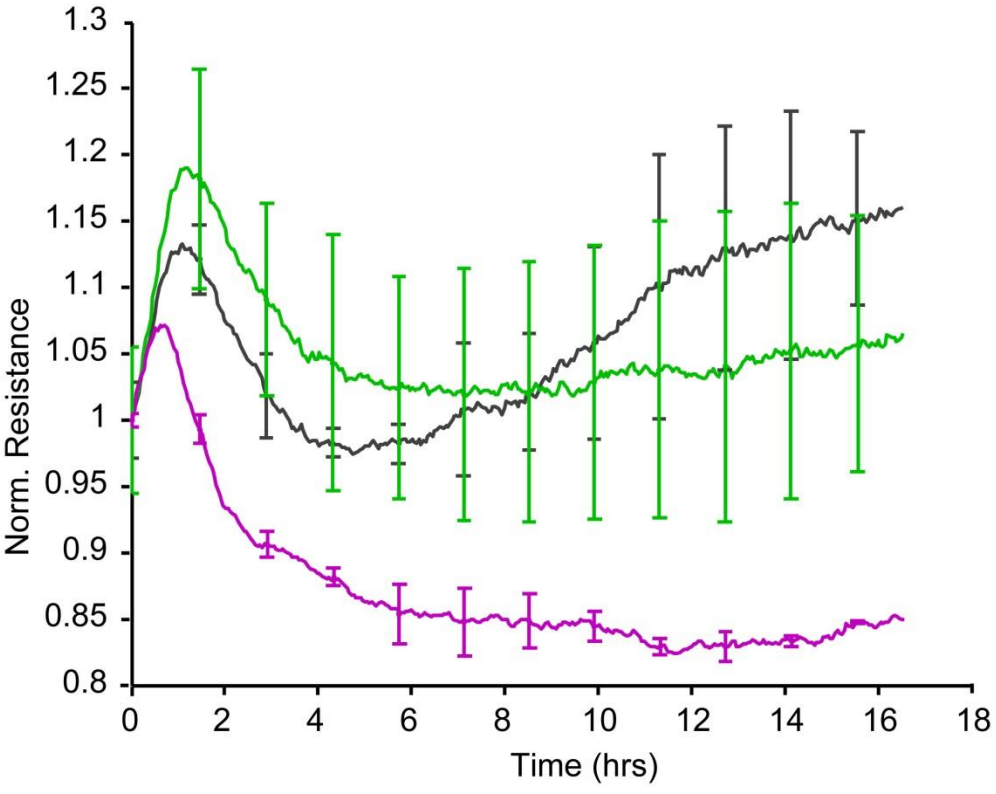
Norm. Resistance
1.3
1.25
1.2
1.15
1.1
1.05
1
0.95
0.9
0.85
0.8
0
2
4
6
8
10
12
14
16
18
Time (hrs)

Figure 5. ECIS barrier function assays in HCAEC. Uniform confluent monolayers of HCAEC cultured in stabilized and collagen coated 8W10E+ ECIS culture chambers (see Methods and Figure 5 of Online Supplement) were treated with Wnt5A and IL-1β. Resistance of HCAEC monolayers was continuously recorded in Ohms every 5 min at multiple frequencies ranging from 62.6 Hz to 64 kHz, normalized to its value at time zero, and plotted with respect to time. Resistance measured from duplicate wells were grouped and averaged to plot as a single curve with error bars representing the SD. Data shown are the resistance measurements conducted at 4000 Hz from four independent experiments. (**A**) Un transfected HCAEC. Black, Untreated; Green, Wnt5A; Purple, IL-1β. (**B**) Ryk siRNA transfected HCAEC. Black, Untreated; Green, Wnt5A; Purple, IL-1β.

Figure 6

A

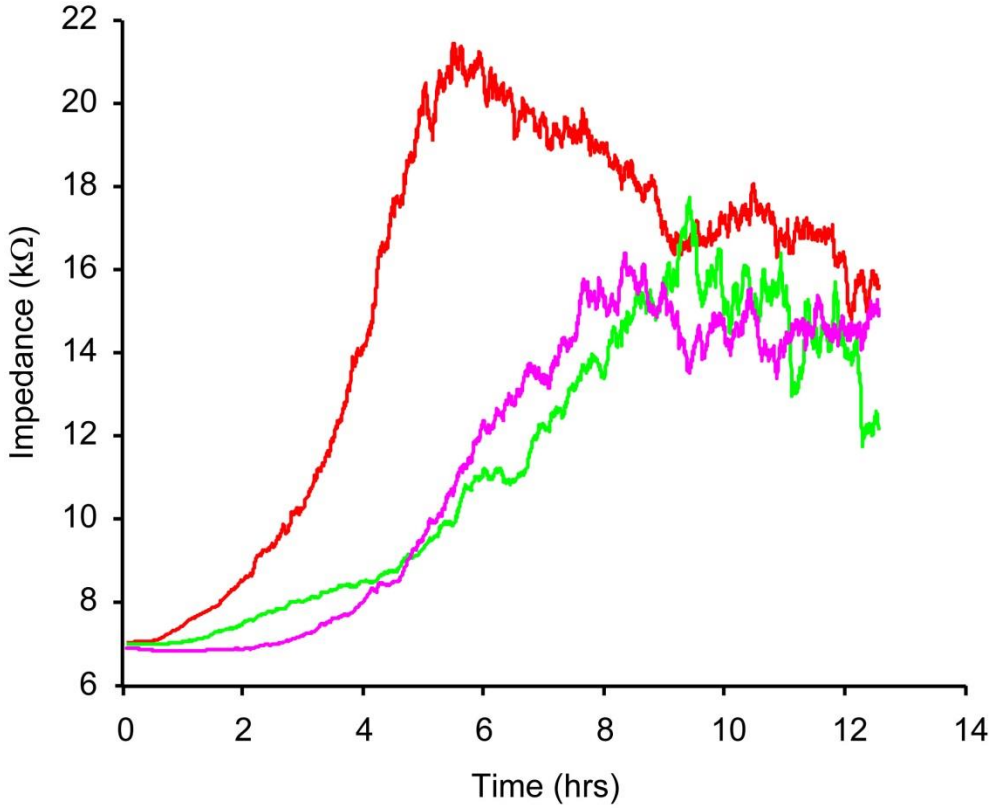
Impedance (kΩ)
22
20
18
16
14
12
10
8
6
0
2
4
6
8
10
12
14
Time (hrs)

B

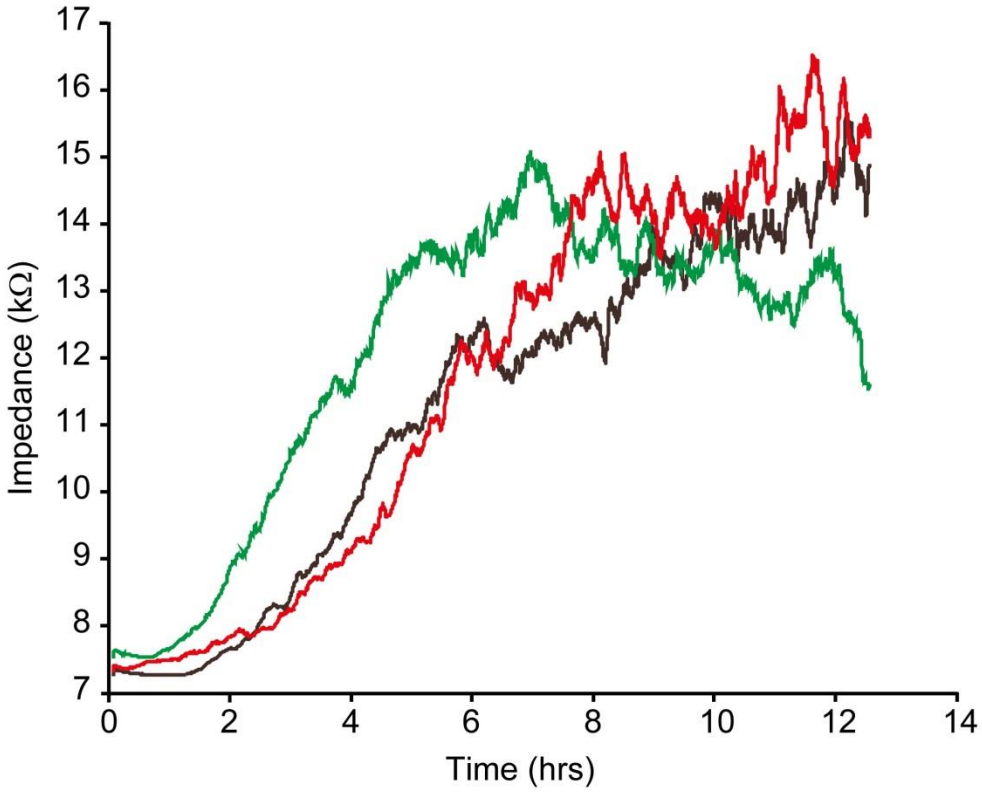
Impedance (kΩ)
17
16
15
14
13
12
11
10
9
8
7
0
2
4
6
8
10
12
14
Time (hrs)

Figure 6. ECIS assisted wound healing assay. Uniform confluent monolayers of HCAEC cultured in stabilized and collagen coated single electrode 8W1E ECIS culture chambers (Methods, Online Supplement) were treated with Wnt5A and IL-1β either alone or in combination with the ROCK inhibitor Y-27632 for 3 h. At time 0 h, a defined wound with a diameter of 250 µm was created in each of the eight wells by applying an elevated electric field at 1400 µA, 60 kHz for 20 sec. Immediately after wounding, impedance of HCAEC was continuously recorded in Ohms every 5 min at multiple frequencies ranging from 62.6 Hz to 64 kHz and plotted with respect to time. Data shown represent the measurements conducted at 4000 Hz from four independent experiments. (**A**) HCAEC without ROCK inhibition. Red, Untreated; Purple, Wnt5A; Green, IL-1β. (**B**) HCAEC with ROCK inhibition. Black, Control with Y-27632; Red, Wnt5A+Y-27632; Green IL-1β+Y-27632.

Materials and Methods

Cell Culture

HCAEC (Clonetics, Lonza, Switzerland) were propagated in EBM-2 medium (Clonetics, Lonza) supplemented with EGM-2MV Single Quots with 5% FBS (Clonetics, Lonza) as described[1]. Cells were cultured under standard conditions (37°C, 5% CO2, 80% humidity) in a Class 100 HEPA air filtered system (SteriCult, Fisher Scientific, Switzerland). To avoid masked low-level contamination in cultures, culture medium without antibiotics was used throughout the study. In experimental settings, cells from passages three to six were used and serum concentration of the medium was reduced to 2% FBS. HCAEC were treated with recombinant human/mouse Wnt5A (250 ng/mL; CHO-derived Gln38-Lys380, purity >80%, endotoxin level <1.0 EU/µg of protein; Cat. No. 645-WN, R&D systems, USA), recombinant human IL-1β (20 U/mL; purity >98%; PeproTech, USA), recombinant human secreted Frizzled-related peptide (sFRP)1 (10 µg/mL; purity >95%; Cat. No.1384-SF, R&D systems, USA), recombinant human WIF1 (15 µg/mL; purity >97%; Cat. No. 1341-WF-050, R&D systems, USA). For all pipetting steps, Biopure ep Dualfilter T.I.P.S. sterile filter tips (Eppendorf, Germany) were used.

RNA Isolation and Quantitative Real Time-PCR (qRT-PCR) Analyses

RNA isolation and qRT-PCR were performed as described[2] with the following modifications and primers. RNA was reverse transcribed into cDNA using TaqMan® Kit (Applied Biosystems, USA). qRT-PCR was performed using Fast SYBR® Green Master Mix and a 7500 Fast Real-Time PCR System (Applied Biosystems, USA). Relative quantification analyses were performed with HPRT gene as endogenous control using RQ Study SDS software v1.4 (Applied Biosystems, USA). Sequence specific PCR detection primers used for Wnt5A, IL-6, IL-8, HPRT, MCP-1, ICAM-1, Ryk and Fzd5 are as follows: Wnt5A forward, 5'-AGT TGC CTA CCC TAG C-3'; Wnt5A reverse, 5'-GTG CCT TCG TGC CTA T-3'; IL-6 forward, 5'-CCT GAC CCA ACC ACA AA-3'; IL-6 reverse, 5'-AGT GTC CTA ACG CTC ATA C-3'; IL-8 forward, 5'-AGA CAG CAG AGC ACA CAA GC-3'; IL-8 reverse, 5'-ATG GTT CCT TCC GGT GGT-3'; HPRT forward, 5'-CCA GTC AAC AGG GGA CAT AAA-3'; HPRT reverse, 5'-CAC AAT CAA GAC ATT CTT TCC AGT-3'; MCP-1 forward, 5'-CAG CCA GAT GCA ATC AAT GC-3'; MCP-1 reverse, 5'-GTG GTC CAT GGA ATC CTG AA-3'; ICAM-1 forward, 5'-TTG GAA GCC TCA TCC G-3'; ICAM-1 reverse, 5'-CAA TGT TGC GAG ACC C-3'; Ryk forward, 5'-TGC CCT CTC CAG AGA CTT GT-3'; Ryk reverse, 5'-CAT CTC GAA GGG GTC AAT GT-3'; Fzd5 forward, 5'-CAT CGA CAT GGA ACG C-3'; Fzd5 reverse, 5'-CGT GAT GGA CTT GAC GC-3'. Temperature cycling conditions of the PCR were as

follows; an initial denaturation step (10 min, 95°C) followed by 40 cycles of denaturation (15 sec, 95°C), annealing (30 sec, 55°C), and extension (30 sec, 72°C).
Constitutively expressed mRNA levels of Fzd5 and Ryk in HCAEC were calculated by the 1/ΔCt method and values were given as arbitrary units.

Microarray Based Differential Gene Expression Profiling

Gene expression profiling by competitive two-color hybridization of cRNA probes onto 4×44K Human Whole Genome Oligonucleotide microarrays (Agilent Technologies) was performed as described[3]. Briefly, total RNA was isolated using RNeasy Mini Kit (Qiagen, Basel, Switzerland). Total RNA was quantified by Nanodrop spectrophotometry and RNA integrity was confirmed using the Agilent 2100 Bioanalyzer System (Agilent Tech., Basel, Switzerland). Only RNA samples with a RNA integrity number (RIN) >9 were used for microarray experiments. From each sample, 500 ng of total RNA was reverse transcribed and labeled with Cy3- and Cy5-CTP using the two-color Quick Amp Labeling Kit (Agilent Tech., Switzerland), containing internal control probes and spike in's (labeled Spike A mix with Cy-3 and Spike B mix with Cy-5) for control of reaction performance and background normalization of arrays. cRNA fragmentation and hybridization onto the Human GE 4×44K V2 Microarray chips were performed as per the Quick Amp Labeling protocol (Agilent Techno., version 5.7, 2008). To avoid ozone-induced deterioration of cyanine dyes, array chips were washed with stabilization and drying solution (Agilent Tech., Switzerland).

Microarray Data Analyses

Scanning, feature extraction and preprocessing including data normalization of the microarrays were done by Microarray Scanner and Feature Extraction Software 10.7 (Agilent Tech. Inc.) with default settings for Agilent 4×44 K two-color arrays. The preprocessed data was further analyzed using GeneSpring GX 9.0 Software (Agilent Tech. Inc.) with default settings for two-color arrays using fold change cutoff of 1.5. Gene ontology analysis was performed using Metacore GeneGO software (Thomson Reuters, http://portal.genego.com). Genes regulated ≥2-fold in their expression and satisfying a *P* value <0.05 were grouped into pathways according to their biological functions and gene ontology classes.

Immunofluorescence Staining

HCAEC were cultured in four-chamber culture slides coated with rat tail collagen type I (diluted 0.01% in sterile pyrogen-free water; BD Biosciences, USA). To stain for the adherens junction proteins β-catenin and VE-cadherin, HCAEC were grown to a confluent monolayer. After treatment with the stimuli indicated, cells were fixed with 4% formalin in PBS (in case of detecting adherens junction proteins) for 20 min or with a mixture of acetone

and methanol (1:1) for 5 min (in case of Fzd5, Ryk and Wnt5A detection). Slides were washed three times with PBS (pH 7.4) at room temperature (RT). Slides were treated with blocking solution containing 10% goat serum and 1% BSA in PBS for 1 h at RT in case of secondary antibodies derived from goat. Rabbit blocking solution (10% rabbit serum and 1% BSA in PBS) was used in case of secondary antibodies derived from rabbit. Slides were again washed with PBS at RT and incubated with primary antibodies diluted in blocking solution at 4°C overnight. The following antibodies were used for immunofluorescence: goat-anti-Wnt5A (1:50; Cat. No. AF645, R&D Systems), rabbit-anti-Ryk (1:500; Product No. Ab5518, Abcam), rabbit-anti-Fzd5 (1:100; Product No. Ab14475, Abcam), rabbit-anti-β-catenin (1:150; Product No. 9562, Cell Signaling Technology), rabbit-anti-VE-cadherin (1:100; Product No. 2158, Cell Signaling Technology), rabbit-anti-phosphorylated LIMK2 (1:300; pT505; Product No. Ab131343, Abcam), rabbit-anti-phosphorylated CFL1 (1:500; pS3; Product No. Ab100836, Abcam). After three washes with PBS at RT, slides were incubated with Alexa 568 labeled goat anti-rabbit or rabbit anti-goat secondary antibodies (1:2000; Molecular Probes, Invitrogen, USA) depending on the first antibody's species. Incubations with secondary antibodies were combined with Alexa Fluor 488 Phalloidin (1:80; Molecular Probes, Invitrogen, USA) for 1 h at RT in the dark. After three washes with PBS at RT, slides were counterstained with 10 µg/mL diamidino-phenylindole (DAPI; Sigma-Aldrich) and mounted using ProLong Gold Antifade^{R} (Life Technologies, USA). Images were captured by Axioskope microscope equipped with an Axio-CamMRm digital camera using AxioVision Rel.4.6 software (Carl Zeiss, Feldbach, Switzerland). The intensity of cellular fluorescent signals was quantified from five different positions of the respective fluorescent images using ImageJ based Fiji software (Fiji is Just ImageJ) and corrected for background fluorescence.

Live Cell Imaging of Actin

HCAEC grown in rat tail collagen type I coated optical 96 microwell culture plates (Thermoscientific, USA) were transduced with CellLight Actin-RFP probe (Cat. No. C10583, Life Technologies, USA) as per manufacturer's instructions. Cells were treated with Wnt5A or IL-1β alone or in combination with either sFRP1 or WIF1 for 8 h. Images of the cultures were captured with an Axio Observer.Z1 inverted microscope equipped with Axio-Cam MRm digital camera using ZEN 2012 software (Carl Zeiss, Feldbach, Switzerland).

Endothelial Barrier Function Assays

The response of endothelial barrier to a particular stimulus can be assessed non-invasively in a fully standardized manner by continuously recording changes in trans-endothelial electric resistance using Electric Cell-substrate Impedance Sensing (ECIS)[4, 5]. Endothelial barrier function was recorded in real-time using the ECIS Z Theta system (Applied Biophysics) with

associated software v.1.2.126 PC, as described[6] with the following modifications. 8W10E+ electrode chamber arrays were equilibrated with EBM-2 basal medium (Clonetics, Lonza, USA) for 24 h and coated with rat tail collagen type I (diluted 0.01% in sterile pyrogen-free water; BD Biosciences, USA) for 12 h. Then HCAEC in EGM2MV complete medium (Clonetics, Lonza, USA) were added to the wells with a density of 80,000- 90,000 cells/well and grown up to 24 h to form dense monolayers (Supplemental Figure 5). Treatments were then conducted by replacing the medium with fresh medium without or with stimuli (Wnt5A, IL-1β). Measurements were conducted at multiple frequencies ranging from 62.6 Hz to 64 kHz. 8W10E+ contains 40 electrodes per each of its eight wells that traced the cells at 40 different locations in each well and averaged the measurements.

ECIS Assisted Cell Migration Assay

Motility/wound healing assays were performed in ECIS single electrode arrays as described[7] with the following modifications. 8W1E single electrode chambers were equilibrated with EBM-2 basal medium (Clonetics, Lonza, USA) for 24 h and coated with rat tail collagen type I (BD Biosciences, USA) for 12 h. HCAEC in EGM2MV complete medium (Clonetics, Lonza, USA) were added to the wells with a cell a density of 80,000- 90,000 cells/well. To attain confluent HCAEC monolayers, single electrode array chambers were further incubated for up to 24 h. Stimuli were then added as described above for barrier function assays. 3 h after stimulation, wounding was activated with default conditions for 8W1E arrays (1400 µA, 60000 Hz, for 20 sec). This fully standardized method produces a highly reproducible wound with an exact diameter of 250 µm surrounded by undamaged living cells in 8W1E chambers. After wounding, impedance was continuously recorded to observe the migration of cells and formation of confluent monolayer within the defined wounded area.

Ryk Silencing

Specific and functionally validated small interfering RNA (siRNA) against human Ryk (Hs-RYK-9, Cat No. SI02223074) was obtained from Qiagen. To control for “off target” effects of siRNAs, validated AllStars negative control siRNA (Qiagen) with no homology to any mammalian gene was used. For knockdown of Ryk expression, transfection complexes formed of Ryk-siRNA (5 nM) and 6 µL/mL HiPerFect Transfection reagent (Qiagen GmbH, Hilden, Germany) in EBM-2 basal medium were added to 80% confluent cultures of HCAEC in 24-well plates in a total volume of 500 µL/well. After 24 h of incubation, transfected cells were split using Trypsin EDTA, seeded onto collagen coated 6 well plates, retransfected for a second round as above and incubated until the cells attained 90% confluency. At this stage, cells were either stimulated with Wnt5A or IL-1β for 8 h and lysed (for qRT-PCR analyses) or trypsinized and transferred into collagen-coated 8W10E+ arrays (for ECIS barrier function

measurements). Alternatively, HCAEC after one round of Ryk-siRNA transfection were harvested by trypsinization and seeded into collagen-coated BD Falcon 4 chamber culture slides (BD Biosciences, USA). There, a second round of Ryk-siRNA transfection was performed as in 24-well plates. After growing to a confluent monolayer, cells were fixed for immunostainings. Stimulations were carried out in complete EGM medium with 2% FBS devoid of transfection complexes.

ROCK Inhibition

To inhibit ROCK activity, Y-27632 (Cat. No. 688000, Calbiochem; Millipore, USA) was used[8] at an optimal concentration for this system of 10 μmol/L. HCAEC were incubated in medium containing Y-27632 (10 μmol/L) alone or in combination with either Wnt5A or IL-1β for 1 h and 4 h.

Flow Cytometry

HCAEC stimulated with Wnt5A, IL-1β or combination of these two agents for 24 h were trypsinized and resuspended in PBS supplemented with 0.1% BSA (sample buffer) such that cell density did not exceed more than 10^5 cells/tube. Cells were incubated on ice with directly labeled mouse antibodies against human VCAM-1 (CD106, fluorescein isothiocyanate label, BD pharmingen), ICAM-1 (CD54, phycoerithrin labeled, BD pharmingen), E selectins (CD62E, allophycocyanin label, BD pharmingen) and human integrin b1 chain (CD29, allophycocyanin label, BD pharmingen) at a final concentration of 2 μg/ml. Isotype controls were performed using mouse IgG polyclonal antibodies. After washing twice with FACS buffer, samples were analyzed using FACS CantoII cell sorting system (BD Biosciences, Allschwil, Switzerland). Cells were gated according to their forward- and side-scatter pattern, at least 10'000 gated events were acquired for analysis. The fluorescence intensity of corresponding samples labeled with the isotype control antibody was used to set the individual threshold of antigen positivity. Data were analyzed using FlowJo 7.2.5 software.

Statistical Analysis

Data were analyzed using GraphPad Prism software version 5.04 (GraphPad Software, San Diego, CA). An unpaired 2-tailed Student's *t*-test was used and differences were considered statistically significant at $P<0.05$.

References

1. Franscini N, Bachli EB, Blau N, Leikauf M-S, Schaffner A, Schoedon G. Gene expression profiling of inflamed human endothelial cells and influence of Activated protein C. Circulation. 2004:110:2903-2909.
2. Pereira C, Schaer DJ, Bachli EB, Kurrer MO, Schoedon G. Wnt5A/CaMKII signaling contributes to the inflammatory response of macrophages and is a target for the antiinflammatory action of Activated Protein C and Interleukin-10. Arterioscler Thromb Vasc Biol. 2008:28:504-510.
3. Schaer CA, Deuel JW, Bittermann AG, Rubio IG, Schoedon G, Spahn DR, Wepf RA, Vallelian F, Schaer DJ. Mechanisms of haptoglobin protection against hemoglobin peroxidation triggered endothelial damage. Cell Death Differ. 2013:20:1569-1579.
4. Bernas MJ, Cardoso FL, Daley SK, Weinand ME, Campos AR, Ferreira AJG, Hoying JB, Witte MH, Brites D, Persidsky Y, Ramirez SH, Brito MA. Establishment of primary cultures of human brain microvascular endothelial cells to provide an in vitro cellular model of the blood-brain barrier. Nat Protocols. 2010:5:1265-1272.
5. Szulcek R, Bogaard HJ, van Nieuw Amerongen GP. Electric cell-substrate impedance sensing for the quantification of endothelial proliferation, barrier function, and motility. J Vis Exp. 2014:85:e51300.
6. Sun S, Sursal T, Adibnia Y, Zhao C, Zheng Y, Li H, Otterbein LE, Hauser CJ, Itagaki K. Mitochondrial DAMPs increase endothelial permeability through neutrophil dependent and independent pathways. PLoS One. 2013:8:e59989.
7. Keese CR, Wegener J, Walker SR, Giaever I. Electrical wound-healing assay for cells in vitro. *Proc Natl Acad Sci U. S. A.* 2004:101:1554-1559.
8. Watanabe K, Ueno M, Kamiya D, Nishiyama A, Matsumura M, Wataya T, Takahashi JB, Nishikawa S, Nishikawa S-i, Muguruma K, Sasai Y. A ROCK inhibitor permits survival of dissociated human embryonic stem cells. Nat Biotech. 2007:25:681-686.

SUPPLEMENTAL MATERIAL

SUPPLEMENTAL RESULTS

Effects of Wnt5A on the Expression of Pro-inflammatory Cytokines

To investigate whether Wnt5A regulates the expression of pro-inflammatory cytokines, HCAEC were treated with Wnt5A (250 ng/mL) for 4 h and 8 h and the regulation of IL-6, IL-8 and MCP-1 mRNA levels were analyzed by qRT-PCR. In parallel, HCAEC were treated with IL-1β for 4 h and 8 h to validate the biological function of the system. Expression of IL-6 was not significantly regulated by 4 h and 8 h Wnt5A treatments (Online Supplement Figure 1A). Similarly, HCAEC treated with Wnt5A for 4 h and 8 h showed no significant difference in the expression of IL-8 compared with non-treated cells (Online Supplement Figure 1B). Upon Wnt5A treatments for 4 h, but not 8 h, the expression of MCP-1 was significantly upregulated in HCAEC (Online Supplement Figure 1C).

Treatment with IL-1β significantly upregulated the expression of IL-6, IL-8 and MCP-1 in HCAEC. The highest expression of IL-6 was observed 4 h after IL-1β treatment (Online Supplement Figure 1D), whereas the expression level of induced IL-8 remained unchanged after 4 h and 8 h IL-1β treatments (Online Supplement Figure 1E). IL-1β caused more than 10- fold increase in MCP-1 expression, with its highest expression observed following 8 h treatment (Online Supplement Figure 1F).

Wnt5A Does Not Regulate the Expression of Cell Adhesion Molecules

Pro-inflammatory mediators secreted by activated immune cells activate endothelial cells by upregulating cell adhesion molecules. To determine if Wnt5A regulates the expression of cell adhesion molecules in vascular endothelial cells, HCAEC were treated with Wnt5A as described above for 24 h and the expression of VCAM-1, ICAM-1, E selectins and integrin b1 chain were analyzed by flow cytometry. Wnt5A did not regulate or alter the expression of VCAM-1, ICAM-1, E selectins and integrin b1 chain. HCAEC treated with IL-1β, which served as a positive control, showed significant upregulation of all four adhesion molecules (Online Supplement Figure 2A).

These findings were confirmed by qRT-PCR. ICAM-1 mRNA expression was not changed following 4 h, 8 h and 24 h Wnt5A treatments (Online Supplement Figure 2B) while ICAM-1 mRNA level was significantly upregulated following 4 h and 8 h IL-1β treatments (Online Supplement Figure 2C).

IL-1β Induces the Expression of Wnt5A in HCAEC

Pro-inflammatory cytokines secreted by activated immune cells upregulate inflammatory mediators in endothelial cells. To investigate if the pro-inflammatory cytokine IL-1β induces

the expression of Wnt5A in vascular endothelial cells, HCAEC were treated with IL-1β (20 U/mL) for 8 h and the expression of Wnt5A mRNA level was measured by qRT-PCR. Treatment with IL-1β significantly upregulated Wnt5A mRNA level in HCAEC (Online Supplement Figure 4A). Immunofluorescence staining confirmed increased expression of Wnt5A protein in HCAEC upon IL-1β treatment (Online Supplement Figure 4B).

SUPPLEMENTAL TABLES

Table 1. Detailed list of the 200 genes highest regulated by Wnt5A in HCAEC.

Gene symbol	Accession number	Sequence description	Fold change
ACOT6	NM_001037162	Homo sapiens acyl-CoA thioesterase 6	-8.324418
MCHR2	NM_001040179	Homo sapiens melanin-concentrating hormone receptor 2	-7.2782345
SNORD3B-1	NR_003271	Homo sapiens small nucleolar RNA, C/D box 3B-1	-6.936168
FGG	NM_000509	Homo sapiens fibrinogen gamma chain A	-6.7145305
SNORD3B-1	NR_003271	Homo sapiens small nucleolar RNA, C/D box 3B-1	-6.5760064
TRPA1	NM_007332	Homo sapiens transient receptor potential cation channel, subfamily A, member 1	-6.389514
ZSCAN5D	XM_001725568	PREDICTED: Homo sapiens zinc finger and SCAN domain containing 5D	-6.2849603
OR9G4	NM_001005284	Homo sapiens olfactory receptor, family 9, subfamily G, member 4	-5.88169
CELSR1	NM_014246	Homo sapiens cadherin, EGF LAG seven-pass G-type receptor 1	-5.839751
RIMBP2	NM_015347	Homo sapiens RIMS binding protein 2	-5.6184063
KAZN	NM_015209	Homo sapiens kazrin, periplakin interacting protein	-5.4967346
FLG	NM_002016	Homo sapiens filaggrin	-5.4960876
SCAND2	NR_003654	Homo sapiens SCAN domain containing 2 pseudogene	-5.4488153
LILRB5	NM_006840	Homo sapiens leukocyte immunoglobulin-like receptor, subfamily B (with TM and ITIM domains), member 5	-5.210473
DEFB113	NM_001037729	Homo sapiens defensin, beta 113	-5.1864524
RNU1-5	NR_004400	Homo sapiens RNA, U1 small nuclear 5	-5.1660633
CEACAM7	NM_006890	Homo sapiens carcinoembryonic antigen-related cell adhesion molecule 7	-5.1170654
FCRL5	NM_001195388	Homo sapiens Fc receptor-like 5	-5.115607
DOK2	NM_003974	Homo sapiens docking protein 2	-5.030525
IL31	NM_001014336	Homo sapiens interleukin 31	-4.9612994
SERPINI2	NM_006217	Homo sapiens serpin peptidase inhibitor, clade I (pancpin), member 2	-4.946744
NDOR1	NM_001144026	Homo sapiens NADPH dependent diflavin oxidoreductase 1	-4.8756633
PRO0611	NR_002762	Homo sapiens PRO0611 protein	-4.8346343
CSN3	NM_005212	Homo sapiens casein kappa	-4.832802
KRT42P	NR_033415	Homo sapiens keratin 42 pseudogene	-4.7667203

TRIM3	NM_006458	Homo sapiens tripartite motif containing 3	-4.7564874
NCRNA00307	NR_038855	Homo sapiens non-protein coding RNA 307	-4.746788
CEP44	NM_001145314	Homo sapiens centrosomal protein 44kDa	-4.694463
CNPY1	NM_001103176	Homo sapiens canopy 1 homolog	-4.687589
SEC14L3	NM_174975	Homo sapiens SEC14-like 3	-4.6785803
FAM83C	NM_178468	Homo sapiens family with sequence similarity 83, member C	-4.6747828
EPB41	NM_203342	Homo sapiens erythrocyte membrane protein band 4.1	-4.670895
NCRNA00308	NR_038400	Homo sapiens non-protein coding RNA 308	-4.635309
ZNF560	NM_152476	Homo sapiens zinc finger protein 560	-4.614581
ZSCAN10	NM_032805	Homo sapiens zinc finger and SCAN domain containing 10	-4.59965
CHI3L1	NM_001276	Homo sapiens chitinase 3-like 1	-4.5791106
LANCL2	NM_018697	Homo sapiens LanC lantibiotic synthetase component C-like 2	-4.5460114
GNG2	NM_053064	Homo sapiens guanine nucleotide binding protein (G protein), gamma 2	-4.5214796
FBF1	NM_001080542	Homo sapiens Fas (TNFRSF6) binding factor 1	-4.501989
RD3	NM_183059	Homo sapiens retinal degeneration 3	-4.49653
RBM23	NM_001077351	Homo sapiens RNA binding motif protein 23	-4.475341
TAX1BP3	NM_014604	Homo sapiens Tax1 (human T-cell leukemia virus type I) binding protein 3	-4.469355
CLMP	NM_024769	Homo sapiens CXADR-like membrane protein	-4.465107
HHIPL1	NM_032425	Homo sapiens HHIP-like 1	-4.443919
XIRP2	NM_152381	Homo sapiens xin actin-binding repeat containing 2	-4.426423
EEF1A1	NM_001402	Homo sapiens eukaryotic translation elongation factor 1 alpha 1	-4.4053526
CAGE1	NM_001170692	Homo sapiens cancer antigen 1	-4.352445
MSH4	NM_002440	Homo sapiens mutS homolog 4	-4.3516383
STK31	NM_032944	Homo sapiens serine/threonine kinase 31	-4.348402
C1QC	NM_172369	Homo sapiens complement component 1, q subcomponent, C chain	-4.298029
OR52B4	NM_001005161	Homo sapiens olfactory receptor, family 52, subfamily B, member 4	-4.287528
HPGD	NM_000860	Homo sapiens hydroxyprostaglandin dehydrogenase 15	-4.2874207
NPPC	NM_024409	Homo sapiens natriuretic peptide C	-4.269714
KCNG2	NM_012283	Homo sapiens potassium voltage-gated channel, subfamily G, member 2	-4.261782
CRIP3	NM_206922	Homo sapiens cysteine-rich protein 3	-4.221094
CFHR2	NM_005666	Homo sapiens complement factor H-related 2	-4.197347
OR2T8	NM_001005522	Homo sapiens olfactory receptor, family 2, subfamily T, member 8	-4.196567
SCARNA16	NR_003013	Homo sapiens small Cajal body-specific RNA 16	-4.1780257
FRY	NM_023037	Homo sapiens furry homolog	-4.1688576
BEST1	NM_004183	Homo sapiens bestrophin 1	-4.1176815
RNU2-2	NR_002761	Homo sapiens RNA, U2 small nuclear 2	-4.1092715
BTBD9	NM_052893	Homo sapiens BTB (POZ) domain containing 9	-4.07787
FGF22	NM_020637	Homo sapiens fibroblast growth factor 22	-4.0691175

TTTY21	NR_001535	Homo sapiens testis-specific transcript, Y-linked 21	-4.0551863
RNU12	NR_029422	Homo sapiens RNA, U12 small nuclear	-4.0501595
HTR3B	NM_006028	Homo sapiens 5-hydroxytryptamine (serotonin) receptor 3B	-4.042065
ELAC2	NM_173717	Homo sapiens elaC homolog 2	-4.0066185
OR6N2	NM_001005278	Homo sapiens olfactory receptor, family 6, subfamily N, member 2	-4.006343
STIP1	NM_006819	Homo sapiens stress-induced-phosphoprotein 1	-4.003879
PRB4	NM_002723	Homo sapiens proline-rich protein BstNI subfamily 4	-3.9900327
KCNJ15	NM_170736	Homo sapiens potassium inwardly-rectifying channel, subfamily J, member 15	-3.9797218
GATA1	NM_002049	Homo sapiens GATA binding protein 1	-3.9709651
SLC10A6	NM_197965	Homo sapiens solute carrier family 10 (sodium/bile acid cotransporter family), member 6	-3.9443247
CYTH4	NM_013385	Homo sapiens cytohesin 4	-3.939965
PLEKHM3	NM_001080475	Homo sapiens pleckstrin homology domain containing, family M, member 3	-3.9233177
SLC4A5	NM_021196	Homo sapiens solute carrier family 4, sodium bicarbonate cotransporter, member 5	-3.9189212
CACNA1I	NM_021096	Homo sapiens calcium channel, voltage-dependent, T type, alpha 1I subunit	-3.9179988
CER1	NM_005454	Homo sapiens cerberus 1, cysteine knot superfamily, homolog	-3.9090295
PDE1C	NM_001191057	Homo sapiens phosphodiesterase 1C	-3.8955886
TTN	NM_133379	Homo sapiens titin	-3.8821275
PIGS	NM_033198	Homo sapiens phosphatidylinositol glycan anchor biosynthesis, class S	-3.8780873
TSPAN2	NM_005725	Homo sapiens tetraspanin 2	-3.870439
GABRQ	NM_018558	Homo sapiens gamma-aminobutyric acid (GABA) receptor, theta	-3.8608994
TBC1D3B	NM_001001417	Homo sapiens TBC1 domain family, member 3B	-3.8530922
FLJ16341	NR_033980	Homo sapiens hypothetical LOC400957	-3.850772
ADAM30	NM_021794	Homo sapiens ADAM metallopeptidase domain 30	-3.849467
WNT7A	NM_004625	Homo sapiens wingless-type MMTV integration site family, member 7A	-3.8393934
LRFN5	NM_152447	Homo sapiens leucine rich repeat and fibronectin type III domain containing 5	-3.7527678
PCLO	NM_014510	Homo sapiens piccolo (presynaptic cytomatrix protein)	-3.7487924
PRSS58	NM_001001317	Homo sapiens protease, serine, 58	-3.7485342
TARP	NM_001003799	Homo sapiens TCR gamma alternate reading frame protein	-3.7370687
DAPL1	NM_001017920	Homo sapiens death associated protein-like 1	-3.7273319
HYAL4	NM_012269	Homo sapiens hyaluronoglucosaminidase 4	-3.7211566
HEMGN	NM_018437	Homo sapiens hemogen	-3.7154548
CHST10	NM_004854	Homo sapiens carbohydrate sulfotransferase 10	-3.7049973
ISX	NM_001008494	Homo sapiens intestine-specific homeobox	-3.6912203
ZSCAN5B	NM_001080456	Homo sapiens zinc finger and SCAN domain containing 5B	-3.673115

ANKRD30B	NM_001145029	Homo sapiens ankyrin repeat domain 30B	-3.6584432
RNU105A	NR_004404	Homo sapiens RNA, U105A small nucleolar	-3.6451502
PROZ	NM_003891	Homo sapiens protein Z, vitamin K-dependent plasma glycoprotein	-3.63101
KLK10	NM_002776	Homo sapiens kallikrein-related peptidase 10	6.575816
EFCAB9	NM_001171183	Homo sapiens EF-hand calcium binding domain 9	6.2932844
TMEM26	NM_178505	Homo sapiens transmembrane protein 26	6.0545125
SLC10A7	NM_032128	Homo sapiens solute carrier family 10 (sodium/bile acid cotransporter family), member 7	5.8828216
PLCB4	NM_182797	Homo sapiens phospholipase C, beta 4	5.841824
MCM9	NM_153255	Homo sapiens minichromosome maintenance complex component 9	5.7155905
UGT8	NM_003360	Homo sapiens UDP glycosyltransferase 8	5.6220107
PTPRC	NM_002838	Homo sapiens protein tyrosine phosphatase, receptor type, C	5.4459214
FOXJ1	NM_001454	Homo sapiens forkhead box J1	5.2694902
KIAA0754	NM_015038	Homo sapiens KIAA0754	4.940688
PPM1A	NM_177951	Homo sapiens protein phosphatase, Mg2+/Mn2+ dependent, 1A	4.856635
MYL10	NM_138403	Homo sapiens myosin, light chain 10, regulatory	4.8453765
DLG2	NM_001364	Homo sapiens discs, large homolog 2	4.8151875
MYOZ2	NM_016599	Homo sapiens myozenin 2	4.7882605
NARG2	NM_024611	Homo sapiens NMDA receptor regulated 2	4.770257
KRTAP3-3	NM_033185	Homo sapiens keratin associated protein 3-3	4.7615805
GHR	NM_000163	Homo sapiens growth hormone receptor	4.7060866
HPCA	NM_002143	Homo sapiens hippocalcin	4.619414
FBXW2	NM_012164	Homo sapiens F-box and WD repeat domain containing 2	4.504634
HAND1	NM_004821	Homo sapiens heart and neural crest derivatives expressed 1	4.4445825
NPSR1	NM_207173	Homo sapiens neuropeptide S receptor 1	4.4138284
SRD5A2	NM_000348	Homo sapiens steroid-5-alpha-reductase, alpha polypeptide 2	4.39622
OR2M2	NM_001004688	Homo sapiens olfactory receptor, family 2, subfamily M, member 2	4.385679
IL2RG	NM_000206	Homo sapiens interleukin 2 receptor, gamma	4.3586574
SLC7A4	NM_004173	Homo sapiens solute carrier family 7 (orphan transporter), member 4	4.31417
C6	NM_000065	Homo sapiens complement component 6	4.3134027
C10orf81	NM_001193434	Homo sapiens chromosome 10 open reading frame 81	4.31175
NUP62CL	NM_017681	Homo sapiens nucleoporin 62kDa C-terminal like	4.2600613
RAP1GAP	NM_002885	Homo sapiens RAP1 GTPase activating protein	4.2497783
LNX1	NM_032622	Homo sapiens ligand of numb-protein X 1	4.212433
C4orf19	NM_018302	Homo sapiens chromosome 4 open reading frame 19	4.1853323
C16orf73	NM_152764	Homo sapiens chromosome 16 open reading frame 73	4.15877
OOEP	NM_001080507	Homo sapiens oocyte expressed protein	4.137426

MYH11	NM_001040114	Homo sapiens myosin, heavy chain 11	4.1324053
CBLN4	NM_080617	Homo sapiens cerebellin 4 precursor	4.1233478
EPDR1	NM_017549	Homo sapiens ependymin related protein 1	4.118658
HTR3E	NM_182589	Homo sapiens 5-hydroxytryptamine (serotonin) receptor 3, family member E	4.114653
FILIP1L	NM_182909	Homo sapiens filamin A interacting protein 1-like	4.04679
ISLR2	NM_020851	Homo sapiens immunoglobulin superfamily containing leucine-rich repeat 2	4.0254397
C10orf111	NM_153244	Homo sapiens chromosome 10 open reading frame 111	4.023104
ADAM7	NM_003817	Homo sapiens ADAM metallopeptidase domain 7	3.98616
C1orf116	NM_023938	Homo sapiens chromosome 1 open reading frame 116	3.9734225
KLK3	NM_001030050	Homo sapiens kallikrein-related peptidase 3	3.9705615
L1CAM	NM_000425	Homo sapiens L1 cell adhesion molecule	3.9692035
MALT1	NM_006785	Homo sapiens mucosa associated lymphoid tissue lymphoma translocation gene 1	3.9679544
FPGT-TNNI3K	NM_001199327	Homo sapiens FPGT-TNNI3K readthrough	3.967866
TRIM43	NM_138800	Homo sapiens tripartite motif containing 43	3.966672
C22orf41	NM_001123225	Homo sapiens chromosome 22 open reading frame 41	3.941643
BRSK1	NM_032430	Homo sapiens BR serine/threonine kinase 1	3.9395163
TUBAL3	NM_024803	Homo sapiens tubulin, alpha-like 3	3.9376917
SULT1C4	NM_006588	Homo sapiens sulfotransferase family, cytosolic, 1C, member 4	3.9312081
EPM2AIP1	NM_014805	Homo sapiens EPM2A (laforin) interacting protein 1	3.9263732
FBXL16	NM_153350	Homo sapiens F-box and leucine-rich repeat protein 16	3.88959
FLJ33360	NR_028351	Homo sapiens FLJ33360 protein	3.8839903
B3GAT1	NM_054025	Homo sapiens beta-1,3-glucuronyltransferase 1	3.8738415
KIF21A	NM_017641	Homo sapiens kinesin family member 21A	3.857627
CCK	NM_000729	Homo sapiens cholecystokinin	3.8558495
UMODL1	NM_173568	Homo sapiens uromodulin-like 1	3.854163
C1orf126	NR_027136	Homo sapiens chromosome 1 open reading frame 126	3.8402214
FAM184A	NM_024581	Homo sapiens family with sequence similarity 184, member A	3.837973
GYPE	NM_002102	Homo sapiens glycophorin E	3.8379157
ALDH8A1	NM_022568	Homo sapiens aldehyde dehydrogenase 8 family, member A1	3.8279617
DBF4	NM_006716	Homo sapiens DBF4	3.8249915
TDRG1	NR_024015	Homo sapiens testis development related protein 1	3.8203418
CNTD1	NM_173478	Homo sapiens cyclin N-terminal domain containing 1	3.8109999
ST8SIA2	NM_006011	Homo sapiens ST8 alpha-N-acetyl-neuraminide alpha-2,8-sialyltransferase 2	3.8014293
FLJ33534	NR_040080	Homo sapiens hypothetical LOC285150	3.7999313
ARHGEF26	NM_015595	Homo sapiens Rho guanine nucleotide exchange factor (GEF) 26	3.795749
CD83	NM_004233	Homo sapiens CD83 molecule	3.7942684

PRSS56	NM_001195129	Homo sapiens protease, serine, 56	3.7854364
GJC3	NM_181538	Homo sapiens gap junction protein, gamma 3	3.7840154
DAO	NM_001917	Homo sapiens D-amino-acid oxidase	3.7802026
ZMAT1	NM_001011657	Homo sapiens zinc finger, matrin-type 1	3.7773993
COL4A4	NM_000092	Homo sapiens collagen, type IV, alpha 4	3.766722
HOXB9	NM_024017	Homo sapiens homeobox B9	3.7637649
FAM135A	NM_020819	Homo sapiens family with sequence similarity 135, member A	3.7612922
OR2M3	NM_001004689	Homo sapiens olfactory receptor, family 2, subfamily M, member 3	3.7432675
CCDC87	NM_018219	Homo sapiens coiled-coil domain containing 87	3.7388036
GPR98	NM_032119	Homo sapiens G protein-coupled receptor 98	3.7176704
DNAH5	NM_001369	Homo sapiens dynein, axonemal, heavy chain 5	3.668384
HPR	NM_020995	Homo sapiens haptoglobin-related protein	3.6548119
ACPL2	NM_152282	Homo sapiens acid phosphatase-like 2	3.6438594
COL1A1	NM_000088	Homo sapiens collagen, type I, alpha 1	3.6359794
INPP4B	NM_003866	Homo sapiens inositol polyphosphate-4-phosphatase, type II	3.6334362
NXF2	NM_022053	Homo sapiens nuclear RNA export factor 2	3.631438
RGS1	NM_002922	Homo sapiens regulator of G-protein signalling 1	3.6119537
IL36G	NM_019618	Homo sapiens interleukin 36, gamma	3.6095219
SLC8A1	NM_021097	Homo sapiens solute carrier family 8 (sodium/calcium exchanger), member 1	3.5803816
ARHGEF7	NM_145735	Homo sapiens Rho guanine nucleotide exchange factor (GEF) 7	3.576161
C10orf93	NM_173572	Homo sapiens chromosome 10 open reading frame 93	3.5718787
C11orf40	NM_144663	Homo sapiens chromosome 11 open reading frame 40	3.570219
TEX19	NM_207459	Homo sapiens testis expressed 19	3.568851
LEUTX	NM_001143832	Homo sapiens leucine twenty homeobox	3.5589292
GPCRLTM7	NM_001195021	Homo sapiens putative olfactory receptor GPCRLTM7	3.5525014
RUFY2	NM_001042417	Homo sapiens RUN and FYVE domain containing 2	3.5239537
SLC7A8	NM_182728	Homo sapiens solute carrier family 7 (amino acid transporter light chain, L system), member 8	3.5139337
NBPF7	NM_001047980	Homo sapiens neuroblastoma breakpoint family, member 7	3.5125823
SORBS1	NM_001034954	Homo sapiens sorbin and SH3 domain containing 1	3.5078912
ARHGAP42	NM_152432	Homo sapiens Rho GTPase activating protein 42	3.4985898
SOX3	NM_005634	Homo sapiens SRY (sex determining region Y)-box 3	3.493397

Table 2. Detailed list of the 200 genes highest regulated by IL-1β in HCAEC.

Gene symbol	Accession number	Sequence description	Fold change
MYCN	NM_005378	Homo sapiens v-myc myelocytomatosis viral related oncogene, neuroblastoma derived	-48.749245
INHBB	NM_002193	Homo sapiens inhibin, beta B	-29.917957
CLEC4GP1	NR_002931	Homo sapiens C-type lectin domain family 4, member G pseudogene 1	-19.890667
DNASE1L3	NM_004944	Homo sapiens deoxyribonuclease I-like 3	-10.576039
ADRA1B	NM_000679	Homo sapiens adrenergic, alpha-1B-, receptor	-9.219272
GJA4	NM_002060	Homo sapiens gap junction protein, alpha 4	-8.887568
PLEKHA7	NM_175058	Homo sapiens pleckstrin homology domain containing, family A member 7	-8.722773
HRCT1	NM_001039792	Homo sapiens histidine rich carboxyl terminus 1	-8.206352
LIMCH1	NM_014988	Homo sapiens LIM and calponin homology domains 1	-7.9732385
EBF3	NM_001005463	Homo sapiens early B-cell factor 3	-7.9386687
LYVE1	NM_006691	Homo sapiens lymphatic vessel endothelial hyaluronan receptor 1	-7.8651233
ZNF395	NM_018660	Homo sapiens zinc finger protein 395	-7.3937955
CCDC48	NM_024768	Homo sapiens coiled-coil domain containing 48	-7.049505
LHX6	NM_014368	Homo sapiens LIM homeobox 6	-6.879648
KHK	NM_000221	Homo sapiens ketohexokinase	-6.8313956
TMEM236	NM_001098844	Homo sapiens transmembrane protein 236	-6.775998
ZNF366	NM_152625	Homo sapiens zinc finger protein 366	-6.765643
TMEM37	NM_183240	Homo sapiens transmembrane protein 37	-6.6180515
FRY	NM_023037	Homo sapiens furry homolog	-6.5588756
AQP1	NM_198098	Homo sapiens aquaporin 1	-6.194014
NRG2	NM_013982	Homo sapiens neuregulin 2	-6.034277
AMICA1	NM_153206	Homo sapiens adhesion molecule, interacts with CXADR antigen 1	-6.0145006
PRO0611	NR_002762	Homo sapiens PRO0611 protein	-5.9683604
B4GALNT4	NM_178537	Homo sapiens beta-1,4-N-acetyl-galactosaminyl transferase 4	-5.8034816
THBD	NM_000361	Homo sapiens thrombomodulin	-5.7642055
FAM26D	NM_153036	Homo sapiens family with sequence similarity 26, member D	-5.702154
NCRNA00323	NR_024100	Homo sapiens non-protein coding RNA 323	-5.6987195
PRICKLE1	NM_153026	Homo sapiens prickle homolog 1	-5.6285944
CLDN19	NM_148960	Homo sapiens claudin 19	-5.538379
SEC14L3	NM_174975	Homo sapiens SEC14-like 3	-5.520614
NCRNA00320	NR_024090	Homo sapiens non-protein coding RNA 320	-5.5172276
EHD3	NM_014600	Homo sapiens EH-domain containing 3	-5.488953
GALNTL2	NM_054110	Homo sapiens UDP-N-acetyl-alpha-D-galactosamine:polypeptide N-acetylgalactosaminyltransferase-like 2	-5.475902
RASSF9	NM_005447	Homo sapiens Ras association (RalGDS/AF-6) domain family (N-terminal) member 9	-5.4308662
ADAM11	NM_002390	Homo sapiens ADAM metallopeptidase domain 11	-5.4001203

FRY	NM_023037	Homo sapiens furry homolog	-5.3702507
SNX22	NM_024798	Homo sapiens sorting nexin 22	-5.349246
SSX2IP	NM_014021	Homo sapiens synovial sarcoma, X breakpoint 2 interacting protein	-5.312884
HES7	NM_001165967	Homo sapiens hairy and enhancer of split 7	-5.297948
DBP	NM_001352	Homo sapiens D site of albumin promoter (albumin D-box) binding protein	-5.2756314
RAB37	NM_175738	Homo sapiens RAB37, member RAS oncogene family	-5.251631
GIMAP7	NM_153236	Homo sapiens GTPase, IMAP family member 7	-5.246414
RUNX1T1	NM_004349	Homo sapiens runt-related transcription factor 1; translocated to, 1	-5.2318254
RPRML	NM_203400	Homo sapiens reprimo-like	-5.2271395
CLEC14A	NM_175060	Homo sapiens C-type lectin domain family 14, member A	-5.111908
CLDN22	NM_001111319	Homo sapiens claudin 22	-5.0853024
SOCS2	NM_003877	Homo sapiens suppressor of cytokine signalling 2	-5.0844283
CLDN3	NM_001306	Homo sapiens claudin 3	-5.064153
BDNF	NM_170735	Homo sapiens brain-derived neurotrophic factor	-5.0212407
FAM201A	NR_027294	Homo sapiens family with sequence similarity 201, member A	-5.014723
GIMAP5	NM_018384	Homo sapiens GTPase, IMAP family member 5	-4.9949155
SYN2	NM_133625	Homo sapiens synapsin II	-4.962457
NR0B1	NM_000475	Homo sapiens nuclear receptor subfamily 0, group B, member 1	-4.959428
BMP4	NM_001202	Homo sapiens bone morphogenetic protein 4	-4.9232016
GSTTP2	NR_003082	Homo sapiens glutathione S-transferase theta pseudogene 2	-4.8909044
NCRNA00277	NR_026949	Homo sapiens non-protein coding RNA 277	-4.854132
FILIP1	NM_015687	Homo sapiens filamin A interacting protein 1	-4.845783
TXNRD3NB	NM_001039783	Homo sapiens thioredoxin reductase 3 neighbor	-4.7800193
ANKRD34A	NM_001039888	Homo sapiens ankyrin repeat domain 34A	-4.7779975
KIAA1875	NR_024207	Homo sapiens KIAA1875	-4.774847
TRIL	NM_014817	Homo sapiens TLR4 interactor with leucine-rich repeats	-4.7655497
IMPA2	NM_014214	Homo sapiens inositol(myo)-1(or 4)-monophosphatase 2	-4.7185154
FLYWCH1	NM_032296	Homo sapiens FLYWCH-type zinc finger 1	-4.7098217
ANKRD20A9P	NR_027995	Homo sapiens ankyrin repeat domain 20 family, member A9, pseudogene	-4.7062373
LMCD1	NM_014583	Homo sapiens LIM and cysteine-rich domains 1	-4.7046704
TMEM178	NM_152390	Homo sapiens transmembrane protein 178	-4.6681147
SOX18	NM_018419	Homo sapiens SRY (sex determining region Y)-box 18	-4.6410155
HRK	NM_003806	Homo sapiens harakiri, BCL2 interacting protein	-4.603894
CELSR1	NM_014246	Homo sapiens cadherin, EGF LAG seven-pass G-type receptor 1	-4.5569406
TRIM45	NM_025188	Homo sapiens tripartite motif containing 45	-4.5300555
LHX9	NM_020204	Homo sapiens LIM homeobox 9	-4.5149674

ACOT6	NM_001037162	Homo sapiens acyl-CoA thioesterase 6	-4.5146165
RLN2	NM_005059	Homo sapiens relaxin 2	-4.510096
IGSF6	NM_005849	Homo sapiens immunoglobulin superfamily, member 6	-4.4997478
SERTAD4	NM_019605	Homo sapiens SERTA domain containing 4	-4.455149
NFE2L2	NM_006164	Homo sapiens nuclear factor (erythroid-derived 2)-like 2	-4.4319816
ERV3-1	NM_001007253	Homo sapiens endogenous retrovirus group 3, member 1	-4.407914
NHSL2	NM_001013627	Homo sapiens NHS-like 2	-4.3638372
CCDC165	NM_015210	Homo sapiens coiled-coil domain containing 165	-4.3601694
ST8SIA4	NM_005668	Homo sapiens ST8 alpha-N-acetyl-neuraminide alpha-2,8-sialyltransferase 4	-4.3535028
FAM183B	NR_028347	Homo sapiens family with sequence similarity 183, member B	-4.3384457
PNMAL1	NM_018215	Homo sapiens PNMA-like 1	-4.3220973
ARHGAP20	NM_020809	Homo sapiens Rho GTPase activating protein 20	-4.322003
NLRP12	NM_033297	Homo sapiens NLR family, pyrin domain containing 12	-4.293668
LYPD1	NM_144586	Homo sapiens LY6/PLAUR domain containing 1	-4.2919726
RARB	NM_000965	Homo sapiens retinoic acid receptor, beta	-4.282265
SAMD13	NM_001010971	Homo sapiens sterile alpha motif domain containing 13	-4.2682867
OR4C12	NM_001005270	Homo sapiens olfactory receptor, family 4, subfamily C, member 12	-4.255225
GIMAP1	NM_130759	Homo sapiens GTPase, IMAP family member 1	-4.236272
DPRXP4	NR_002221	Homo sapiens divergent-paired related homeobox pseudogene 4	-4.225941
CSPG5	NM_006574	Homo sapiens chondroitin sulfate proteoglycan 5	-4.224571
CCDC30	NM_001080850	Homo sapiens coiled-coil domain containing 30	-4.208119
WNT7A	NM_004625	Homo sapiens wingless-type MMTV integration site family, member 7A	-4.1847167
PPARG	NM_138711	Homo sapiens peroxisome proliferator-activated receptor gamma	-4.1499724
MAMLD1	NM_005491	Homo sapiens mastermind-like domain containing 1	-4.1428905
PLB1	NM_153021	Homo sapiens phospholipase B1	-4.141613
BCL11A	NM_022893	Homo sapiens B-cell CLL/lymphoma 11A	-4.129264
ZNF521	NM_015461	Homo sapiens zinc finger protein 521	-4.1025825
NEURL1B	NM_001142651	Homo sapiens neuralized homolog 1B	-4.080128
FAM90A7	NM_001136572	Homo sapiens family with sequence similarity 90, member A7	-4.076752
IL1B	NM_000576	Homo sapiens interleukin 1, beta	628.58215
CCL8	NM_005623	Homo sapiens chemokine (C-C motif) ligand 8	567.51654
SELE	NM_000450	Homo sapiens selectin E	523.0239
CXCL1	NM_001511	Homo sapiens chemokine (C-X-C motif) ligand 1	501.29193
CXCL3	NM_002090	Homo sapiens chemokine (C-X-C motif) ligand 3	429.9673
CXCL2	NM_002089	Homo sapiens chemokine (C-X-C motif) ligand	364.44318

		2	
IL8	NM_000584	Homo sapiens interleukin 8	324.8047
TNF	NM_000594	Homo sapiens tumor necrosis factor	271.97995
CCL3	NM_002983	Homo sapiens chemokine (C-C motif) ligand 3	239.2062
CCL20	NM_004591	Homo sapiens chemokine (C-C motif) ligand 20	206.19748
CXCR7	NM_020311	Homo sapiens chemokine (C-X-C motif) receptor 7	193.35707
C15orf48	NM_032413	Homo sapiens chromosome 15 open reading frame 48	188.21423
CXCL6	NM_002993	Homo sapiens chemokine (C-X-C motif) ligand 6	182.55176
C2CD4A	NM_207322	Homo sapiens C2 calcium-dependent domain containing 4A	119.190605
NEURL3	NR_026875	Homo sapiens neuralized homolog 3 (Drosophila) pseudogene	110.60467
UBD	NM_006398	Homo sapiens ubiquitin D	100.76968
CD69	NM_001781	Homo sapiens CD69 molecule	90.45913
TRAF1	NM_005658	Homo sapiens TNF receptor-associated factor 1	84.80847
IL6	NM_000600	Homo sapiens interleukin 6	82.71982
CXCL11	NM_005409	Homo sapiens chemokine (C-X-C motif) ligand 11	81.203156
RSAD2	NM_080657	Homo sapiens radical S-adenosyl methionine domain containing 2	80.846924
BIRC3	NM_001165	Homo sapiens baculoviral IAP repeat containing 3	67.27173
LTB	NM_002341	Homo sapiens lymphotoxin beta	65.086105
IL1A	NM_000575	Homo sapiens interleukin 1, alpha	63.525673
TNFAIP3	NM_006290	Homo sapiens tumor necrosis factor, alpha-induced protein 3	60.4407
TNIP3	NM_024873	Homo sapiens TNFAIP3 interacting protein 3	59.825535
VCAM1	NM_001078	Homo sapiens vascular cell adhesion molecule 1	57.014397
TLR2	NM_003264	Homo sapiens toll-like receptor 2	56.306362
F3	NM_001993	Homo sapiens coagulation factor III	50.284866
PTGS2	NM_000963	Homo sapiens prostaglandin-endoperoxide synthase 2	44.905956
CXCL1	NM_001511	Homo sapiens chemokine (C-X-C motif) ligand 1	40.032032
SGPP2	NM_152386	Homo sapiens sphingosine-1-phosphate phosphatase 2	38.973095
RGS16	NM_002928	Homo sapiens regulator of G-protein signalling 16	38.702847
RCSD1	NM_052862	Homo sapiens RCSD domain containing 1	38.01366
SOD2	NM_001024465	Homo sapiens superoxide dismutase 2, mitochondrial	36.718346
TNFAIP2	NM_006291	Homo sapiens tumor necrosis factor, alpha-induced protein 2	35.506237
CSF3	NM_000759	Homo sapiens colony stimulating factor 3	35.368214
TNFAIP6	NM_007115	Homo sapiens tumor necrosis factor, alpha-induced protein 6	35.234
C3	NM_000064	Homo sapiens complement component 3	33.966663
C1S	NM_001734	Homo sapiens complement component 1, s subcomponent	33.94064
NFKBIZ	NM_031419	Homo sapiens nuclear factor of kappa light	33.30885

		polypeptide gene enhancer in B-cells inhibitor, zeta	
CCL2	NM_002982	Homo sapiens chemokine (C-C motif) ligand 2	31.177633
CLEC2D	NM_013269	Homo sapiens C-type lectin domain family 2, member D	30.127642
FAM65C	NM_080829	Homo sapiens family with sequence similarity 65, member C	29.93501
IL18R1	NM_003855	Homo sapiens interleukin 18 receptor 1	29.57203
NOD2	NM_022162	Homo sapiens nucleotide-binding oligomerization domain containing 2	29.374725
CXCL10	NM_001565	Homo sapiens chemokine (C-X-C motif) ligand 10	27.42973
CFB	NM_001710	Homo sapiens complement factor B	27.262953
CCL5	NM_002985	Homo sapiens chemokine (C-C motif) ligand 5	26.525106
NR4A3	NM_173200	Homo sapiens nuclear receptor subfamily 4, group A, member 3	25.799444
BDKRB2	NM_000623	Homo sapiens bradykinin receptor B2	25.538664
EBI3	NM_005755	Homo sapiens Epstein-Barr virus induced 3	25.296314
MAP3K8	NM_005204	Homo sapiens mitogen-activated protein kinase kinase kinase 8	24.689005
TNFRSF9	NM_001561	Homo sapiens tumor necrosis factor receptor superfamily, member 9	24.13026
SLC7A2	NM_001008539	Homo sapiens solute carrier family 7 (cationic amino acid transporter, y+ system), member 2	24.04523
CXCL10	NM_001565	Homo sapiens chemokine (C-X-C motif) ligand 10	23.984573
KIRREL2	NM_199180	Homo sapiens kin of IRRE like 2	23.426357
LITAF	NM_004862	Homo sapiens lipopolysaccharide-induced TNF factor	23.305717
ICAM1	NM_000201	Homo sapiens intercellular adhesion molecule 1	23.237846
RTP4	NM_022147	Homo sapiens receptor (chemosensory) transporter protein 4	22.30666
C3	NM_000064	Homo sapiens complement component 3	21.691349
SELE	NM_000450	Homo sapiens selectin E	21.351578
MMP10	NM_002425	Homo sapiens matrix metallopeptidase 10	21.229311
CMPK2	NM_207315	Homo sapiens cytidine monophosphate (UMP-CMP) kinase 2, mitochondrial	21.192596
GOT1L1	NM_152413	Homo sapiens glutamic-oxaloacetic transaminase 1-like 1	20.017305
CLDN1	NM_021101	Homo sapiens claudin 1	19.82994
IL18R1	NM_003855	Homo sapiens interleukin 18 receptor 1	19.33128
BCL2A1	NM_004049	Homo sapiens BCL2-related protein A1	19.308804
SLC6A4	NM_001045	Homo sapiens solute carrier family 6	18.38842
VSTM1	NM_198481	Homo sapiens V-set and transmembrane domain containing 1	18.058065
CCL4	NM_002984	Homo sapiens chemokine (C-C motif) ligand 4	17.710985
CCL4	NM_002984	Homo sapiens chemokine (C-C motif) ligand 4	17.653017
LAD1	NM_005558	Homo sapiens ladinin 1	17.627607
OASL	NM_003733	Homo sapiens 2'-5'-oligoadenylate synthetase-like	17.497292
CLDN14	NM_144492	Homo sapiens claudin 14	17.131746
SOCS1	NM_003745	Homo sapiens suppressor of cytokine signalling 1	16.820028
CXCL2	NM_002089	Homo sapiens chemokine (C-X-C motif) ligand	16.501673

		2	
PITX2	NM_153426	Homo sapiens paired-like homeodomain 2	15.021445
IFIT2	NM_001547	Homo sapiens interferon-induced protein with tetratricopeptide repeats 2	15.00921
PRRX1	NM_006902	Homo sapiens paired related homeobox 1	14.835137
OXTR	NM_000916	Homo sapiens oxytocin receptor	14.744355
CSF3	NM_000759	Homo sapiens colony stimulating factor 3	14.631831
NFKBIA	NM_020529	Homo sapiens nuclear factor of kappa light polypeptide gene enhancer in B-cells inhibitor, alpha	14.564752
MX2	NM_002463	Homo sapiens myxovirus (influenza virus) resistance 2	14.004878
ITGB8	NM_002214	Homo sapiens integrin, beta 8	13.91287
CSF2	NM_000758	Homo sapiens colony stimulating factor 2	13.673741
C6orf58	NM_001010905	Homo sapiens chromosome 6 open reading frame 58	13.255741
IL7R	NM_002185	Homo sapiens interleukin 7 receptor	13.228039
LIF	NM_002309	Homo sapiens leukemia inhibitory factor	13.028622
NPTX1	NM_002522	Homo sapiens neuronal pentraxin I	12.880365
IFIT2	NM_001547	Homo sapiens interferon-induced protein with tetratricopeptide repeats 2	12.85912
FGF18	NM_003862	Homo sapiens fibroblast growth factor 18	12.7818
GBP1	NM_002053	Homo sapiens guanylate binding protein 1, interferon-inducible	12.647643
RAB11FIP1	NM_001002814	Homo sapiens RAB11 family interacting protein 1	12.551967
ELOVL7	NM_024930	Homo sapiens ELOVL fatty acid elongase 7	12.131871
C11orf96	NM_001145033	Homo sapiens chromosome 11 open reading frame 96	12.129249
CSF1	NM_172210	Homo sapiens colony stimulating factor 1	12.096482
TMEM106A	NM_145041	Homo sapiens transmembrane protein 106A	12.058173
CD69	NR_026672	Homo sapiens CD69 molecule	12.0577545
GBP5	NM_052942	Homo sapiens guanylate binding protein 5	11.924029

SUPPLEMENTAL FIGURES

Figure 1

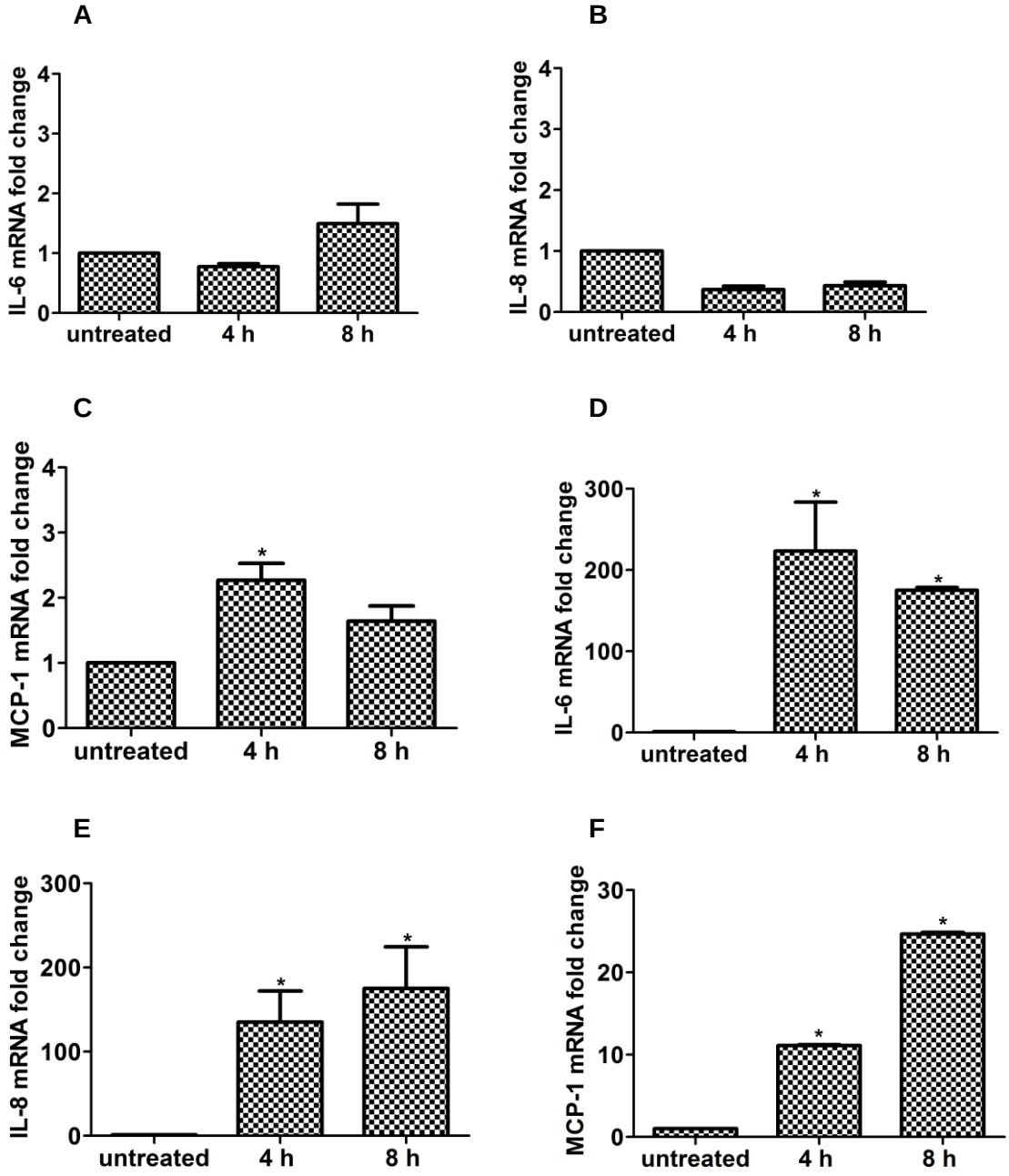

Figure 1. Regulation of inflammatory cytokines by Wnt5A and IL-1β. Expression of mRNA levels of IL-6 (**A, D**), IL-8 (**B, E**) and MCP-1 (**C, F**) in HCAEC treated with Wnt5A (**A, B, C**) or IL-1β (**D, E, F**) for 4 h and 8 h. Data were obtained from three independent qRT-PCR experiments run in duplicates and expressed as the mean ± S.E.M. **P*<0.05 by Student's *t*-test

Figure 2

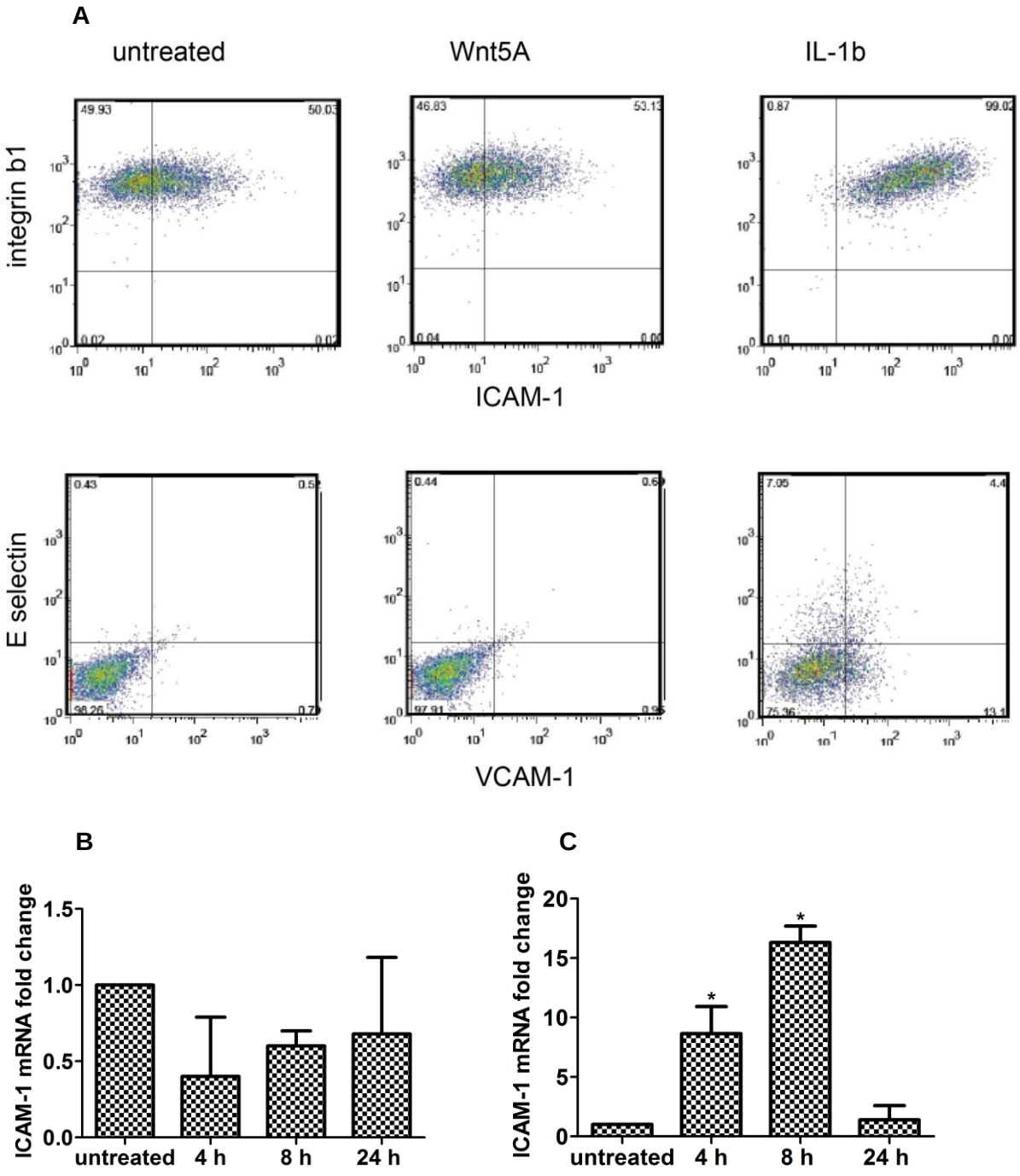

Figure 2. Endothelial cell adhesion molecules expression. (**A**) Flow cytometry analyses of VCAM-1 (CD106), ICAM-1 (CD54), E selectins (CD62E) and human integrin b1 chain (CD29) expression in Wnt5A and IL-1β (IL-1b)-treated HCAEC. (**B,C**) qRT-PCR analyses of ICAM-1 mRNA expression in HCAEC treated with **(B)** Wnt5A and **(C)** IL-1β for 4 h, 8 h and 24 h. Data were obtained from three independent experiments run in duplicates and expressed as the mean ± S.E.M. **P*<0.05 by Student's *t*-test.

Figure 3

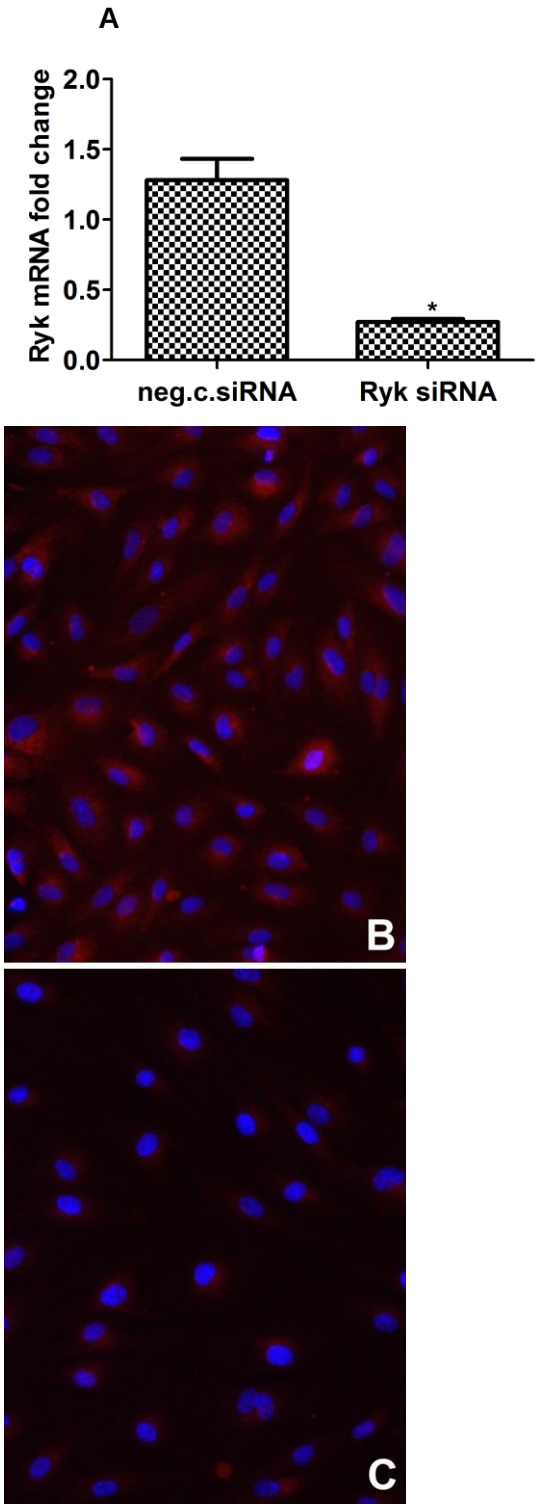

Figure 3. Knockdown of Ryk expression. (A) Changes in the mRNA expression level of Ryk in HCAEC transfected with 5 nM negative control siRNA (neg.c.siRNA) and Ryk siRNA. Data were obtained from three independent qRT-PCR experiments run in duplicates and expressed as the mean ± S.E.M. *P<0.05 by Student's t-test. Immunofluorescence staining for Ryk protein expression in **(B)** negative control siRNA transfected and **(C)** Ryk-siRNA transfected HCAEC. Ryk (red), nuclei (DAPI, blue). Zeiss Axioskope, magnification 200 fold.

Figure 4

A

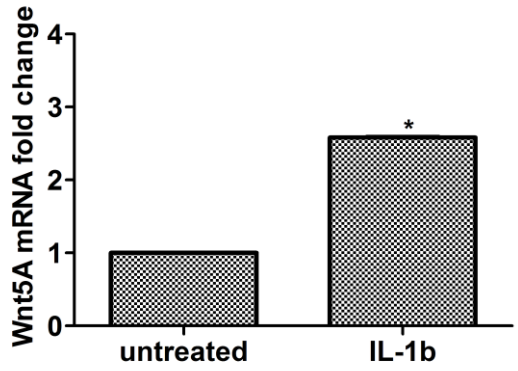

B

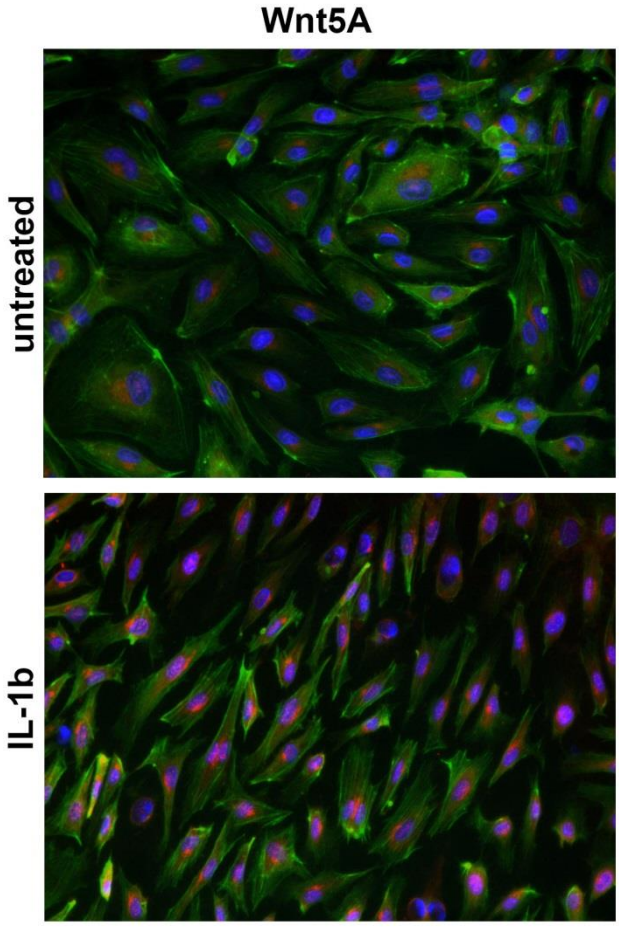

Figure 4. Wnt5A expression induced by IL-1β treatment. (**A**) Fold changes in the expression of Wnt5A mRNA in HCAEC treated with IL-1β (IL-1b) for 8 h. Data were obtained from three independent qRT-PCR experiments run in duplicates and expressed as the mean ± S.E.M. **P*<0.05 by Student's *t*-test. (**B**) Immunofluorescence staining for Wnt5A protein expression in non-treated and 8 h IL-1β-treated HCAEC. Wnt5A (red), F-actin (phalloidin, green), and nuclei (DAPI, blue). Zeiss Axioskope, magnification 200 fold.

Figure 5

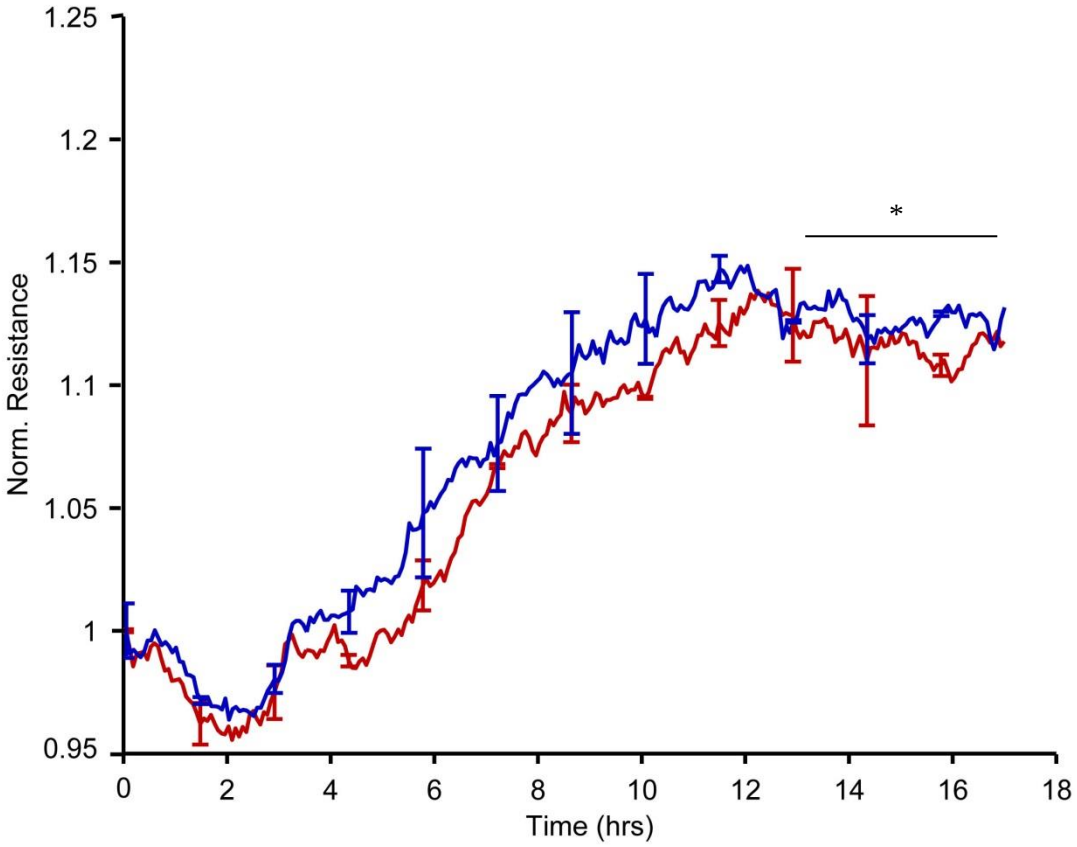

Figure 5. Formation of confluent HCAEC monolayer in 8W10E+ ECIS array. HCAEC seeded into an 8W10E+ array with a density of 80,000- 90,000 cells/well. Soon after cell seeding, resistance measurements (in Ohms) were started and are shown as normalized resistance (subsequent values were divided by initial values). Rise in resistance with respect to time indicates that cells were forming contacts between each other. The steady state (marked by *) indicates the stage at which maximum resistance is reached to form a tight monolayer. Resistance measurements were conducted in duplicate wells which were grouped and averaged to plot as single curve. Error bars of curves represent SD. Figure shown depict the resistance measurements conducted at 4000 Hz. Red and Blue, Untreated.

6.2 IL-4 Causes Hyperpermeability of Vascular Endothelial Cells through Wnt5A Signaling

Tom Skaria, Julia Burgener, Esther Bachli, Gabriele Schoedon

IL-4 Causes Hyperpermeability of Vascular Endothelial Cells through Wnt5A Signaling

Tom Skaria[1], Julia Burgener[1], Esther Bachli[2], Gabriele Schoedon[1]*

[1]Inflammation Research Unit, Department of Medicine, Division of Internal Medicine, University Hospital Zürich, Zürich, Switzerland
[2]Department of Medicine, Uster Hospital, Uster, Switzerland

* Corresponding author
Email: klinsog@usz.uzh.ch (GS)

Abstract

Microvascular leakage due to endothelial barrier dysfunction is a prominent feature of T helper 2 (Th2) cytokine mediated allergic inflammation. Interleukin-4 (IL-4) is a potent Th2 cytokine, known to impair the barrier function of endothelial cells. However, the effectors mediating IL-4 induced cytoskeleton remodeling and consequent endothelial barrier dysfunction remain poorly defined. Here we have used whole genome transcriptome profiling and gene ontology analyses to identify the genes and processes regulated by IL-4 signaling in human coronary artery endothelial cells (HCAEC). The study revealed Wnt5A as an effector that can mediate actin cytoskeleton remodeling in IL-4 activated HCAEC through the regulation of LIM kinase (LIMK) and Cofilin (CFL). Following IL-4 treatment, LIMK and CFL were phosphorylated, thereby indicating the possibility of actin stress fiber formation. Imaging of actin showed the formation of stress fibers in IL-4 treated live HCAEC. Stress fiber formation was notably decreased in the presence of Wnt inhibitory factor 1 (WIF1). Non-invasive impedance measurements demonstrated that IL-4 increased the permeability and impaired the barrier function of HCAEC monolayers. Silencing Wnt5A significantly reduced permeability and improved the barrier function of HCAEC monolayers upon IL-4 treatment. Our study identifies Wnt5A as a novel marker of IL-4 activated vascular endothelium and demonstrates a critical role for Wnt5A in mediating IL-4 induced endothelial barrier dysfunction. Wnt5A could be a potential therapeutic target for reducing microvascular leakage and edema formation in Th2 driven inflammatory diseases.

Introduction

Interleukin-4 (IL-4) is a multifunctional pleiotropic type I cytokine secreted by activated T helper (Th) 2 cells, basophils, eosinophils and mast cells [1,2]. Functionally, IL-4 induces the differentiation of antigen stimulated naïve T cells to a Th2 phenotype [3,4]. It also regulates immunoglobulin (Ig) class switching so that B lymphocytes express IgE [5], and regulates apoptosis, cell proliferation and expression of several genes in different cell types such as fibroblasts, macrophages, endothelial and epithelial cells [1,2]. IL-4 drives the 'alternative activation of macrophages' to produce the M2 phenotype, which is crucially involved in type 2 immunity. Thus, through its effects on multiple cell types and by binding to alternative cell surface receptors [1], IL-4 plays critical roles in allergic inflammation [6], immune response to extracellular parasites including helminths, autoimmunity [2] and tumor inflammation and metastasis [1,7].

Recent evidence suggests a potential role for IL-4 in generating a proinflammatory environment in vascular endothelial cells (VEC) [8]. VEC are essential for maintaining vascular homeostasis in normal physiological conditions [9]. Under pathophysiological conditions, activated blood components, pathogens or inflammatory mediators such as cytokines act upon VEC and heavily alter their functions, conferring on them an inflamed phenotype. These alterations include a change from the anticoagulant phenotype to a procoagulant state, increased production of vasoactive substances, expression of cell adhesion molecules, synthesis of inflammatory mediators including chemoattractants, and endothelial barrier dysfunction causing microvascular leakage. It has been demonstrated that IL-4 upregulates the expression of vascular cell adhesion molecule (VCAM)-1 [10-12], IL-6 [12-14] and monocyte chemotactic protein (MCP) [12,14] in human umbilical vein endothelial cells (HUVEC). Moreover, stimulation with IL-4 increased the adhesion of peripheral blood monocytes [15] and T cells [16] to HUVEC. IL-4 has been shown to induce cytoskeletal rearrangements in HUVEC and significantly regulate their proliferation [17]. Further, IL-4 acts as a modest mitogen for both macro and microvascular endothelial cells [8,17-19]. IL-4 has proatherogenic effects and induces the apoptosis of endothelial cells causing increased endothelial cell turnover [20]. It has been demonstrated that IL-4 induces hyperpermeability of HUVEC, causing vascular leakage [21], however, effectors responsible for IL-4 induced endothelial hyperpermeability and consequent barrier dysfunction remain unidentified. Moreover, these previous studies addressing the effects of IL-4 on endothelial inflammation used HUVEC as the primary endothelial cell model system. HUVEC that are obtained from the immune naïve foetal tissue shows significant variations in function compared with adult vascular endothelium and hence may be an inappropriate primary cell model of vascular endothelium [22]. The targets and effects of IL-4 signaling in adult VEC, therefore, may vary from HUVEC and have to be elucidated.

In the present study, we used transcriptome profiling to identify the genes regulated by paracrine IL-4 signaling in our established *in vitro* model of adult VEC, cultured human coronary artery endothelial cells (HCAEC) [23]. Here we identify Wnt5A as one of the genes significantly upregulated by IL-4 treatment. We further demonstrate a critical role for IL-4 induced Wnt5A in impairing barrier function of endothelial monolayers. Our findings suggest a prominent role for Wnt5A in causing microvascular leakage associated with IL-4 driven allergic inflammation and other pathophysiological conditions.

Methods

Cell Culture

HCAEC and human pulmonary artery endothelial cells (HPAEC) purchased from Clonetics (Lonza, USA) were cultured in EBM-2 medium (Clonetics, Lonza, USA) supplemented with EGM-2MV Single Quots and 5% FBS (Clonetics, Lonza) as described previously [23]. For experiments, cells at passages three to six were used and the serum in culture medium was decreased to 2% FBS. Macrophages derived from human PBMC were cultured as described [24]. Cells were cultured under standard conditions (37°C, 5% CO2, 80% humidity) in a Class 100 HEPA air filtered system (SteriCult, Fisher Scientific, Switzerland). Culture medium without antibiotics was used to prevent masked low-level contamination in cell cultures. Treatments were carried out using recombinant human (rh) IL-4 (4 ng/mL; purity >98%; PeproTech, USA), rh IL-6 (20 U/mL; purity >98%; PeproTech, USA), rh soluble Frizzled-related peptide-1 (sFRP1; 10 µg/mL; purity > 95%; R&D systems, USA), rh/mouse Wnt5A (250 ng/mL; CHO-derived Gln38-Lys380, purity >80%, endotoxin level <1.0 EU/µg of protein; R&D systems, USA) and rh Wnt inhibitory factor 1 (WIF1; 15 µg/mL; purity >97%; R&D systems, USA). Sterile biopure ep Dualfilter T.I.P.S.sterile filter tips (Eppendorf, Germany) were used throughout the study.

RNA Isolation and Quantitative Real-Time PCR (qRT-PCR) Analyses

RNA isolation and qRT-PCR using the HPRT gene as endogenous control were performed as described previously [25]. Sequence specific PCR detection primers used for Wnt5A, IL-6 and HPRT are as follows: Wnt5A forward, 5'-AGT TGC CTA CCC TAG C-3'; Wnt5A reverse, 5'-GTG CCT TCG TGC CTA T-3'; IL-6 forward, 5'-CCT GAC CCA ACC ACA AA-3'; IL-6 reverse, 5'-AGT GTC CTA ACG CTC ATA C-3'; HPRT forward, 5'-CCA GTC AAC AGG GGA CAT AAA-3'; HPRT reverse, 5'-CAC AAT CAA GAC ATT CTT TCC AGT-3'. Thermal cycling conditions set in the 7500 Fast Real-Time PCR System (Applied Biosystems, USA) involved an initial denaturation step (10 min, 95°C) followed by 40 cycles of denaturation (15 sec, 95°C), annealing (30 sec, 55°C), and extension (30 sec, 72°C).

Differential Gene Expression Profiling

Microarray based gene expression profiling and scanning, feature extraction and data normalization of microarrays were performed as described previously [25]. Complete data sets for the IL-4 regulated transcriptome in HCAEC are available in the NCBI GEO data repository, accession number GSE64860.

Microarray Data Analyses

The preprocessed microarray data was analyzed using GeneSpring GX 9.0 Software (Agilent Tech. Inc.) with default settings for two color arrays and a fold change (FC) cutoff of 2. Using MetaCore™ GeneGO software (Thomson Reuters, http://portal.genego.com), genes regulated ≥2 fold in their expression and satisfying a *P* value <0.05 were grouped into pathways according to their biologic functions and gene ontology (GO) classes.

Immunofluorescence Staining

HCAEC were grown in four-chamber culture slides coated with rat tail collagen type I (diluted 0.01% in sterile pyrogen-free water; BD Biosciences, USA). To stain for VE-cadherin, HCAEC were grown to a confluent monolayer. After treatment with appropriate stimuli, cells were fixed with 4% formalin in PBS for 20 min. After washing three times with PBS (pH 7.4) at room temperature (RT), slides were treated with blocking solution for 1 h at RT. Depending on the source of secondary antibodies, blocking solution containing either 10% goat serum and 1% BSA (for secondary antibodies derived from goat) or 10% rabbit serum and 1% BSA in PBS (for secondary antibodies derived from rabbit) was used. After washing three times with PBS at RT, slides were incubated with primary antibodies diluted in blocking solution at 4°C overnight. The following antibodies were used with dilutions indicated: rabbit anti-VE-cadherin, polyclonal (1:100; Product No. 2158, Cell Signaling Technology), rabbit anti-phospho LIMK2, polyclonal (1:300; Product No. Ab131343, Abcam), rabbit anti-phospho CFL, polyclonal (1:500; Product No. Ab100836, Abcam), goat anti-Wnt5A, polyclonal (1:500; Cat. No. AF645, R&D Systems). Slides were then washed three times with PBS at RT. Depending on the first antibody's species, slides were incubated with Alexa 568 labelled goat anti-rabbit or rabbit anti-goat secondary antibodies (1:2000; Molecular Probes, Invitrogen, USA) for 1 h at RT in the dark. Incubations with secondary antibody were combined with Alexa Fluor 488 Phalloidin (1:80; Molecular Probes, Invitrogen, USA) to visualize F-actin. Slides were washed three times with PBS at RT, counterstained with 10 µg/mL diamidino-phenylindole (DAPI; Sigma-Aldrich) and mounted using ProLong® Gold Antifade (Life Technologies, USA). Images were captured using an Axioskope microscope equipped with an AxioCam MRm digital camera and the associated AxioVision Rel.4.6 software (Carl Zeiss, Feldbach Switzerland). Fluorescent intensity was quantified from five different areas of the

respective fluorescent images using ImageJ based Fiji software (Fiji is just ImageJ) and corrected for background fluorescence to obtain cellular fluorescent intensity.

Inhibition of Rho associated protein serine/threonine kinases (ROCK)

Y-27632 (Calbiochem; Millipore, USA) at a concentration of 10 μM [26] was used to inhibit the activation of ROCK. ROCK inhibition experiments were performed by incubating cells in medium containing Y-27632 alone or in combination with IL-4 for 1 h and 4 h.

Live Cell Imaging of Actin

HCAEC monolayers were grown in rat tail collagen type I coated optical 96 microwell culture plates (Thermo Scientific, USA). Cells were incubated with CellLight® Actin-RFP probe (Cat. No. C10583, Life Technologies, USA) according to manufacturer's instructions. After medium change, cells were treated with IL-4 or Wnt5A alone or in combination with sFRP1 or WIF1. Cells were further incubated up to 12 h. Images of live actin cytoskeleton organization were obtained using the Axio Observer.Z1 inverted microscope equipped with an AxioCam MRm digital camera and the associated ZEN 2012 software (Carl Zeiss, Feldbach, Switzerland).

Wnt5A Silencing

To knockdown Wnt5A expression, HCAEC grown up to 80% confluency in 24-well plates were incubated with transfection complexes formed from Wnt5A-siRNA (5 nM; Hs_Wnt5A_6, Cat. No. SI03025596; Qiagen) and 6 μL/mL HiPerFect Transfection reagent (Qiagen GmbH, Hilden, Germany) in EBM-2 basal medium (Clonetics, Lonza, USA) for 24 h. After splitting using Trypsin EDTA, transfected cells were seeded onto collagen coated 6 well plates, retransfected for an additional round as above and incubated until the cells reached 90% confluency. HCAEC were also transfected with validated AllStars negative control siRNA (Qiagen) in parallel to control for 'off target' effects of siRNAs. Cells were then either treated with IL-4 for 8 h and lysed (for qRT-PCR analyses) or trypsinized and seeded into collagen-coated 8W10E+ arrays (for ECIS barrier function assays, see below). Treatments were carried out in EGM-2 MV medium with 2% FBS devoid of transfection complexes. To immunostain for Wnt5A, HCAEC transfected once with Wnt5A-siRNA were harvested by trypsinization and seeded into collagen-coated BD Falcon 4 chamber culture slides (BD Biosciences, USA). There, an additional round of Wnt5A-siRNA transfection was performed as in 24-well plates, incubated until the cells attained monolayer confluency and fixed for immunostaining.

Electric Cell-substrate Impedance Sensing (ECIS) of Endothelial Barrier Function

Using ECIS, the response of endothelial barrier to the stimulus can be assessed by continuously recording changes in transendothelial resistance (TEER) [27,28]. Endothelial barrier function was detected in real time using the ECIS® Z-theta system (Applied Biophysics) with associated software v.1.2.126 PC as follows: after equilibrating with EBM-2 basal medium (Clonetics, Lonza, USA) for 24 h, 8W10E+ arrays were coated with rat tail collagen type I (diluted 0.01% in sterile pyrogen-free water; BD Biosciences, USA) for 12 h. A monodisperse suspension of HCAEC in EGM-2 MV medium (Clonetics, Lonza, USA) supplemented with 5% FBS was added to the arrays at a density of 80,000–90,000 cells/well and incubated up to 24 h to form a uniform dense monolayer (S1 Fig.). Treatments were carried out in fresh medium with or without stimuli. Resistance of HCAEC monolayer was measured in Ohms at multiple frequencies ranging from 62.6 Hz to 64 kHz. Each of the eight wells of the 8W10E+ arrays contain 40 electrodes that trace the cells at 40 different locations in each well. The measurements from each well were averaged.

Automated Cell Migration Assay Using ECIS

The non-invasive ECIS assisted wound healing assay makes a highly reproducible wound with a specific diameter of 250 μm without damaging cells in the surrounding region in 8W1E arrays [29]. It was used for studying cell migration and was performed as follows: equilibration and collagen coating of 8W1E single electrode arrays were performed as described above for 8W10E+ arrays. A monodisperse suspension of HCAEC in EGM-2 MV medium (Clonetics, Lonza, USA) supplemented with 5% FBS was added to the arrays at a density of 80,000–90,000 cells/well and incubated up to 24 h to form a uniform dense monolayer. Treatments were carried out as described above for barrier function assays. Three hours after treatment, wounding was activated with default conditions for 8W1E arrays (1400 μA, 60000 Hz for 20 sec). This killed the treated cells adhering to the electrode surface in 8W1E slides to create a wound. Thereafter, impedance was continuously recorded to observe the migration of cells to the wounded area to form a confluent HCAEC monolayer.

Statistical Analysis

Data were analyzed using GraphPad Prism software version 5.04 (GraphPad Software, San Diego, CA). An unpaired 2-tailed Student's *t*-test was used and differences were considered statistically significant at $P<0.05$.

Results

Gene expression changes in IL-4 treated adult human VEC

To identify all genes regulated by IL-4 treatment in HCAEC, we performed dual channel oligonucleotide based transcriptome profiling. The transcriptome profile of HCAEC treated with IL-4 for 8 h was compared to that of non-treated cells using whole human genome oligomicroarrays. The preprocessed gene expression data was analyzed by GeneSpring software to identify the genes in treated cells that showed a minimum two fold change in expression compared with non-treated cells. IL-4 regulated 2747 genes, of which 1395 genes were upregulated and 1352 genes were down regulated. *PMCH, HAS3*, *CCL26, OTOGL, TMTC1, CH25H, VCAM1, DKK2, SLC10A7, MASP1, COL3A1* and *WNT5A* were the genes most upregulated by IL-4. The top one hundred genes upregulated by IL-4 in HCAEC are listed in S1 Table. *LRRC14B, DNAH2*, *TMEM191B, FAM47B, GPR116, TTC9, NOG, OR13C8, GPRC6A, CSN3, TMEM236* and *PRKG2* were the genes most downregulated by IL-4. The top one hundred genes downregulated by IL-4 in HCAEC are listed in S2 Table.

All differentially regulated genes contained in the preprocessed microarray data were subjected to GO analyses using MetaCore™ GeneGO software. Using this tool, genes regulated at least two fold in their expression were clustered on the basis of their function to generate statistically significant cellular pathways. Among the top twenty five biological pathways regulated by IL-4, six were associated with immune responses (Figs. 1A and 1B). The 'Immune response_Oncostatin M signaling via JAK-Stat in human cells' is the pathway most significantly regulated by IL-4 treatment in HCAEC (Fig. 1A). Genes of this pathway regulated by IL-4 (e.g. *CCL2, IL6ST, MMP1* and *VEGFA*; Table 1) are mainly associated with immune responses involving monocyte-endothelial interactions and endothelial permeabilization. The 'Development_Regulation of epithelial-to-mesenchymal transition (EMT)' is the second most significant biological process for IL-4 in HCAEC (Fig. 1A). Among the genes of this pathway regulated by IL-4 (Table 1), *DLL4* and *PDGFB* are involved in cell proliferation and migration, *SNAI1* and *ZEB1* are involved in promoting the transition of cells from epithelial to mesenchymal state, *SNAI2* is involved in repressing the expression of cellular junctional proteins and *Wnt5A* is involved in cell migration and inflammation.

The 'Cytoskeleton remodeling_TGF, Wnt and cytoskeletal remodeling' pathway is the third most significant biological process for IL-4 in HCAEC (Fig. 1A). Among the genes regulated in this pathway are *Wnt5A, Wnt1, VEGFA, LIMK2* and *CFL1* (Table 1). The MetaCore™ map of this pathway showing these genes within their signaling context indicates that IL-4 upregulates Wnt as most significant ligand for the cytoskeleton remodeling (Fig. 2, upper right quarter), and causes downstream regulation of LIMK2 and CFL1 (Fig. 2, lower left quarter). *LIMK2* and *CFL1* are responsible for actin polymerization. Among the other genes

of this pathway are *KDR* and *FZDs* (Fig. 2, Table 1), which are involved in VEGF and Wnt signaling.

Data from our study confirm previous findings that IL-4 upregulatesVCAM-1 [10-12], IL-6 [12-14], MCP [12,14] and LIFR [12] in VEC (S1 Table). Thus, it corroborates the proposed role of IL-4 as an 'alternative inflammatory' cytokine. With respect to transcription factors mediating IL-4 induced gene expression in VEC, the present study demonstrates that IL-4 upregulates the expression of genes encoding FOSB (a member of the activator protein-1 family), GATA3 and EGR1 (S3 Table).

Confirmation of Wnt5A expression by qRT-PCR and immunofluorescence staining

Since Wnt5A was previously identified as an inflammatory mediator, and expression of the gene is shown to be significantly upregulated by IL-4 in microarray analysis, we measured Wnt5A mRNA levels in HCAEC treated with IL-4 for 8 h using qRT-PCR. Consistent with the microarray data, IL-4 significantly upregulated Wnt5A mRNA levels (Fig. 3A). The induction of IL-6 mRNA was considered as indication of positive IL-4 stimulation of HCAEC (Fig. 3B). To confirm that IL-4 induced Wnt5A expression is not only specific for HCAEC but also for endothelial cells from different vascular beds, we measured Wnt5A mRNA level in IL-4 treated HPAEC. Consistent with findings obtained in HCAEC, 8 h treatment with IL-4 significantly upregulated Wnt5A in HPAEC (Fig. 3A). We further confirmed Wnt5A induction at the protein level by immunofluorescence staining. In accordance with qRT-PCR and microarray data, treatment with IL-4 notably increased the levels of Wnt5A protein in HCAEC (Fig. 3C).

LIM kinase (LIMK) 2 and Cofilin-1 (CFL1) are phosphorylated in IL-4 treated HCAEC

GO analysis of gene expression data shows that IL-4 regulated the *LIMK2* and *CFL1* genes, which are involved in cytoskeleton remodeling (Fig. 2, Table 1). LIMK2, a serine/threonine/tyrosine kinase, is a downstream target of ROCK. When phosphorylated by the activated ROCK, LIMK2 phosphorylates the actin depolymerization factor CFL1 [30-32]. Therefore, we investigated whether LIMK2 and CFL1 proteins are phosphorylated following IL-4 treatment in HCAEC. Immunofluorescence staining employing specific antibodies were used to detect the phosphorylated forms of LIMK2 (pLIMK2) and CFL1 (pCFL1). Compared to non-treated cells, pLIMK2 (Fig. 4, upper panel) and pCFL1 (Fig. 4, lower panel) levels were markedly increased in HCAEC treated with IL-4 for 1 h and 4 h respectively. Combining IL-4 with the ROCK inhibitor Y-27632 notably suppressed the phosphorylation of LIMK2 (Figs. 4A and 4B) and CFL1 (Figs. 4A and 4B) in HCAEC.

IL-4 induced stress fiber formation can be decreased by Wnt antagonist

Since inactivation of CFL1 by phosphorylation prevents actin depolymerization resulting in F-actin stress fiber formation [31-33], and IL-4 treatment induced its phosphorylation, we next investigated whether IL-4 causes stress fiber formation. Alterations in actin organization and stress fiber formation were visualized by imaging actin-RFP in IL-4 treated live HCAEC. Actin-RFP showed only a few thin stress fibers in non-treated HCAEC whereas formation of thick actin stress fibers were visible in IL-4 treated cells (Fig. 5).

Functional clustering of the IL-4 regulated transcriptome showed upregulation of Wnt5A, and this occurs upstream of LIMK2 and CFL1 regulation in the cytoskeleton remodeling process (Fig. 2). Having verified upregulated Wnt5A expression and increased stress fiber formation through LIMK2 and CFL1 phosphorylation in IL-4 treated HCAEC, we next investigated the role of Wnt5A in IL-4 induced stress fiber formation using Wnt antagonists. As Frizzleds (Fzds) have long been considered the receptors for Wnts, and transcriptome profiling in this study showed upregulation of some *Fzd* genes by IL-4 in HCAEC, we first attempted to block Wnt5A/Fzd signaling using sFRP1. Treating HCAEC with IL-4 in the presence of sFRP1 did not influence actin stress fiber formation (Fig. 5). As Ryk is described as an alternative receptor for Wnts [34], we next tested whether inhibiting Wnt5A/Ryk interaction by using WIF1 has an effect on IL-4 induced stress fiber formation. Stress fiber formation was notably suppressed when HCAEC were treated with a combination of IL-4 and WIF1 (Fig. 5). HCAEC showed increased stress fiber formation upon Wnt5A treatment, however this was notably suppressed after treatment with a combination of Wnt5A and WIF1 (Fig. 5).

IL-4 disrupts the assembly of VE-cadherin in inter-endothelial junctions (IEJs)

Actin stress fiber formation leads to disassembly of VE-cadherin in IEJs and causes intercellular gap formation in endothelial monolayers [35]. Since IL-4 induced stress fiber formation, we next investigated if IL-4 affected VE-cadherin assembly in HCAEC. Immunofluorescence staining showed continuous distribution of VE-cadherin along the cellular periphery, and tight intercellular contacts in non-treated HCAEC monolayers (Fig. 6A). In contrast, IL-4 treated HCAEC monolayers showed small inter-endothelial gaps with marked loss of VE-cadherin at intercellular regions (Fig. 6B).

IL-4 induced endothelial hyperpermeability is decreased by silencing Wnt5A

Stress fiber formation and IEJ disruption accompanied by inter-endothelial gap formation impairs barrier function and increases permeability of endothelial monolayers [35]. Since IL-4 upregulated Wnt5A, and inhibiting Wnt5A with WIF1 decreased IL-4 induced stress fiber formation in HCAEC, we investigated whether Wnt5A mediated IL-4 induced endothelial hyperpermeability. Alterations in TEER of tight HCAEC monolayers cultured in 8W10E+

slides were recorded in real time by ECIS. Treatment with IL-4 significantly reduced the TEER of HCAEC monolayers to alternating current (AC). Notably, IL-4 induced alterations in TEER became apparent 3 h after treatment with IL-4 and persisted for more than 8 h (Fig. 7A).

Next, we tested whether silencing Wnt5A improves the barrier function of IL-4 treated HCAEC monolayers. HCAEC were transfected with siRNA against Wnt5A. qRT-PCR showed that Wnt5A mRNA expression was approximately 60% lower in Wnt5A-siRNA transfected cells than in cells transfected with negative control siRNA (S2A Fig.). Accordingly, immunofluorescence staining showed decreased Wnt5A protein expression in Wnt5A-siRNA transfected HCAEC compared with negative control siRNA transfected cells (S2B and S2C Figs.).

Upon IL-4 treatment, Wnt5A silenced HCAEC showed significantly increased TEER compared with non-transfected HCAEC (Fig. 7A). In HCAEC transfected with negative control siRNA, the response to IL-4 was not altered (Fig. 7B).

Since IL-4 upregulated IL-6 in HCAEC in the present study (Fig. 3B), and IL-6 has been reported to increase permeability of HUVEC [36] and bovine vascular endothelial cells (BVEC) [37], we also investigated whether IL-6 increased permeability of HCAEC monolayers. Treatment with IL-6 did not alter the TEER of HCAEC monolayer to AC, thereby indicating that IL-6 does not influence the permeability characteristics of HCAEC (Fig. 7C).

IL-4 impairs migration of HCAEC, which can be restored by ROCK inhibition

Since IL-4 increased the formation of actin stress fibers and caused inter-endothelial gap formation, we investigated whether IL-4 would also affect the motility of HCAEC. In an ECIS supported wound healing and cell migration assay, IL-4 treated HCAEC exhibited a lower impedance and required a longer time to heal the wound compared with non-treated cells (Fig. 8A). This indicates that IL-4 significantly reduces endothelial cell motility, causing delayed wound closure.

The present study shows that IL-4 induced phosphorylation of LIMK2 and CFL1 can be decreased by inhibiting ROCK. Since ROCK regulates cytoskeleton remodeling, cell–cell adhesion and cell motility [32], we investigated whether inhibiting ROCK prevents IL-4 induced impairment of HCAEC motility. Cells treated with a combination of IL-4 and the ROCK inhibitor Y-27632 showed signifcantly higher motility rates and faster wound closure than cells treated with only IL-4 (Fig. 8B).

IL-4 upregulates Wnt5A expression in human macrophages

Since macrophages also play a pivotal role in Th2 inflammation, we asked whether Wnt5A expression is also upregulated in IL-4 activated human M2 type macrophages. Treatment with IL-4 significantly upregulated Wnt5A mRNA expression in macrophages (Fig. 9).

Discussion

VEC play an important role in maintaining vascular homeostasis. During inflammation, soluble mediators secreted by activated immune cells paracrinically act on VEC and significantly alter their functions to confer 'inflamed' or 'activated' phenotypes on them. IL-4 is a potent Th2 cytokine known to cause activation of VEC and induce endothelial barrier dysfunction [21]. However, the exact mechanisms responsible for IL-4 dependent endothelial dysfunction in VEC remained unclear. In the present study, we detected all genes regulated by paracrine IL-4 signaling in adult VEC by whole human genome microarray based transcriptome profiling (Fig. 1, S1 and S2 Tables).

This is the first study to demonstrate that IL-4 significantly upregulates Wnt5A expression in adult VEC. A previous study demonstrated that HUVEC treated with a combination of TNF-α, IL-1 and IL-8 upregulated the expression of Wnt5A mRNA [38]. Wnt5A is a non-canonical Wnt ligand, recently identified as a pro-inflammatory mediator of macrophage activation in vascular inflammation [24]. Wnt5A has been demonstrated to enhance the permeability of HUVEC monolayers in a ^{14}C sucrose permeability test [39] and IL-4 caused morphological changes and induced inter-endothelial gap formation in HUVEC [17]. Furthermore IL-4 has been demonstrated to induce hyperpermeability of HUVEC [21]. Inter-endothelial gap formation caused by cytoskeletal rearrangements impairs the barrier functions of endothelial monolayers and is the principal pathway causing endothelial hyperpermeability and subsequent edema formation in inflammation [40]. Endothelial hyperpermeability accounts for increased efflux of plasma through microvessel walls into neighboring tissues, leading to the formation of protein rich tissue edema. Edema formation resulting from vascular leakage is an important consequence of allergic inflammation [21] and a most common side effect of IL-4 therapy in human cancer patients [41]. Addressing a potential role for Wnt5A in IL-4 induced endothelial cytoskeleton remodeling, GO analyses for the current study point to Wnt5A as a potential ligand for the 'Cytoskeleton remodeling_TGF, Wnt and cytoskeletal remodeling' pathway (Fig. 2). A prominent role for Wnt5A in mediating IL-4 induced cytoskeleton remodeling is evident from our observation that IL-4 induced actin stress fiber formation can be prevented by blocking Wnt5A signaling (Fig. 5). Further proof for the involvement of Wnt5A is provided by functional experiments demonstrating that the enhanced permeability of HCAEC monolayers upon IL-4 treatment can be significantly decreased by silencing Wnt5A expression (Fig. 7A). Our findings support the crucial role of

Wnt5A in stress fiber formation and inter-endothelial gap formation, leading to impaired barrier function in IL-4 treated HCAEC.

Wnt5A signals mainly through Fzd receptors but can also function through Ryk, a member of the family of atypical receptor tyrosine-protein kinases (RTKs). Ryk consists of an extracellular Wnt-binding domain, a PDZ binding motif and an intracellular inactive tyrosine kinase domain. Its Wnt-binding domain is homologous to the extracellular Wnt antagonist, WIF protein. sFRP1 is another Wnt antagonist that contains a frizzled like cysteine-rich domain (CRD) homologous to the extracellular Wnt-binding domains of Fzd receptors [34]. The availability of the receptor, presence of Wnt antagonists and the cellular environment determines which receptors Wnts engages and the signals that are generated. The involvement of Ryk, but not Fzd receptors, in IL-4 induced Wnt5A signaling in HCAECs is obvious from our observation that stress fiber formation was prevented in the presence of WIF1 but not sFRP1 (Fig. 5). Others have demonstrated that Wnt5A/Ryk signaling through Rho-kinase activation inhibits axon growth in rats [42]. We propose that in HCAEC, Wnt5A signaling through Ryk receptor activates ROCK that in turn phosphorylates LIMK2. Activated pLIMK2 in turn phosphorylates CFL1 that is then deactivated, and as a consequence, allows actin fiber polymerization. This disrupts VE-cadherin assembly in IEJs leading to the formation of inter-endothelial gaps, as we have observed in the present study (Fig. 6B). The involvement of ROCK as a downstream effector of Wnt5A/Ryk signaling in HCAEC is very well supported by the observations that phosphorylation of LIMK2 and CFL1 following IL-4 treatment can be decreased by inhibiting ROCK (Fig. 4). The function of ROCK in IL-4 induced cytoskeleton remodeling is further evident from the standardized ECIS cell migration assay that shows improved migratory and wound healing capacity of cells treated with a combination of IL-4 and ROCK inhibitor (Figs. 8A and 8B).

Intriguingly, the present study confirms that IL-6 is upregulated by IL-4 in HCAEC but IL-6 does not influence TEER in the ECIS based standardized permeability assay (Fig. 7C), even though it increases permeability in HUVEC [36] and BVEC [37]. Further studies are warranted to confirm that IL-6 is not responsible for increased VEC permeability, or whether this effect of IL-6 varies between endothelial cells from different vascular beds and thus depends on endothelial heterogeneity.

The whole genome transcriptome analysis of IL-4 treated HCAEC further revealed induction of vascular endothelial growth factor (VEGF)-A (Table 1, Fig. 2). A previous study showed that IL-4 increased the production of VEGF in unstimulated synovial fibroblasts [43]. VEGF-A acts as a proangiogenic factor in wound healing. It enhances endothelial cell migration from pre-existing blood vessels and promotes the recruitment of endothelial progenitor cells (EPCs) from peripheral circulation [44]. Surprisingly, the present study demonstrates an inhibitory effect of IL-4 on endothelial cell migration while upregulating VEGF-A. Even though

this contradicts the effects of VEGF in stimulating endothelial cell migration, it could be explained by the observation that IL-4 downregulates expression of VEGFR-2 (Table 1, Fig. 2). VEGFR-2 (also known as KDR) is a receptor specific for VEGF [44] and downregulation would block autocrine VEGF-A signaling in endothelial cells. This is a likely feedback mechanism inhibiting angiogenesis. As soluble factors secreted by VEC paracrinically act on other immune cells such as macrophages, it is also possible that VEGF-A produced by VEC interacts with VEGF receptors expressed on other immune cells. This view is well supported by previous studies which demonstrated that VEGF-A acted as a chemoattractant for monocytes expressing VEGF receptor 1 [45-48].

Among the genes highly expressed upon IL-4 treatment of HCAEC (S1 Table), pro-melanin-concentrating hormone (PMCH) has also been described previously as highly induced by activated Th2 cells [49]. IL-4 triggered expression of hyaluronan synthase 3 (HAS3) may facilitate the adhesion and migration of activated immune cells and cancer cells during inflammatory response and cancer metastasis, respectively. Induction of CCL26 by IL-4 has already been described in VEC and it acts as a chemokine for eosinophils [50].

Conclusions

Our study indicates that Wnt5A is crucially involved in cytoskeleton rearrangement mediated by IL-4 in VEC. We further show that Wnt5A signals downstream through the ROCK–LIMK2–CFL1 pathway and show that Ryk is a possible receptor for Wnt5A signaling in VEC. Here we demonstrate a crucial role for Wnt5A in IL-4 induced actin cytoskeleton remodeling and consequent barrier dysfunction and hyperpermeability of VEC. Therapeutic approaches targeting Wnt5A may reduce microvascular leakage and subsequent edema formation associated with IL-4 driven pathophysiological conditions such as allergic inflammation, tumor inflammation, and angioedema. Moreover, we show for the first time that IL-4 induces Wnt5A in human M2 type macrophages, which is different to the Toll-like receptor (TLR) mediated Wnt5A induction described previously [24]. Together, this establishes Wnt5A as a component of both classically and alternatively activated macrophages. Further studies delineating the specific role of Wnt5A in alternatively activated macrophages would provide novel insights into the inflammatory responses in diseases associated with Th2 activity.

Acknowledgments

We thank Cheryl Pech, PhD, for critical reading of the manuscript.

References

1. Luzina IG, Keegan AD, Heller NM, Rook GA, Shea-Donohue T, et al. (2012) Regulation of inflammation by interleukin-4: a review of "alternatives". J Leukoc Biol 92: 753-764.
2. Nelms K, Keegan AD, Zamorano J, Ryan JJ, Paul WE (1999) The IL-4 receptor: signaling mechanisms and biologic functions. Annu Rev Immunol 17: 701-738.
3. Seder RA, Paul WE, Davis MM, Fazekas de St Groth B (1992) The presence of interleukin 4 during in vitro priming determines the lymphokine-producing potential of CD4+ T cells from T cell receptor transgenic mice. J Exp Med 176: 1091-1098.
4. Hsieh CS, Heimberger AB, Gold JS, O'Garra A, Murphy KM (1992) Differential regulation of T helper phenotype development by interleukins 4 and 10 in an alpha beta T-cell-receptor transgenic system. Proc Natl Acad Sci U S A 89: 6065-6069.
5. Gascan H, Gauchat JF, Roncarolo MG, Yssel H, Spits H, et al. (1991) Human B cell clones can be induced to proliferate and to switch to IgE and IgG4 synthesis by interleukin 4 and a signal provided by activated CD4+ T cell clones. J Exp Med 173: 747-750.
6. Li-Weber M, Krammer PH (2003) Regulation of IL4 gene expression by T cells and therapeutic perspectives. Nat Rev Immunol 3: 534-543.
7. Li Z, Chen L, Qin Z (2009) Paradoxical roles of IL-4 in tumor immunity. Cell Mol Immunol 6: 415-422.
8. Kotowicz K, Callard RE, Friedrich K, Matthews DJ, Klein N (1996) Biological activity of IL-4 and IL-13 on human endothelial cells: functional evidence that both cytokines act through the same receptor. Int Immunol 8: 1915-1925.
9. Galley HF, Webster NR (2004) Physiology of the endothelium. Br J Anaesth 93: 105-113.
10. Thornhill MH, Wellicome SM, Mahiouz DL, Lanchbury JS, Kyan-Aung U, et al. (1991) Tumor necrosis factor combines with IL-4 or IFN-gamma to selectively enhance endothelial cell adhesiveness for T cells. The contribution of vascular cell adhesion molecule-1-dependent and -independent binding mechanisms. J Immunol 146: 592-598.
11. Beekhuizen H, Verdegaal EM, Blokland I, van Furth R (1992) Contribution of ICAM-1 and VCAM-1 to the morphological changes in monocytes bound to human venous endothelial cells stimulated with recombinant interleukin-4 (rIL-4) or rIL-1 alpha. Immunology 77: 469-472.
12. Lee YW, Eum SY, Chen KC, Hennig B, Toborek M (2004) Gene expression profile in interleukin-4-stimulated human vascular endothelial cells. Mol Med 10: 19-27.

13. Howells G, Pham P, Taylor D, Foxwell B, Feldmann M (1991) Interleukin 4 induces interleukin 6 production by endothelial cells: synergy with interferon-gamma. Eur J Immunol 21: 97-101.
14. Colotta F, Sironi M, Borre A, Luini W, Maddalena F, et al. (1992) Interleukin 4 amplifies monocyte chemotactic protein and interleukin 6 production by endothelial cells. Cytokine 4: 24-28.
15. Luscinskas FW, Kansas GS, Ding H, Pizcueta P, Schleiffenbaum BE, et al. (1994) Monocyte rolling, arrest and spreading on IL-4-activated vascular endothelium under flow is mediated via sequential action of L-selectin, beta 1-integrins, and beta 2-integrins. J Cell Biol 125: 1417-1427.
16. Thornhill MH, Kyan-Aung U, Haskard DO (1990) IL-4 increases human endothelial cell adhesiveness for T cells but not for neutrophils. J Immunol 144: 3060-3065.
17. Klein NJ, Rigley KP, Callard RE (1993) IL-4 regulates the morphology, cytoskeleton, and proliferation of human umbilical vein endothelial cells: relationship between vimentin and CD23. Int Immunol 5: 293-301.
18. Lee IY, Kim J, Ko EM, Jeoung EJ, Kwon YG, et al. (2002) Interleukin-4 inhibits the vascular endothelial growth factor- and basic fibroblast growth factor-induced angiogenesis in vitro. Mol Cells 14: 115-121.
19. Toi M, Harris AL, Bicknell R (1991) Interleukin-4 is a potent mitogen for capillary endothelium. Biochem Biophys Res Commun 174: 1287-1293.
20. Lee YW, Kim PH, Lee WH, Hirani AA (2010) Interleukin-4, Oxidative Stress, Vascular Inflammation and Atherosclerosis. Biomol Ther (Seoul) 18: 135-144.
21. Kotowicz K, Callard RE, Klein NJ, Jacobs MG (2004) Interleukin-4 increases the permeability of human endothelial cells in culture. Clin Exp Allergy 34: 445-449.
22. Tan PH, Chan C, Xue SA, Dong R, Ananthesayanan B, et al. (2004) Phenotypic and functional differences between human saphenous vein (HSVEC) and umbilical vein (HUVEC) endothelial cells. Atherosclerosis 173: 171-183.
23. Franscini N, Bachli EB, Blau N, Leikauf MS, Schaffner A, et al. (2004) Gene expression profiling of inflamed human endothelial cells and influence of activated protein C. Circulation 110: 2903-2909.
24. Pereira C, Schaer DJ, Bachli EB, Kurrer MO, Schoedon G (2008) Wnt5A/CaMKII signaling contributes to the inflammatory response of macrophages and is a target for the antiinflammatory action of activated protein C and interleukin-10. Arterioscler Thromb Vasc Biol 28: 504-510.
25. Schaer CA, Deuel JW, Bittermann AG, Rubio IG, Schoedon G, et al. (2013) Mechanisms of haptoglobin protection against hemoglobin peroxidation triggered endothelial damage. Cell Death Differ 20: 1569-1579.

26. Watanabe K, Ueno M, Kamiya D, Nishiyama A, Matsumura M, et al. (2007) A ROCK inhibitor permits survival of dissociated human embryonic stem cells. Nat Biotechnol 25: 681-686.
27. Bernas MJ, Cardoso FL, Daley SK, Weinand ME, Campos AR, et al. (2010) Establishment of primary cultures of human brain microvascular endothelial cells to provide an in vitro cellular model of the blood-brain barrier. Nat Protocols 5: 1265-1272.
28. Sun S, Sursal T, Adibnia Y, Zhao C, Zheng Y, et al. (2013) Mitochondrial DAMPs Increase Endothelial Permeability through Neutrophil Dependent and Independent Pathways. PLoS ONE 8: e59989.
29. Szulcek R, Bogaard HJ, van Nieuw Amerongen GP (2014) Electric Cell-substrate Impedance Sensing for the Quantification of Endothelial Proliferation, Barrier Function, and Motility. e51300.
30. Rath N, Olson MF (2012) Rho-associated kinases in tumorigenesis: re-considering ROCK inhibition for cancer therapy. EMBO Rep 13: 900-908.
31. Maekawa M, Ishizaki T, Boku S, Watanabe N, Fujita A, et al. (1999) Signaling from Rho to the actin cytoskeleton through protein kinases ROCK and LIM-kinase. Science 285: 895-898.
32. Liao JK, Seto M, Noma K (2007) Rho kinase (ROCK) inhibitors. J Cardiovasc Pharmacol 50: 17-24.
33. Fazal F, Bijli KM, Minhajuddin M, Rein T, Finkelstein JN, et al. (2009) Essential role of cofilin-1 in regulating thrombin-induced RelA/p65 nuclear translocation and intercellular adhesion molecule 1 (ICAM-1) expression in endothelial cells. J Biol Chem 284: 21047-21056.
34. Green J, Nusse R, van Amerongen R (2014) The role of Ryk and Ror receptor tyrosine kinases in Wnt signal transduction. Cold Spring Harb Perspect Biol 6: a009175.
35. Vandenbroucke E, Mehta D, Minshall R, Malik AB (2008) Regulation of endothelial junctional permeability. Ann N Y Acad Sci 1123: 134-145.
36. Desai TR, Leeper NJ, Hynes KL, Gewertz BL (2002) Interleukin-6 causes endothelial barrier dysfunction via the protein kinase C pathway. J Surg Res 104: 118-123.
37. Maruo N, Morita I, Shirao M, Murota S (1992) IL-6 increases endothelial permeability in vitro. Endocrinology 131: 710-714.
38. Cheng CW, Yeh JC, Fan TP, Smith SK, Charnock-Jones DS (2008) Wnt5a-mediated non-canonical Wnt signalling regulates human endothelial cell proliferation and migration. Biochem Biophys Res Commun 365: 285-290.
39. Kim J, Kim J, Kim DW, Ha Y, Ihm MH, et al. (2010) Wnt5a induces endothelial inflammation via beta-catenin-independent signaling. J Immunol 185: 1274-1282.

40. Ochoa CD, Stevens T (2012) Studies on the cell biology of interendothelial cell gaps. Am J Physiol Lung Cell Mol Physiol 302: L275-286.
41. Tulpule A, Joshi B, DeGuzman N, Espina BM, Mocharnuk R, et al. (1997) Interleukin-4 in the treatment of AIDS-related Kaposi's sarcoma. Ann Oncol 8: 79-83.
42. Miyashita T, Koda M, Kitajo K, Yamazaki M, Takahashi K, et al. (2009) Wnt-Ryk signaling mediates axon growth inhibition and limits functional recovery after spinal cord injury. J Neurotrauma 26: 955-964.
43. Hong KH, Cho ML, Min SY, Shin YJ, Yoo SA, et al. (2007) Effect of interleukin-4 on vascular endothelial growth factor production in rheumatoid synovial fibroblasts. Clin Exp Immunol 147: 573-579.
44. Hoeben A, Landuyt B, Highley MS, Wildiers H, Van Oosterom AT, et al. (2004) Vascular endothelial growth factor and angiogenesis. Pharmacol Rev 56: 549-580.
45. Sawano A, Iwai S, Sakurai Y, Ito M, Shitara K, et al. (2001) Flt-1, vascular endothelial growth factor receptor 1, is a novel cell surface marker for the lineage of monocyte-macrophages in humans. Blood 97: 785-791.
46. Grunewald M, Avraham I, Dor Y, Bachar-Lustig E, Itin A, et al. (2006) VEGF-induced adult neovascularization: recruitment, retention, and role of accessory cells. Cell 124: 175-189.
47. Kerber M, Reiss Y, Wickersheim A, Jugold M, Kiessling F, et al. (2008) Flt-1 signaling in macrophages promotes glioma growth in vivo. Cancer Res 68: 7342-7351.
48. De Palma M (2012) Partners in crime: VEGF and IL-4 conscript tumour-promoting macrophages. J Pathol 227: 4-7.
49. Sandig H, McDonald J, Gilmour J, Arno M, Lee TH, et al. (2007) Human Th2 cells selectively express the orexigenic peptide, pro-melanin-concentrating hormone. Proc Natl Acad Sci U S A 104: 12440-12444.
50. Shinkai A, Yoshisue H, Koike M, Shoji E, Nakagawa S, et al. (1999) A novel human CC chemokine, eotaxin-3, which is expressed in IL-4-stimulated vascular endothelial cells, exhibits potent activity toward eosinophils. J Immunol 163: 1602-1610.

Supporting Information

S1 Table. The top 100 genes upregulated by IL-4 in HCAEC.

S2 Table. The top 100 genes downregulated by IL-4 in HCAEC.

S3 Table. Regulation of genes coding for transcription factors in IL-4 treated HCAEC.

S1 Fig. HCAECmonolayer formation in ECIS arrays.

S2 Fig. Wnt5A knockdown efficiency.

Table 1. Key genes regulated by IL-4 in 'Immune response_Oncostatin M signaling via JAK-Stat in human cells', 'Development_Regulation of epithelial-to-mesenchymal transition (EMT)' and 'Cytoskeleton remodeling_TGF, Wnt and cytoskeletal remodeling' pathways in HCAEC.

Gene Symbol	Accession	Sequence Description	Regulation
CAV1[c]	NM_001172895	Homo sapiens caveolin 1	Down
CCL2[a]	NM_002982	Homo sapiens chemokine (C-C motif) ligand 2	Up
CFL1[c]	NM_005507	Homo sapiens cofilin 1	Down
CCND1[a,c]	NM_053056	Homo sapiens cyclin D1	Down
DLL4[b]	NM_019074	Homo sapiens delta-like 4	Down
FZD4[b,c]	NM_012193	Homo sapiens frizzled class receptor 4	Up
FZD8[b,c]	NM_031866	Homo sapiens frizzled class receptor 8	Up
FOXO3[c]	NM_001455	Homo sapiens forkhead box O3	Up
HEY1[b]	NM_001040708	Homo sapiens hes-related family bHLH transcription factor with YRPW motif 1	Down
IL6ST[a]	NM_001190981	Homo sapiens interleukin 6 signal transducer	Up
JAG1[b]	NM_000214	Homo sapiens jagged 1	Up
KDR[c]	NM_002253	Homo sapiens kinase insert domain receptor	Down
LIFRα[a]	NM_002310	Homo sapiens leukemia inhibitory factor receptor alpha	Up
LIMK2[c]	NM_001031801	Homo sapiens LIM domain kinase 2	Down
MAPK13[c]	NM_002754	Homo sapiens mitogen-activated protein kinase 13	Down
MAP2K3[c]	NM_002756	Homo sapiens mitogen-activated protein kinase kinase 3	Down
MMP1[a]	NM_002421	Homo sapiens matrix metallopeptidase 1	Up
MMP7[c]	NM_002423	Homo sapiens matrix metallopeptidase 7	Up
MYLK[c]	NM_053025	Homo sapiens myosin light chain kinase	Down
MYLK2[c]	NM_033118	Homo sapiens myosin light chain kinase 2	Down
PDGFβ[b]	NM_002608	Homo sapiens platelet-derived growth factor beta polypeptide	Down
SNAI1[b]	NM_005985	Homo sapiens snail homolog 1	Down
SNAI2[b]	NM_003068	Homo sapiens snail homolog 2	Down
TGFβ2[b]	NM_003238	Homo sapiens transforming growth factor, beta 2	Up
TGFβ3[b]	NM_003239	Homo sapiens transforming growth factor, beta 3	Up
VEGFA[a,c]	NM_001025366	Homo sapiens vascular endothelial growth factor A	Up
WNT5A[b,c]	NM_003392	Homo sapiens wingless-type MMTV integration site family, member 5A	Up
ZEB1[b]	NM_001128128	Homo sapiens zinc finger E-box binding homeobox 1	Down

[a]Genes regulated by IL-4 in 'Immune response_Oncostatin M signaling via JAK-Stat in human cells' pathway.
[b]Genes regulated by IL-4 in 'Development_Regulation of epithelial-to-mesenchymal transition (EMT)' pathway.
[c]Genes regulated by IL-4 in 'Cytoskeleton remodeling_TGF, Wnt and cytoskeletal remodeling' pathway.

Figure 1

A


1 2 3 4 5 6 7
-log(pValue)
1
2
3
4
5
6
7
8
9
10
11
12
1. Immune response_Oncostatin M signaling via JAK-Stat in human cells
2. Development_Regulation of epithelial-to-mesenchymal transition (EMT)
3. Cytoskeleton remodeling_TGF, WNT and cytoskeletal remodeling
4. Development_TGF-beta-dependent induction of EMT via SMADs
5. Cell adhesion_Chemokines and adhesion
6. Cell adhesion_Plasmin signaling
7. Immune response_Oncostatin M signaling via JAK-Stat in mouse cells
8. Immune response_Oncostatin M signaling via MAPK in human cells
9. Cytoskeleton remodeling_Cytoskeleton remodeling
10. G-protein signaling_Regulation of p38 and JNK signaling mediated by G-proteins
11. Airway smooth muscle contraction in asthma
12. NF-AT signaling in cardiac hypertrophy

B

Fig. 1. The twenty five biological pathways most significantly (*P*<0.05) regulated by IL-4 treatment in HCAEC. (A, B) Pathways represented as histograms are ranked by the –log value (*P* value). Length of histogram corresponds to the number of genes associated with that specific pathway.

Figure 2

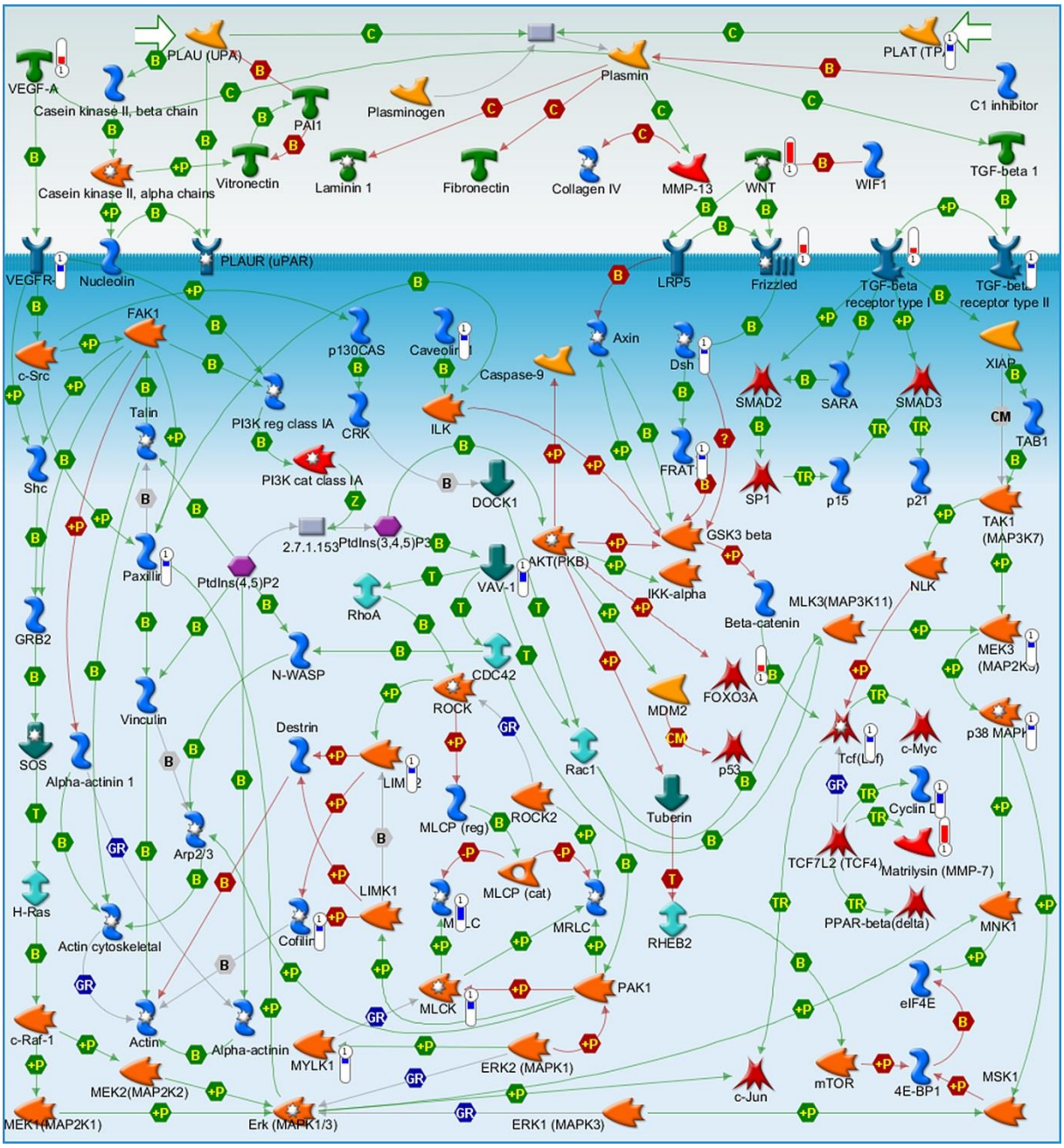

Fig. 2. Metacore™ map showing the signaling context of the genes contained in the 'Cytoskeleton remodeling_TGF, Wnt and cytoskeletal remodeling' pathway. Genes regulated by IL-4 are marked by red and blue thermometer icons representing upregulated and downregulated gene expression respectively.

Figure 3

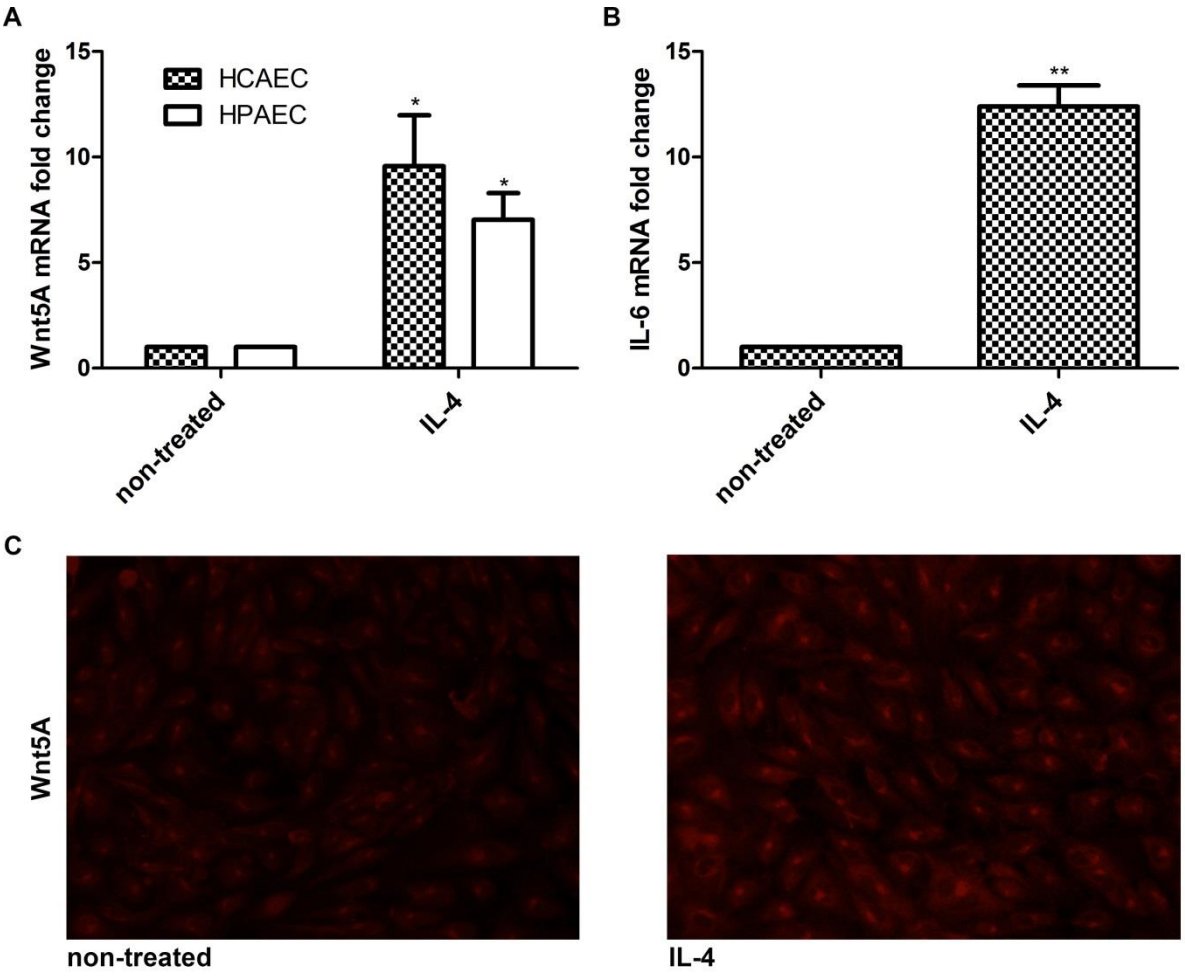

Fig. 3. Expression of Wnt5A in IL-4 treated HCAEC. Fold changes in the expression of (A) Wnt5A mRNA in 8 h IL-4 treated HCAEC and HPAEC and (B) IL-6 mRNA in 8 h IL-4 treated HCAEC. Data were obtained from three independent qRT-PCR experiments run with duplicate samples and expressed as the mean ± SEM. **P*<0.05, ***P*<0.005 using an unpaired Student's *t*-test. (C) Wnt5A protein expression in non-treated and IL-4 treated HCAEC. Wnt5A is immunostained (red). Zeiss Axioskope, magnification 20×.

Figure 4

A

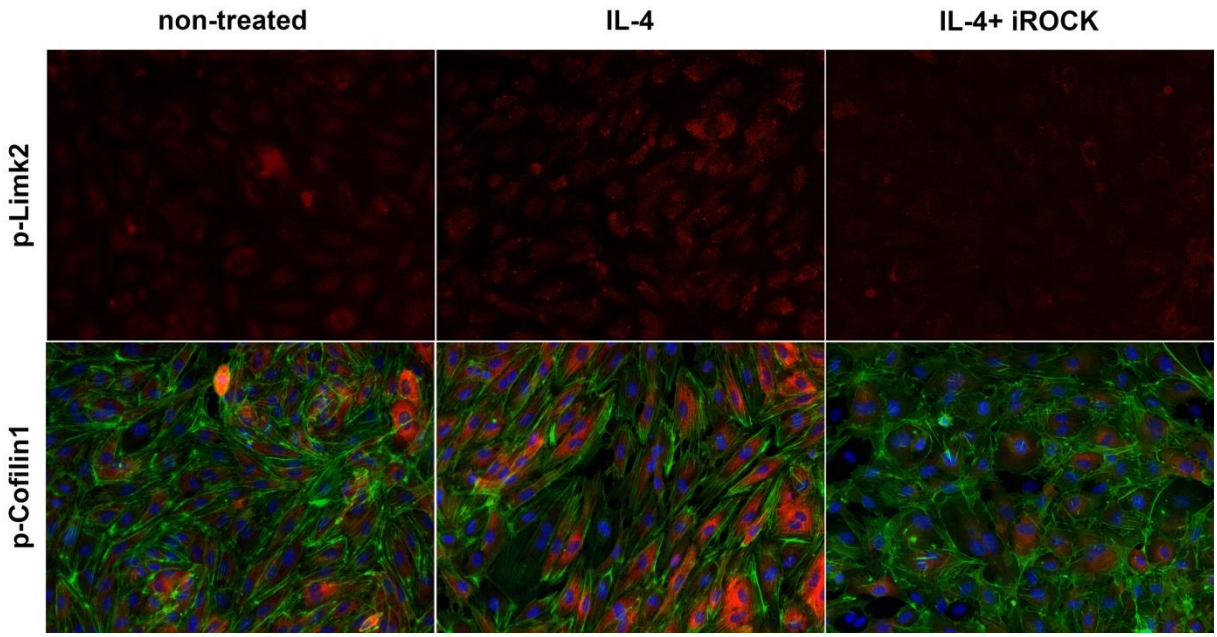
non-treated
IL-4
IL-4+ iROCK
p-Limk2
p-Cofilin1

B

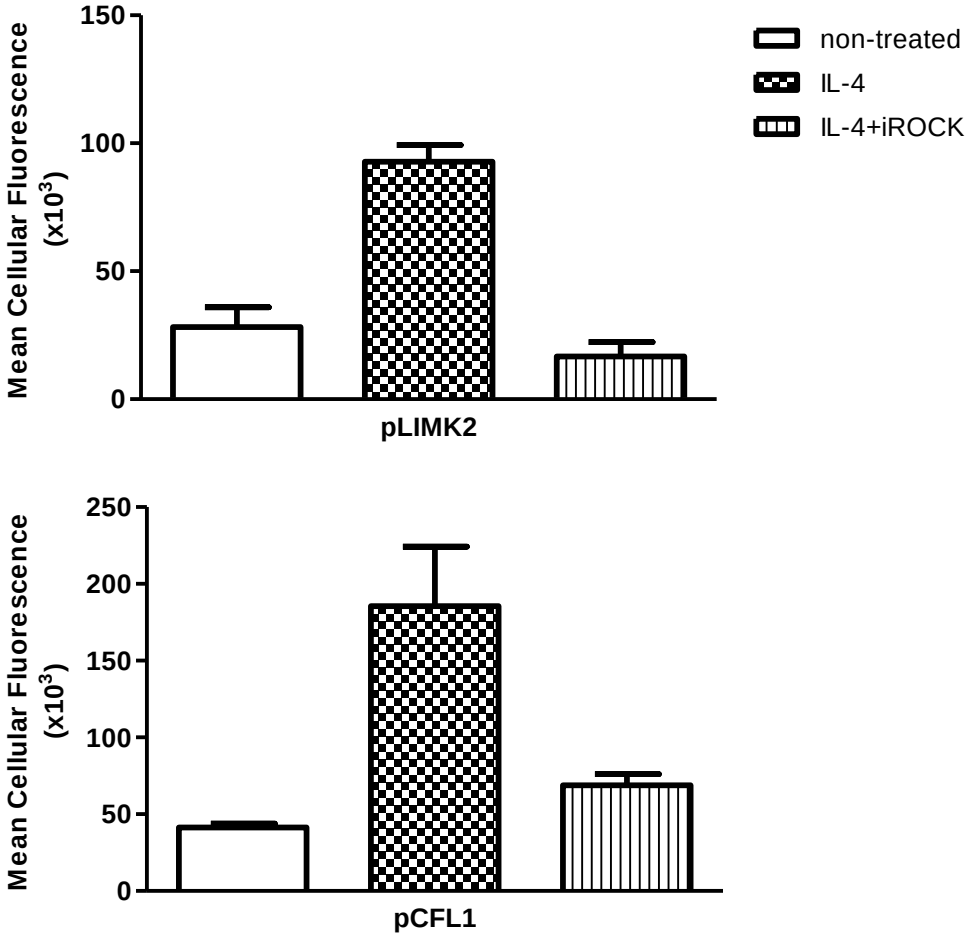
Mean Cellular Fluorescence (x10³)
150
100
50
0
pLIMK2
non-treated
IL-4
IL-4+iROCK
Mean Cellular Fluorescence (x10³)
250
200
150
100
50
0
pCFL1

Fig. 4. Phosphorylation of LIMK2 and CFL1 in IL-4 treated HCAEC. (A) pLIMK2 and pCofilin-1 were immunostained (red) in HCAEC treated with IL-4 either alone or in combination with Y-27632. F-actin (fluorescent phalloidin, green) and nuclei (DAPI, blue) were also stained. Zeiss Axioskope, magnification 20×. (B) Mean cellular fluorescent intensities of pLIMK2 and pCFL1 quantified by Fiji software.

Figure 5

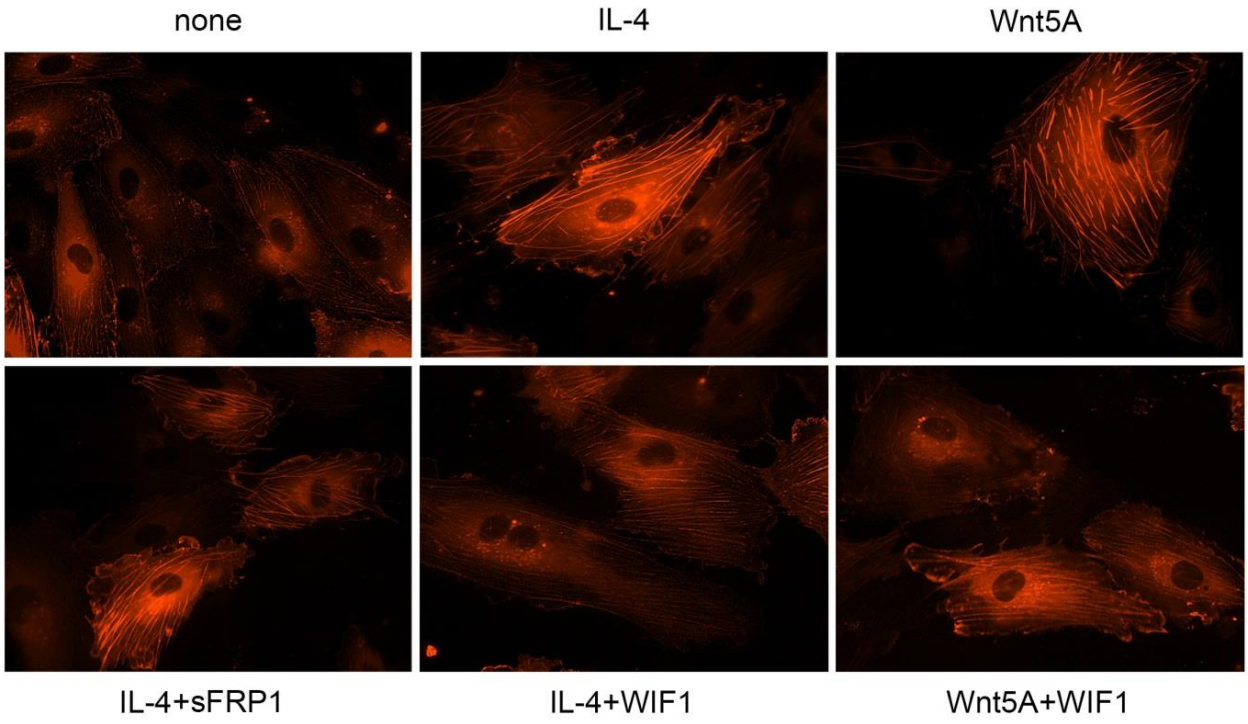

Fig. 5. Stress fiber formation in IL-4 treated HCAEC. Live actin-RFP staining showing the formation of actin stress fibers in HCAEC treated with IL-4 or Wnt5A in the absence or presence of sFRP1 and WIF1. Zeiss Axio Observer.Z1, magnification 40×.

Figure 6

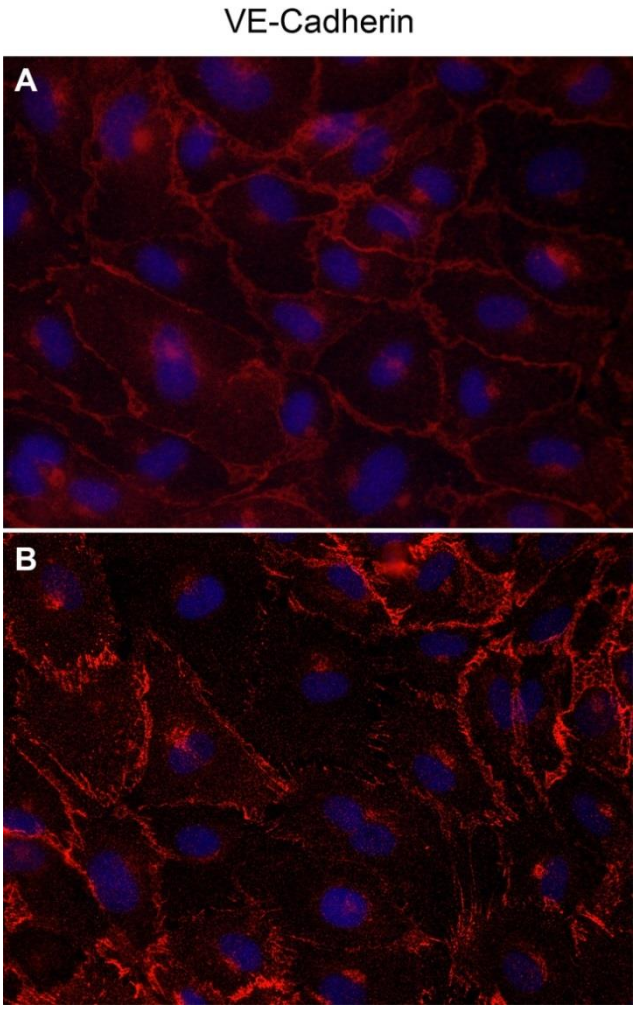

Fig. 6. Assembly of VE-cadherin in IL-4 treated HCAEC. VE-cadherin immunostained (red) in HCAEC either non-treated (A) or treated with IL- 4 for 8 h (B). Nuclei (DAPI, blue). Zeiss Axioskope, magnification 40×.

Figure 7

A

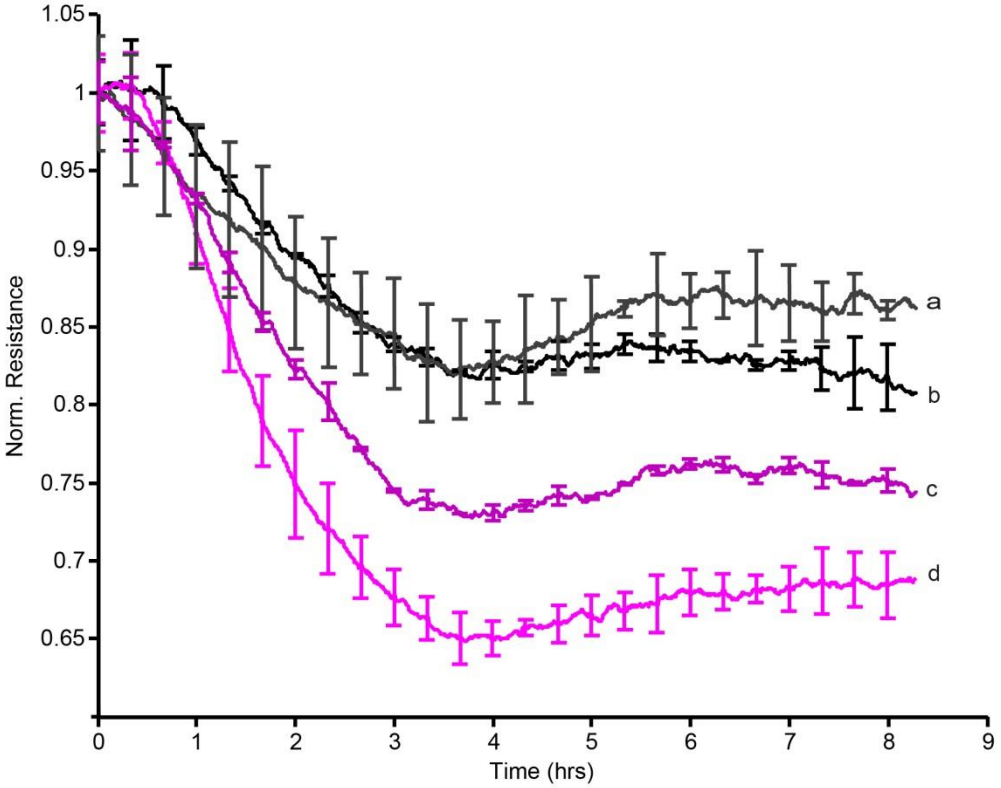

B

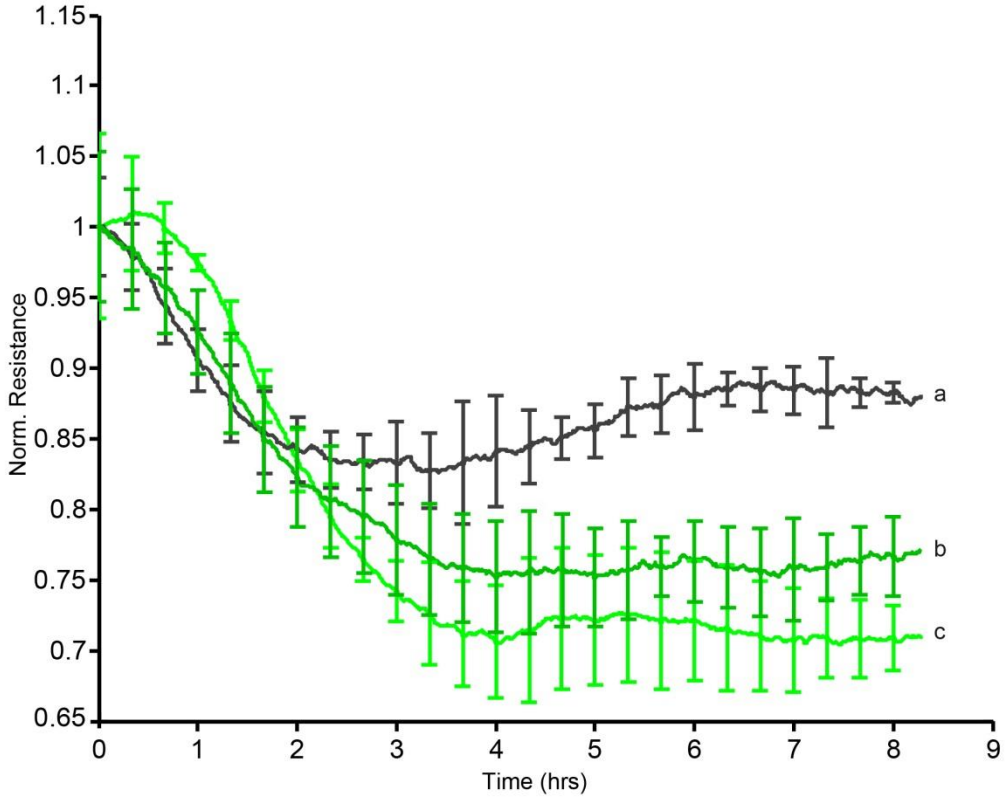

C

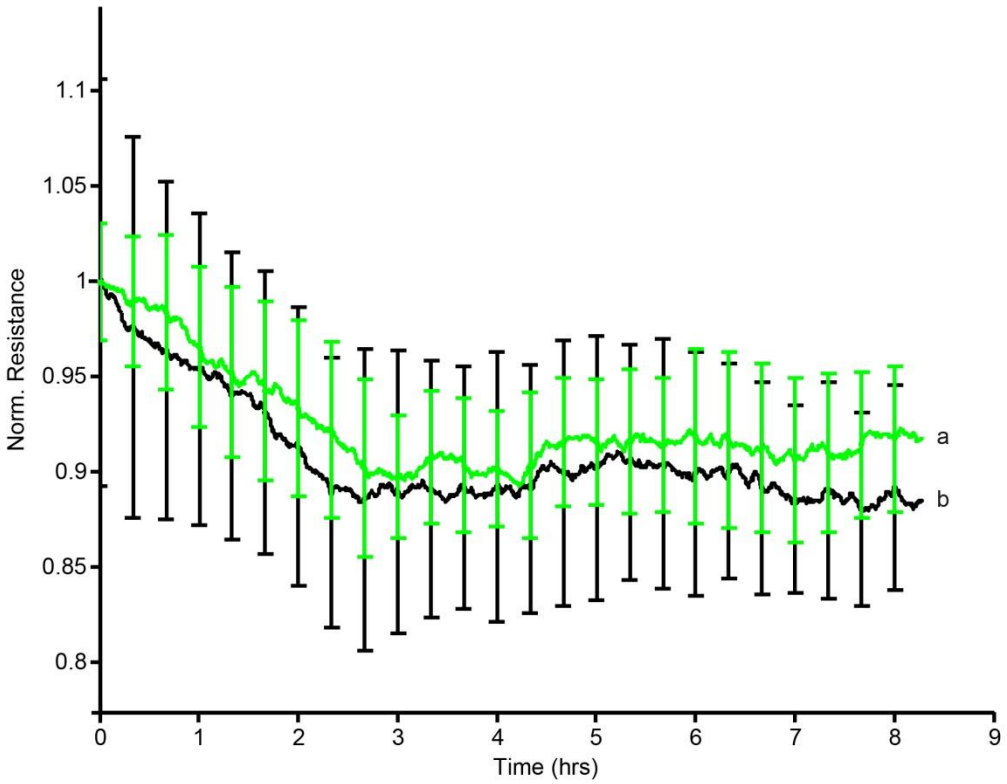

Fig. 7. ECIS barrier function assays showing the effect of Wnt5A in IL-4 induced hyperpermeability of HCAEC. Uniform confluent monolayers of HCAEC cultured in stabilized and collagen coated ECIS 8W10E+ arrays were treated with IL-4. TEER of HCAEC monolayers was measured in Ohms continuously at multiple frequencies ranging from 62.6 Hz to 64 kHz, normalized to its value at time zero and plotted with respect to time. Stimulations conducted in duplicate wells were grouped and averaged to plot a single curve with error bars representing SD. Figures shown depict the resistance measurements conducted at 4000 Hz and represent four independent experiments. (A) 1, non-treated Wnt5A-siRNA transfected HCAEC; 2, non-treated non-transfected HCAEC; 3, IL-4 treated Wnt5A-siRNA transfected HCAEC; 4, IL-4 treated non-transfected HCAEC. (B) 1, non-treated negative control siRNA transfected HCAEC; 2, IL-4 treated negative control siRNA transfected HCAEC; 3, IL-4 treated non-transfected HCAEC. (C) Black, non-treated; green, IL-6.

Figure 8

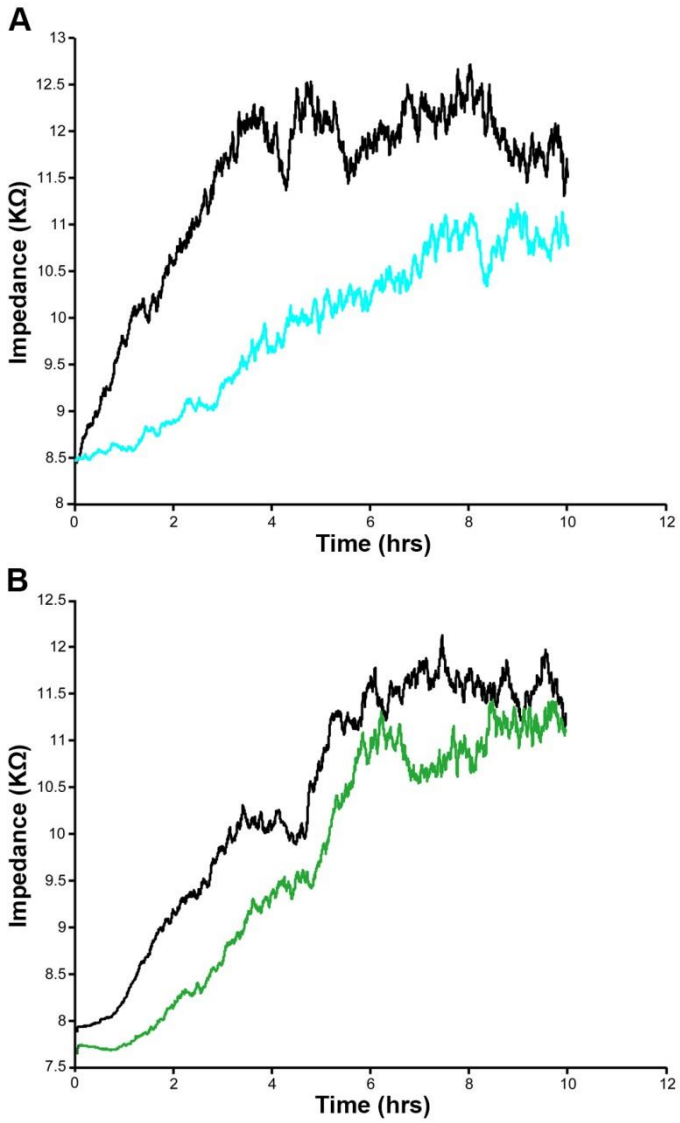

Fig. 8. Automated wound healing assay showing decreased motility of IL-4 treated HCAEC. Uniform confluent monolayers of HCAEC cultured in stabilized and collagen coated ECIS 8W1E cultureware were treated with IL-4 either alone or in combination with Y-27632. Three hours after treatment, wells were subjected to an elevated electric field to create a wound. Measurements were started immediately after wounding. Impedance of HCAEC monolayer was measured in Ohms every 5 min at multiple frequencies ranging from 62.6 Hz to 64 kHz and plotted with respect to time. Representative figures depict the impedance of wells after wounding was applied. Figures shown depict the measurements conducted at 4000 Hz and represent four independent experiments. (A) Black, non-treated; Blue, IL-4. (B) Black, control with Y27632; Green, IL-4 + Y27632.

Figure 9

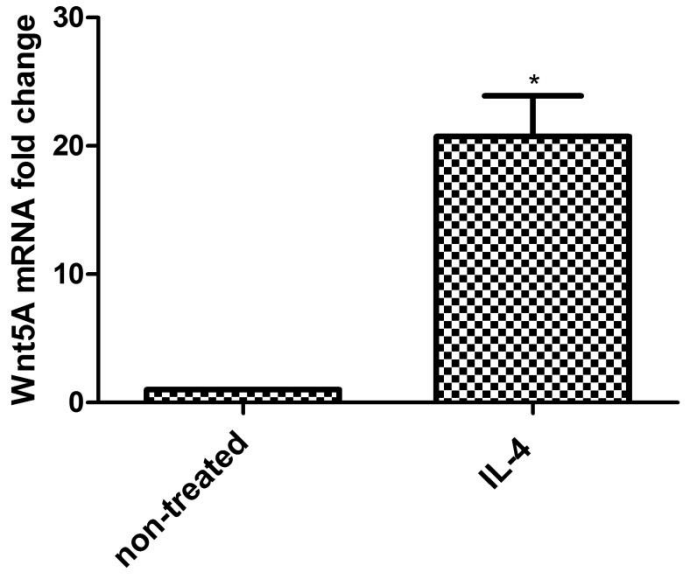

Fig. 9. Wnt5A expression in IL-4 activated human macrophages. Fold changes in the expression of Wnt5A mRNA in IL-4 treated human macrophages. Data were obtained from two independent qRT-PCR experiments run with duplicate samples using RNA isolated from macrophages from four different donors and expressed as the mean ± SEM. **P*<0.05 using an unpaired Student's *t*- test.

SUPPLEMENTAL MATERIAL

SUPPLEMENTAL TABLES

S1 Table. The top 100 genes upregulated by IL-4 in HCAEC.

Gene symbol	Accession	Sequence description	Fold change
PMCH	NM_002674	Homo sapiens pro-melanin-concentrating hormone	41,795143
HAS3	NM_005329	Homo sapiens hyaluronan synthase 3	40,64191
CCL26	NM_006072	Homo sapiens chemokine (C-C motif) ligand 26	37,32348
OTOGL	NM_173591	Homo sapiens otogelin-like	28,089672
TMTC1	NM_175861	Homo sapiens transmembrane and tetratricopeptide repeat containing 1	26,668077
CH25H	NM_003956	Homo sapiens cholesterol 25-hydroxylase	21,65999
VCAM1	NM_001078	Homo sapiens vascular cell adhesion molecule 1	19,443674
DKK2	NM_014421	Homo sapiens dickkopf homolog 2	12,351812
SLC10A7	NM_032128	Homo sapiens solute carrier family 10 (sodium/bile acid cotransporter family), member 7	12,2331505
MASP1	NM_001031849	Homo sapiens mannan-binding lectin serine peptidase 1	11,580042
COL3A1	NM_000090	Homo sapiens collagen, type III, alpha 1	10,082533
WNT5A	NM_003392	Homo sapiens wingless-type MMTV integration site family, member 5A	9,96113
PKD1L1	NM_138295	Homo sapiens polycystic kidney disease 1 like 1	9,657538
SOCS1	NM_003745	Homo sapiens suppressor of cytokine signalling 1	9,610145
IGF1	NM_000618	Homo sapiens insulin-like growth factor 1	9,396036
ERAP1	NM_016442	Homo sapiens endoplasmic reticulum aminopeptidase 1	9,268832
PLCB4	NM_182797	Homo sapiens phospholipase C, beta 4	8,71052
HS3ST1	NM_005114	Homo sapiens heparan sulfate (glucosamine) 3-O-sulfotransferase 1	8,354389
FILIP1L	NM_182909	Homo sapiens filamin A interacting protein 1-like	8,258449
NCF2	NM_000433	Homo sapiens neutrophil cytosolic factor 2	8,030248
MAP3K8	NM_005204	Homo sapiens mitogen-activated protein kinase kinase kinase 8	7,8828645
BMP2	NM_001200	Homo sapiens bone morphogenetic protein 2	7,6503243
LIFR	NM_002310	Homo sapiens leukemia inhibitory factor receptor alpha	7,4233665
BATF3	NM_018664	Homo sapiens basic leucine zipper transcription factor, ATF-like 3	7,255049
FOXC1	NM_001453	Homo sapiens forkhead box C1	7,21699
CISH	NM_145071	Homo sapiens cytokine inducible SH2-	7,0423675

		containing protein	
EGR1	NM_001964	Homo sapiens early growth response 1	7,0303206
MMP7	NM_002423	Homo sapiens matrix metallopeptidase 7	6,91629
AGXT2L1	NM_031279	Homo sapiens alanine-glyoxylate aminotransferase 2-like 1	6,9126115
FAM115C	NM_173678	Homo sapiens family with sequence similarity 115, member C	6,896242
SELP	NM_003005	Homo sapiens selectin P	6,8684745
VSTM1	NM_198481	Homo sapiens V-set and transmembrane domain containing 1	6,8496885
RTP4	NM_022147	Homo sapiens receptor (chemosensory) transporter protein 4	6,7024455
CHRNB2	NM_000748	Homo sapiens cholinergic receptor, nicotinic, beta 2	6,6299343
VIT	NM_001177972	Homo sapiens vitrin	6,553535
GDF6	NM_001001557	Homo sapiens growth differentiation factor 6	6,516541
SLC1A6	NM_005071	Homo sapiens solute carrier family 1 (high affinity aspartate/glutamate transporter), member 6	6,510828
IGFL2	NM_001002915	Homo sapiens IGF-like family member 2	6,4454446
EFCAB9	NM_001171183	Homo sapiens EF-hand calcium binding domain 9	6,444065
OLFML2A	NM_182487	Homo sapiens olfactomedin-like 2A	6,3796315
MYH11	NM_001040114	Homo sapiens myosin, heavy chain 11	6,3696566
SP5	NM_001003845	Homo sapiens Sp5 transcription factor	6,3607006
C5orf46	NM_206966	Homo sapiens chromosome 5 open reading frame 46	6,228292
UBD	NM_006398	Homo sapiens ubiquitin D	6,2165623
C11orf70	NM_001195005	Homo sapiens chromosome 11 open reading frame 70	6,2152133
TMTC1	NM_175861	Homo sapiens transmembrane and tetratricopeptide repeat containing 1	6,153664
DACT1	NM_016651	Homo sapiens dapper, antagonist of beta-catenin, homolog 1	6,1239324
MTMR7	NM_004686	Homo sapiens myotubularin related protein 7	6,1005383
POU4F1	NM_006237	Homo sapiens POU class 4 homeobox 1	5,999347
CXCR7	NM_020311	Homo sapiens chemokine (C-X-C motif) receptor 7	5,9171534
PCDHGC4	NM_032406	Homo sapiens protocadherin gamma subfamily C, 4	5,8364773
FABP4	NM_001442	Homo sapiens fatty acid binding protein 4	5,8192124
CCL11	NM_002986	Homo sapiens chemokine (C-C motif) ligand 11	5,7279153
IL6ST	NM_002184	Homo sapiens interleukin 6 signal transducer	5,718929
DUOX1	NM_017434	Homo sapiens dual oxidase 1	5,7007294
TSLP	NM_033035	Homo sapiens thymic stromal lymphopoietin	5,688645
FXYD1	NM_005031	Homo sapiens FXYD domain containing ion transport regulator 1	5,568317

KCND2	NM_012281	Homo sapiens potassium voltage-gated channel, Shal-related subfamily, member 2	5,4865217
NAP1L3	NM_004538	Homo sapiens nucleosome assembly protein 1-like 3	5,437414
SOX12	NM_006943	Homo sapiens SRY (sex determining region Y)-box 12	5,4160028
TMEM87B	NM_032824	Homo sapiens transmembrane protein 87B	5,389064
C22orf33	NM_178552	Homo sapiens chromosome 22 open reading frame 33	5,3850923
ELMOD1	NM_018712	Homo sapiens ELMO/CED-12 domain containing 1	5,357257
INHBA	NM_002192	Homo sapiens inhibin, beta A	5,324977
HTR3C	NM_130770	Homo sapiens 5-hydroxytryptamine (serotonin) receptor 3, family member C	5,283623
C2orf81	NM_001145054	Homo sapiens chromosome 2 open reading frame 81	5,1805587
PTCH1	NM_001083602	Homo sapiens patched 1	5,1540847
CCL20	NM_004591	Homo sapiens chemokine (C-C motif) ligand 20	5,0769067
ANKRD55	NM_024669	Homo sapiens ankyrin repeat domain 55	4,962989
C2CD4A	NM_207322	Homo sapiens C2 calcium-dependent domain containing 4A	4,910864
HTR2B	NM_000867	Homo sapiens 5-hydroxytryptamine (serotonin) receptor 2B	4,856557
IL6	NM_000600	Homo sapiens interleukin 6	4,831578
C17orf109	NM_001162995	Homo sapiens chromosome 17 open reading frame 109	4,821182
C6	NM_000065	Homo sapiens complement component 6	4,8188324
MYOM1	NM_003803	Homo sapiens myomesin 1	4,792512
LOX	NM_002317	Homo sapiens lysyl oxidase	4,7536435
C1orf172	NM_152365	Homo sapiens chromosome 1 open reading frame 172	4,7347064
RBPMS2	NM_194272	Homo sapiens RNA binding protein with multiple splicing 2	4,720724
ZNF415	NM_001136038	Homo sapiens zinc finger protein 415	4,7036552
IL1RL1	NM_016232	Homo sapiens interleukin 1 receptor-like 1	4,659585
AMIGO2	NM_181847	Homo sapiens adhesion molecule with Ig-like domain 2	4,650363
MYB	NM_005375	Homo sapiens v-myb myeloblastosis viral oncogene homolog	4,6442075
ZFR2	NM_015174	Homo sapiens zinc finger RNA binding protein 2	4,6371136
SERPINB13	NM_012397	Homo sapiens serpin peptidase inhibitor, clade B (ovalbumin), member 13	4,599599
CRHBP	NM_001882	Homo sapiens corticotropin releasing hormone binding protein	4,5980325
FSCN3	NM_020369	Homo sapiens fascin homolog 3, actin-bundling protein, testicular	4,592466
DBF4	NM_006716	Homo sapiens DBF4 homolog	4,5902414
LRP1B	NM_018557	Homo sapiens low density lipoprotein receptor-related protein 1B	4,5893173
AIM1	NM_001624	Homo sapiens absent in melanoma 1	4,5863357

KIR2DS4	NM_012314	Homo sapiens killer cell immunoglobulin-like receptor, two domains, short cytoplasmic tail, 4	4,5634003
HIST2H2BE	NM_003528	Homo sapiens histone cluster 2, H2be	4,558278
NUP62CL	NM_017681	Homo sapiens nucleoporin 62kDa C-terminal like	4,5011163
BCL11A	NM_022893	Homo sapiens B-cell CLL/lymphoma 11A	4,495745
FPR2	NM_001462	Homo sapiens formyl peptide receptor 2	4,471268
EMR2	NM_013447	Homo sapiens egf-like module containing, mucin-like, hormone receptor-like 2	4,437741
FLRT3	NM_198391	Homo sapiens fibronectin leucine rich transmembrane protein 3	4,4005938
OXTR	NM_000916	Homo sapiens oxytocin receptor	4,391427
ADAMTSL3	NM_207517	Homo sapiens ADAMTS-like 3	4,3507504
SPDYE5	NM_001099435	Homo sapiens speedy homolog E5	4,3375187
EFCAB3	NM_173503	Homo sapiens EF-hand calcium binding domain 3	4,3256946

S2 Table. The top 100 genes downregulated by IL-4 in HCAEC.

Gene symbol	Accession	Sequence description	Fold change
LRRC14B	NM_001080478	Homo sapiens leucine rich repeat containing 14B	-12,945567
DNAH2	NM_020877	Homo sapiens dynein, axonemal, heavy chain 2	-9,480801
TMEM191B	NM_001242313	Homo sapiens transmembrane protein 191B	-8,606891
FAM47B	NM_152631	Homo sapiens family with sequence similarity 47, member B	-8,436531
GPR116	NM_001098518	Homo sapiens G protein-coupled receptor 116	-7,9685755
TTC9	NM_015351	Homo sapiens tetratricopeptide repeat domain 9	-7,767549
NOG	NM_005450	Homo sapiens noggin	-7,578256
OR13C8	NM_001004483	Homo sapiens olfactory receptor, family 13, subfamily C, member 8	-7,5168667
GPRC6A	NM_148963	Homo sapiens G protein-coupled receptor, family C, group 6, member A	-7,467667
CSN3	NM_005212	Homo sapiens casein kappa	-7,366031
TMEM236	NM_001098844	Homo sapiens transmembrane protein 236	-7,1928277
PRKG2	NM_006259	Homo sapiens protein kinase, cGMP-dependent, type II	-7,114787
DGKB	NM_145695	Homo sapiens diacylglycerol kinase, beta 90kDa	-7,055235
CSTL1	NM_138283	Homo sapiens cystatin-like 1	-7,038949
GALNT14	NM_024572	Homo sapiens UDP-N-acetyl-alpha-D-galactosamine:polypeptide N-acetylgalactosaminyltransferase 14	-6,925887
N4BP3	NM_015111	Homo sapiens NEDD4 binding protein 3	-6,8579197
ARHGEF38	NM_001242729	Homo sapiens Rho guanine nucleotide exchange factor (GEF) 38	-6,75289
MRVI1	NM_130385	Homo sapiens murine retrovirus integration site 1 homolog	-6,6988463
EPN3	NM_017957	Homo sapiens epsin 3	-6,594775
FSIP2	NM_173651	Homo sapiens fibrous sheath interacting protein 2	-6,4968653
SGPP2	NM_152386	Homo sapiens sphingosine-1-phosphate phosphatase 2	-5,6272907
STARD6	NM_139171	Homo sapiens StAR-related lipid transfer (START) domain containing 6	-5,626096
SLC22A12	NM_144585	Homo sapiens solute carrier family 22 (organic anion/urate transporter), member 12	-5,625856
FCRL6	NM_001004310	Homo sapiens Fc receptor-like 6	-5,603581
GPR151	NM_194251	Homo sapiens G protein-coupled receptor 151	-5,515336
TTC16	NM_144965	Homo sapiens tetratricopeptide repeat domain 16	-5,5019436
SGCD	NM_000337	Homo sapiens sarcoglycan, delta	-5,411149
OSTN	NM_198184	Homo sapiens osteocrin	-5,3031754
PCDHGB1	NM_032095	Homo sapiens protocadherin gamma	-5,2786555

		subfamily B, 1	
NEK10	NM_199347	Homo sapiens NIMA (never in mitosis gene a)- related kinase 10	-5,2474537
FREM3	NM_001168235	Homo sapiens FRAS1 related extracellular matrix 3	-5,1939254
NLRP10	NM_176821	Homo sapiens NLR family, pyrin domain containing 10	-5,183514
REM1	NM_014012	Homo sapiens RAS (RAD and GEM)-like GTP-binding 1	-5,148359
TCHHL1	NM_001008536	Homo sapiens trichohyalin-like 1	-5,1217394
ZNF846	NM_001077624	Homo sapiens zinc finger protein 846	-5,025068
LEKR1	NM_001004316	Homo sapiens leucine, glutamate and lysine rich 1	-5,012441
TPTE2	NM_199254	Homo sapiens transmembrane phosphoinositide 3-phosphatase and tensin homolog 2	-5,006573
TAS2R5	NM_018980	Homo sapiens taste receptor, type 2, member 5	-5,004593
CEACAM3	NM_001815	Homo sapiens carcinoembryonic antigen-related cell adhesion molecule 3	-4,9621882
ZNF551	NM_138347	Homo sapiens zinc finger protein 551	-4,959369
SEMA4D	NM_006378	Homo sapiens sema domain, immunoglobulin domain (Ig), transmembrane domain (TM) and short cytoplasmic domain, (semaphorin) 4D	-4,948316
KIT	NM_000222	Homo sapiens v-kit Hardy-Zuckerman 4 feline sarcoma viral oncogene homolog	-4,931853
ANKRD20A2	NM_001012421	Homo sapiens ankyrin repeat domain 20 family, member A2	-4,89075
EPHA10	NM_173641	Homo sapiens EPH receptor A10	-4,870359
SEMA5B	NM_001031702	Homo sapiens sema domain, seven thrombospondin repeats (type 1 and type 1-like), transmembrane domain (TM) and short cytoplasmic domain, (semaphorin) 5B	-4,8688235
SPRR4	NM_173080	Homo sapiens small proline-rich protein 4	-4,8533287
MYL3	NM_000258	Homo sapiens myosin, light chain 3	-4,8104806
PLB1	NM_153021	Homo sapiens phospholipase B1	-4,73602
CHI3L1	NM_001276	Homo sapiens chitinase 3-like 1	-4,7334285
FMN2	NM_020066	Homo sapiens formin 2	-4,7102337
INMT	NM_001199219	Homo sapiens indolethylamine N-methyltransferase	-4,67023
ZCCHC13	NM_203303	Homo sapiens zinc finger, CCHC domain containing 13	-4,646102
HAPLN1	NM_001884	Homo sapiens hyaluronan and proteoglycan link protein 1	-4,6067057
DNAJB8	NM_153330	Homo sapiens DnaJ (Hsp40) homolog, subfamily B, member 8	-4,6007133
RGS7BP	NM_001029875	Homo sapiens regulator of G-protein signalling 7 binding protein	-4,581259
XAGE5	NM_130775	Homo sapiens X antigen family, member 5	-4,4819264
RNASE2	NM_002934	Homo sapiens ribonuclease, RNase A family, 2	-4,4812913

MUC12	NM_001164462	Homo sapiens mucin 12, cell surface associated	-4,476315
ALPK2	NM_052947	Homo sapiens alpha-kinase 2	-4,464628
FMR1NB	NM_152578	Homo sapiens fragile X mental retardation 1 neighbor	-4,4601526
ACOT6	NM_001037162	Homo sapiens acyl-CoA thioesterase 6	-4,4558067
ZNF436	NM_001077195	Homo sapiens zinc finger protein 436	-4,439032
PPP1R1A	NM_006741	Homo sapiens protein phosphatase 1, regulatory (inhibitor) subunit 1A	-4,4109473
HS6ST3	NM_153456	Homo sapiens heparan sulfate 6-O-sulfotransferase 3	-4,379276
CXorf22	NM_152632	Homo sapiens chromosome X open reading frame 22	-4,3745127
KAZN	NM_015209	Homo sapiens kazrin, periplakin interacting protein	-4,3690753
SPANXB2	NM_145664	Homo sapiens SPANX family, member B2	-4,362014
SPINK5	NM_001127698	Homo sapiens serine peptidase inhibitor, Kazal type 5	-4,3541923
DDIT4L	NM_145244	Homo sapiens DNA-damage-inducible transcript 4-like	-4,311884
VCX2	NM_016378	Homo sapiens variable charge, X-linked 2	-4,2942934
CCKBR	NM_176875	Homo sapiens cholecystokinin B receptor	-4,259044
KIAA1199	NM_018689	Homo sapiens KIAA1199	-4,2481823
ATP2A3	NM_174958	Homo sapiens ATPase, Ca++ transporting, ubiquitous	-4,239258
SPANXN3	NM_001009609	Homo sapiens SPANX family, member N3	-4,2082605
KRT6B	NM_005555	Homo sapiens keratin 6B	-4,2064652
APLN	NM_017413	Homo sapiens apelin	-4,198813
PCDHA1	NM_031410	Homo sapiens protocadherin alpha 1	-4,17986
ZP2	NM_003460	Homo sapiens zona pellucida glycoprotein 2	-4,1756864
SMOC2	NM_022138	Homo sapiens SPARC related modular calcium binding 2	-4,1644816
SPINK4	NM_014471	Homo sapiens serine peptidase inhibitor, Kazal type 4	-4,1478534
C1orf49	NM_032126	Homo sapiens chromosome 1 open reading frame 49	-4,146102
CYP3A43	NM_022820	Homo sapiens cytochrome P450, family 3, subfamily A, polypeptide 43	-4,1281586
GPR112	NM_153834	Homo sapiens G protein-coupled receptor 112	-4,1099563
ZNF253	NM_021047	Homo sapiens zinc finger protein 253	-4,0930114
TPD52L3	NM_033516	Homo sapiens tumor protein D52-like 3	-4,05051
GZMK	NM_002104	Homo sapiens granzyme K	-4,0004787
LOC55908	NM_018687	Homo sapiens hepatocellular carcinoma-associated gene TD26	-3,9874408
SPEF2	NM_024867	Homo sapiens sperm flagellar 2	-3,9677868
ZNF208	NM_007153	Homo sapiens zinc finger protein 208	-3,9518707
PTCHD2	NM_020780	Homo sapiens patched domain containing 2	-3,9511278
PARVG	NM_022141	Homo sapiens parvin, gamma (PARVG), transcript variant 1, mRNA	-3,9182448

FTCD	NM_206965	Homo sapiens formiminotransferase cyclodeaminase (FTCD), transcript variant A, mRNA	-3,9056072
NKAIN2	NM_001040214	Homo sapiens Na+/K+ transporting ATPase interacting 2 (NKAIN2), transcript variant 1, mRNA	-3,877624
DMGDH	NM_013391	Homo sapiens dimethylglycine dehydrogenase (DMGDH), nuclear gene encoding mitochondrial protein, mRNA	-3,8753538
SPATA13	NM_001166271	Homo sapiens spermatogenesis associated 13 (SPATA13), transcript variant 1, mRNA	-3,860474
PTPN3	NM_002829	Homo sapiens protein tyrosine phosphatase, non-receptor type 3 (PTPN3), transcript variant 1, mRNA	-3,79502
C10orf99	NM_207373	Homo sapiens chromosome 10 open reading frame 99 (C10orf99), mRNA	-3,792719
MYH4	NM_017533	Homo sapiens myosin, heavy chain 4, skeletal muscle (MYH4), mRNA	-3,7923658
C5orf52	NM_001145132	Homo sapiens chromosome 5 open reading frame 52 (C5orf52), mRNA	-3,7702193
HAVCR1	NM_012206	Homo sapiens hepatitis A virus cellular receptor 1 (HAVCR1), transcript variant 1, mRNA	-3,7554414

S3 Table. Regulation of genes coding for transcription factors in IL-4 treated HCAEC.

Gene symbol	Accession	Sequence description	Fold change
EGR1	NM_001964	Homo sapiens early growth response 1	7.030321
FOSB	NM_006732	Homo sapiens FBJ murine osteosarcoma viral oncogene homolog B	3.307321
GATA3	NM_001002295	Homo sapiens GATA binding protein 3	3.068881

SUPPLEMENTAL FIGURES

S1 Fig.

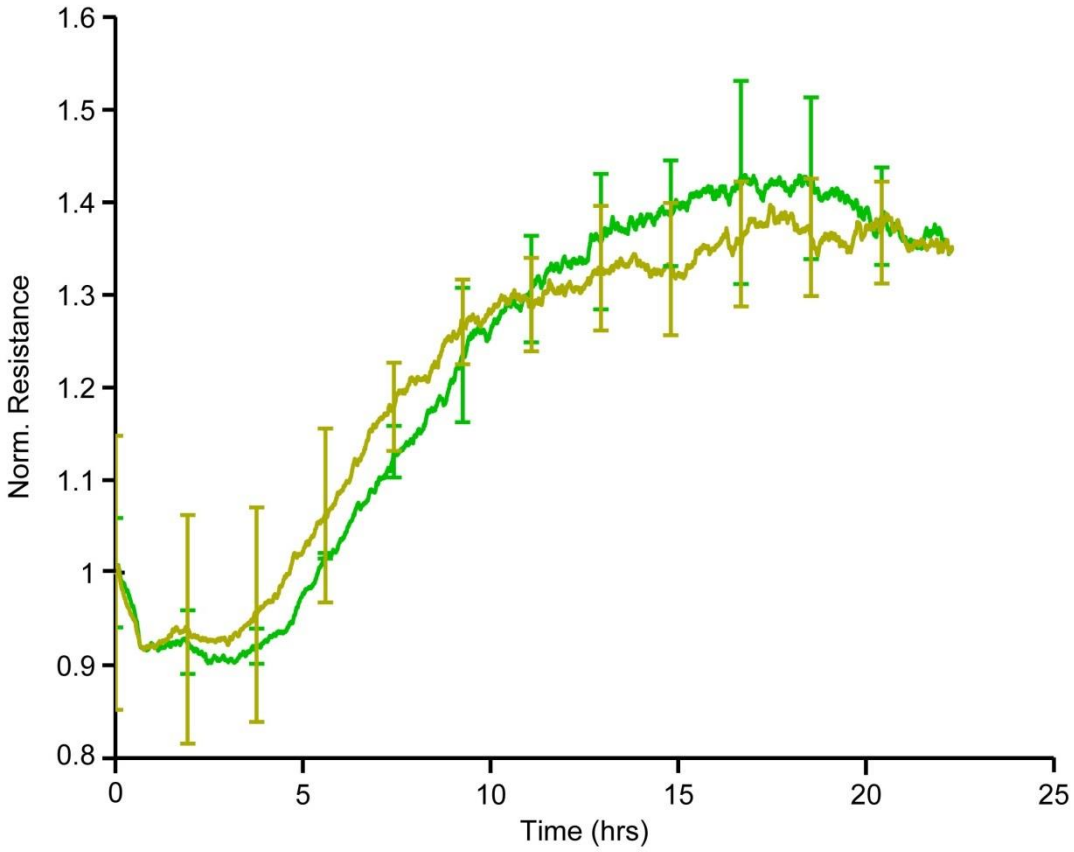

S1 Fig. HCAEC monolayer formation in ECIS arrays. Immediately after seeding HCAEC into 8W10E+ arrays with a density of 80,000- 90,000 cells/well, resistance measurements (in Ohms) were started and are shown as normalized resistance (subsequent values were divided by initial values). Increase in resistance over time indicates an increase in the formation of intercellular contacts. The steady state of resistance represents a tight monolayer stage exhibiting stable barrier function. Each single curve represents the resistance measurements conducted in duplicate wells which were grouped and averaged. Error bars of curves represent SD. Figures shown depict the resistance measurements conducted at 4000 Hz.

S2 Fig.

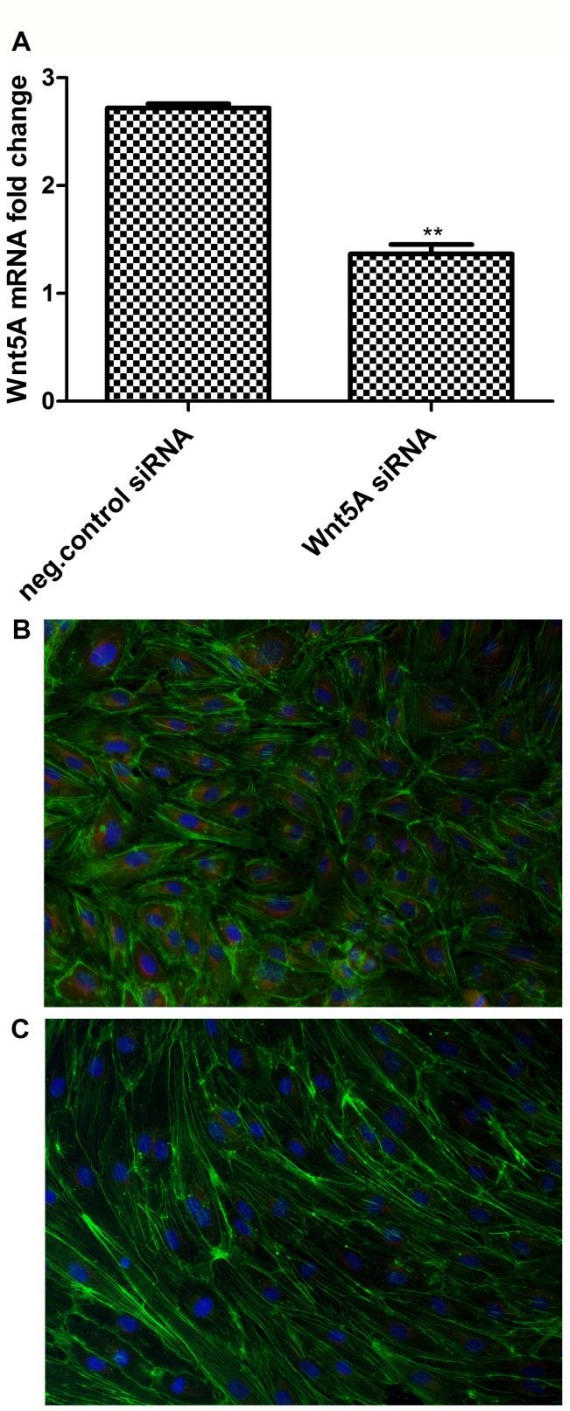

S2 Fig. Wnt5A knockdown efficiency. (A) Expression levels of Wnt5A mRNA in HCAEC transfected with 5 nM negative (neg.) control siRNA and Wnt5A siRNA. Data were obtained from three independent qRT-PCR experiments run with duplicate samples and expressed as the mean ± SEM. **P*<0.005 of Student's *t*-test. Representative immunofluorescence staining depicting Wnt5A protein expression (red) in negative control siRNA transfected (B) and Wnt5A siRNA transfected (C) HCAEC. Green: F-actin, Blue: nuclei. Zeiss Axioskope, Magnification 20×.

7. CONCLUSIONS

The present study describes a novel inflammatory Wnt5A signaling mechanism affecting monolayer integrity and barrier function in human vascular endothelial cells. This pathway acts independent of the presence other inflammatory mediators such as TNF, IL-1 or IL-6 as summarized in Figure 6.

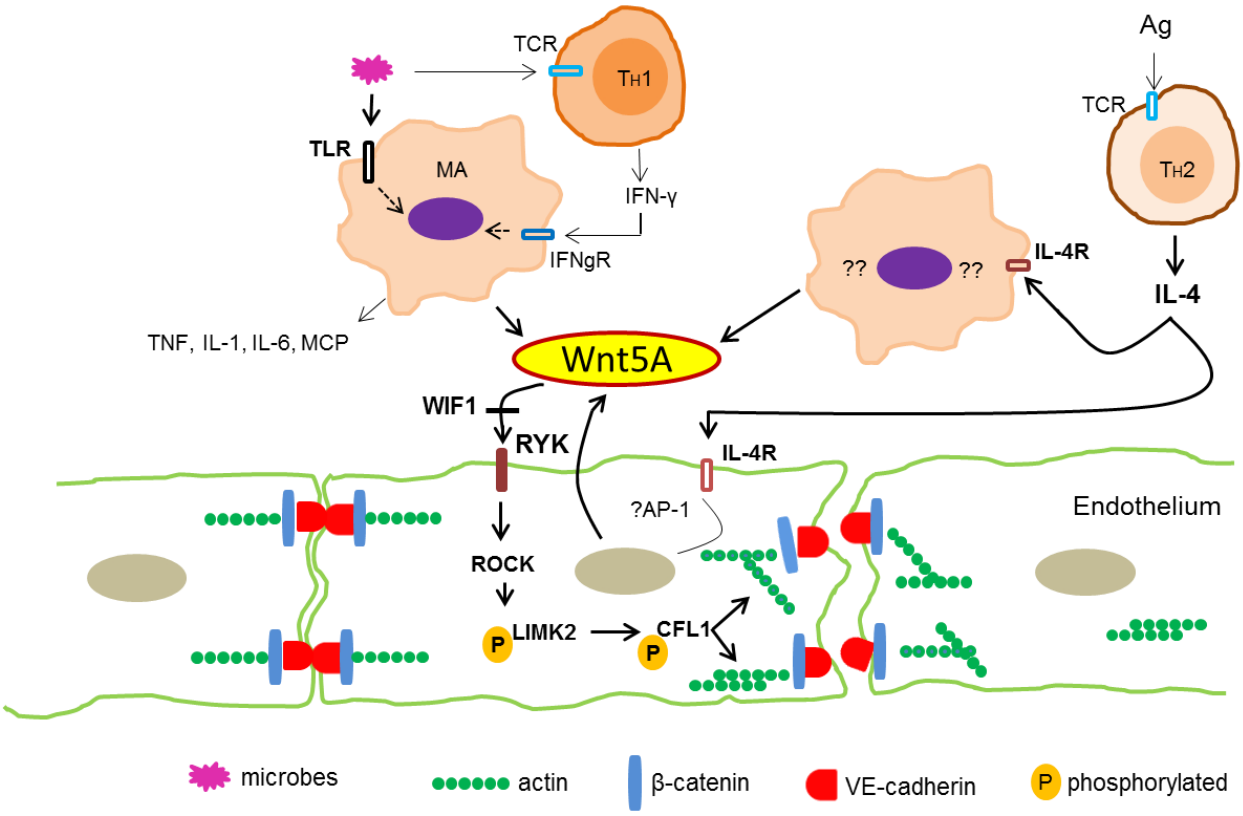

Figure 6. The paracrine and autocrine action of macrophage-derived and IL-4-induced Wnt5A on human vascular endothelial cells. Tight intercellular contacts at AJ in resting endothelial cells (left side of figure) are disrupted upon Wnt5A/Ryk signaling to form inter-endothelial gaps (right side of figure). MA, macrophages; Ag, Antigen; TCR, T cell receptor; IL-4R, IL-4 receptor; IFNgR, Interferon-γ receptor; TH1, type 1 helper T cell.

Whole genome transcriptome profiling and GO analyses revealed that Wnt5A mainly regulated the process of cytoskeleton remodelling involving *LIMK-2* and *CFL-1* in HCAEC. Wnt5A-induced phosphorylation of LIMK-2 and CFL-1 through activation of ROCK increased actin stress fiber formation and disrupted AJ proteins in IEJ (Figure 6). We demonstrated that Wnt5A-induced cytoskeleton remodelling could also affect endothelial cell motility and impair endothelial barrier

function. By application of the Ryk-specific Wnt antagonist WIF-1, and by silencing Ryk expression, we proved Ryk as the Wnt5A receptor upstream to the ROCK/LIMK-2/CFL-1 pathway regulating actin cytoskeleton remodelling. We further identified Wnt5A/Ryk signaling as the effector mechanism responsible for cytoskeleton remodelling and increased permeability in IL-4-treated HCAEC (Figure 6). Data obtained in these studies indicate a critical role for Wnt5A in mediating endothelial permeability in severe systemic inflammatory diseases like sepsis/septic shock, and in IL-4 driven allergic inflammation.

In conclusion, Wnt5A/Ryk signaling is a novel pro-inflammatory mechanism inducing barrier dysfunction in the vascular endothelium. The present study advances the current knowledge of systemic inflammation and opens new perspectives for therapeutic intervention in patients with severe systemic inflammatory diseases.

Further investigations are needed to unravel the intriguing finding of Wnt5A being induced by two different pathways that are evolutionary highly conserved, TLR-dependent and IL-4 dependent signaling.

8. ACKNOWLEDGMENTS

I would first like to thank God for giving me this PhD project through Prof. Schoedon and the knowledge, guidance and strength to successfully complete my doctoral studies.

I am grateful to Prof. Schoedon for the excellent mentoring she has provided throughout the study that has advanced my scientific knowledge and skills. I thank her for interesting discussions and the kindness and support shown to me.

I would like to thank Dr. Mårten Schneider for sharing his knowledge in flow cytometry and Dr. Christian Schaer for his valuable suggestions on microarray technique.

I gratefully acknowledge Prof. Christoph Renner and Prof. Christian Münz for serving as my thesis committee members.

A word of thanks goes to Dr. Julia Burgener, Dr. Esther Bächli and all members of Inflammation Research Unit at Division of Internal Medicine, USZ.

I am indebted to my parents and wife for love, support and understanding.

9. CURRICULUM VITAE

Surname: SKARIA
First Name: Tom
Date of Birth: 28.05.1984
Nationality: Indian

Education

2000-2002	Higher Secondary Examination (Science), Government of Kerala, India.
2002-2005	B.Sc. Biotechnology, Mahatma Gandhi University, Kottayam, Kerala, India.
2005-2007	M.Sc. Biotechnology, Bangalore University, India.
2009-2010	M.Sc. Molecular Biology, University of Skövde, Sweden. Title of Master thesis: “Alterations of complexes of oxidative phosphorylation in gastric carcinoma”.
2010-2015	PhD Dissertation at the Inflammation Research Unit, Division of Internal Medicine, University Hospital of Zurich, University of Zurich. “Mechanisms of Inflammation in Response to Wnt5A and IL-4 in Human Vascular Endothelial Cells” under the supervision of Prof. Gabriele Schoedon, Prof. Christoph Renner and Prof. Christian Münz.